

Supporting Information

for

Pyrrole[3,2-*d*:4,5-*d'*]bisthiazole-Bridged- Bis(naphthalene diimide)s as Electron-Transport Materials

*Yulia A. Getmanenko,¹ Sanjeev Singh,² Bhupinder Sandhu,³ Cheng-Yin Wang,² Tatiana Timofeeva,³
Bernard Kippelen,² Seth R. Marder^{*1}*

¹*Department of Chemistry & Biochemistry and Center for Organic Photonics and Electronics, Georgia
Institute of Technology, 901 Atlantic Drive NW, Atlanta, GA 30332-0400, USA*

²*School of Electrical and Computer Engineering, Center for Organic Photonics and Electronics,
Georgia Institute of Technology, 777 Atlantic Drive NW, Atlanta, GA 30332-0250, USA*

³*Department of Biology and Chemistry, New Mexico Highlands University, Las Vegas, NM 87701, USA*

seth.marder@chemistry.gatech.edu

Contents

General.....	6
Characterization.....	6
Device Fabrication.....	6

Figure S1. Device structure for top-gate bottom-contact organic field-effect transistor.....	7
Device Characteristics	7
Figure S2. Transfer (<i>left</i>) and output (<i>right</i>) characteristics of a particular <i>n</i> -channel top-gate OFET with 6a semiconductor using chloroform solvent and CYTOP/Al ₂ O ₃ gate dielectric layer with Au source / drain electrodes (<i>W/L</i> = 2550 μm / 180 μm).	7
Figure S3. Transfer (<i>left</i>) and output (<i>right</i>) characteristics of a particular <i>n</i> -channel top-gate OFET with 6a semiconductor using chlorobenzene : chloroform (4:1) solvent and CYTOP/Al ₂ O ₃ gate dielectric layer with Au source / drain electrodes (<i>W/L</i> = 2550 μm / 180 μm).	8
Figure S4. Transfer (<i>left</i>) and output (<i>right</i>) characteristics of a particular <i>n</i> -channel top-gate OFET with 6b semiconductor blended with PS using dichlorobenzene solvent and CYTOP/Al ₂ O ₃ gate dielectric layer with Au source / drain electrodes (<i>W/L</i> = 2550 μm / 180 μm).	8
Figure S5. Transfer (<i>left</i>) and output (<i>right</i>) characteristics of a particular <i>n</i> -channel top-gate OFET with 6b semiconductor using 1,1,2,2-tetrachloroethane as a solvent and CYTOP/Al ₂ O ₃ gate dielectric layer with Au source / drain electrodes (<i>W/L</i> = 2550 μm / 180 μm).	9
Figure S6. Transfer (<i>left</i>) and output (<i>right</i>) characteristics of a particular <i>n</i> -channel top-gate OFET with 6c semiconductor using 1,1,2,2-tetrachloroethane solvent and CYTOP/Al ₂ O ₃ gate dielectric layer with Au source / drain electrodes (<i>W/L</i> = 2550 μm / 180 μm).	9
Figure S7. Transfer characteristics of a particular <i>n</i> -channel top-gate OFET with 6e semiconductor using chloroform solvent and CYTOP/Al ₂ O ₃ gate dielectric layer with Au source / drain electrodes (<i>W/L</i> = 2550 μm / 180 μm).	10
Figure S8. Transfer (<i>left</i>) and output (<i>right</i>) characteristics of a particular <i>n</i> -channel top-gate OFET with 8a semiconductor using 1,1,2,2-tetrachloroethane solvent and CYTOP/Al ₂ O ₃ gate dielectric layer with Au source / drain electrodes (<i>W/L</i> = 2550 μm / 180 μm).	10
Figure S9. Transfer (<i>left</i>) and output (<i>right</i>) characteristics of a particular <i>n</i> -channel top-gate OFET with 8a semiconductor using dichlorobenzene as a solvent and CYTOP/Al ₂ O ₃ gate dielectric layer with Au source / drain electrodes (<i>W/L</i> = 1000 μm / 180 μm).	11
Figure S10. Transfer (<i>left</i>) and output (<i>right</i>) characteristics of a particular <i>n</i> -channel top-gate OFET with 8b semiconductor using 1,1,2,2-tetrachloroethane as a solvent and CYTOP/Al ₂ O ₃ gate dielectric layer with Au source / drain electrodes (<i>W/L</i> = 1000 μm / 180 μm).	11
Figure S11. Transfer (<i>left</i>) and output (<i>right</i>) characteristics of a particular <i>n</i> -channel top-gate OFET with 8b semiconductor using 1,2-dichlorobenzene as a solvent and CYTOP/Al ₂ O ₃ gate dielectric layer with Au source / drain electrodes (<i>W/L</i> = 1000 μm / 180 μm).	12
Figure S12. Continuous stress bias inside N ₂ glove box and in ambient atmosphere for a particular <i>n</i> -channel top-gate OFET with 6a semiconductor.....	12
Computational Methodology	12
X-Ray Single Crystal Structural Analysis	13
Table S1. Crystallographic data for 4-hexyl-2,6-bis(triisopropylsilyl)-4 <i>H</i> -pyrrolo[2,3- <i>d</i> :5,4- <i>d'</i>]bisthiazole (2a) and 2,6-dibromo-4-hexyl-4 <i>H</i> -pyrrolo[2,3- <i>d</i> :5,4- <i>d'</i>]bisthiazole (3a)	13
Synthetic Details.....	14
4-Hexyl-2,6-bis(triisopropylsilyl)-4 <i>H</i> -pyrrolo[2,3- <i>d</i> :5,4- <i>d'</i>]bisthiazole (2a).....	14
4-Dodecyl-2,6-bis(triisopropylsilyl)-4 <i>H</i> -pyrrolo[2,3- <i>d</i> :5,4- <i>d'</i>]bisthiazole (2b)	14
Figure S13. CV of 4-dodecyl-2,6-bis(triisopropylsilyl)-4 <i>H</i> -pyrrolo[2,3- <i>d</i> :5,4- <i>d'</i>]bisthiazole (2b) in 0.1 M Bu ₄ PF ₆ in dichloromethane: $E_{1/2}^{0/+} = +0.77$ V.	15
2,6-Dibromo-4-hexyl-4 <i>H</i> -pyrrolo[2,3- <i>d</i> :5,4- <i>d'</i>]bisthiazole (3a)	15

Figure S14. Cyclic voltammetry of 2,6-dibromo-4-hexyl-4 <i>H</i> -pyrrolo[2,3- <i>d</i> :5,4- <i>d'</i>]bisthiazole (3a) in 0.1 M Bu ₄ NPF ₆ in tetrahydrofuran vs. Cp ₂ Fe ⁺⁰ : $E_{pc} = -2.5$ V.....	16
Figure S15. 2,6-Dibromo-4-dodecyl-4 <i>H</i> -pyrrolo[2,3- <i>d</i> :5,4- <i>d'</i>]bisthiazole (3b) (0.1 M Bu ₄ NPF ₆ in tetrahydrofuran vs. Cp ₂ Fe ⁺⁰): (left) CV : $E_{pc} = -2.4$ V; one more peak was observed with $E_{pc} = -2.8$ V; (right) DPV (0.1 M Bu ₄ NPF ₆ in tetrahydrofuran vs. Cp ₂ Fe ⁺⁰): $E_{1/2}^{0/-} = -2.44$ V, $E_{1/2}^{-2-} = -2.71$ V.	17
4-Acetyl-2,7-dihexyl-9-(tributylstannyl)benzo[<i>lmn</i>][3,8]phenanthroline-1,3,6,8(2 <i>H</i> ,7 <i>H</i>)-tetraone (5c).....	18
4-Acetyl-2,7-didodecyl-9-(tributylstannyl)benzo[<i>lmn</i>][3,8]phenanthroline-1,3,6,8(2 <i>H</i> ,7 <i>H</i>)-tetraone (5d)	18
4,4'-(4-Hexyl-4 <i>H</i> -pyrrolo[2,3- <i>d</i> :5,4- <i>d'</i>]bis(thiazole)-2,6-diyl)bis(2,7-dihexylbenzo[<i>lmn</i>][3,8]phenanthroline-1,3,6,8(2 <i>H</i> ,7 <i>H</i>)-tetraone) (6a)	19
Figure S16. DPV analysis of 4,4'-(4-hexyl-4 <i>H</i> -pyrrolo[2,3- <i>d</i> :5,4- <i>d'</i>]bisthiazole-2,6-diyl)bis(2,7-dihexylbenzo[<i>lmn</i>][3,8]phenanthroline-1,3,6,8(2 <i>H</i> ,7 <i>H</i>)-tetraone) (6a) (0.1 M Bu ₄ NPF ₆ in chloroform vs. Cp ₂ Fe ⁺⁰): $E^{red1} = -1.00$ V, $E^{red2} = -1.40$ V.	20
Figure S17. 1 st cycle of the DSC analysis (10 °C/min heating-cooling rate, endo down) of 4,4'-(4-hexyl-4 <i>H</i> -pyrrolo[2,3- <i>d</i> :5,4- <i>d'</i>]bis(thiazole)-2,6-diyl)bis(2,7-dihexylbenzo[<i>lmn</i>][3,8]phenanthroline-1,3,6,8(2 <i>H</i> ,7 <i>H</i>)-tetraone) (6a).	21
4,4'-(4-Dodecyl-4 <i>H</i> -pyrrolo[2,3- <i>d</i> :5,4- <i>d'</i>]bis(thiazole)-2,6-diyl)bis(2,7-didodecylbenzo[<i>lmn</i>][3,8]phenanthroline-1,3,6,8(2 <i>H</i> ,7 <i>H</i>)-tetraone) (6b)	21
Figure S18. DPV analysis of 4,4'-(4-dodecyl-4 <i>H</i> -pyrrolo[2,3- <i>d</i> :5,4- <i>d'</i>]bisthiazole-2,6-diyl)bis(2,7-didodecylbenzo[<i>lmn</i>][3,8]phenanthroline-1,3,6,8(2 <i>H</i> ,7 <i>H</i>)-tetraone) (6b): (left) (0.1 M Bu ₄ NPF ₆ in chloroform vs. Cp ₂ Fe ⁺⁰): $E^{red1} = -1.04$ V, $E^{red2} = -1.42$ V; (right) 0.1 M Bu ₄ NPF ₆ in tetrahydrofuran vs. Cp ₂ Fe ⁺⁰): $E^{red1} = -1.09$ V, $E^{red2} = -1.52$ V, $E^{red3} = -2.33$ V, $E^{red4} = -2.63$ V.	22
Figure S19. DSC analysis (10 °C/min heating-cooling rate, endo down) of 4,4'-(4-dodecyl-4 <i>H</i> -pyrrolo[2,3- <i>d</i> :5,4- <i>d'</i>]bisthiazole-2,6-diyl)bis(2,7-didodecylbenzo[<i>lmn</i>][3,8]phenanthroline-1,3,6,8(2 <i>H</i> ,7 <i>H</i>)-tetraone) (6b): 1st cycle (top); 2nd cycle (bottom).	23
4,4'-(4-Dodecyl-4 <i>H</i> -pyrrolo[2,3- <i>d</i> :5,4- <i>d'</i>]bisthiazole-2,6-diyl)bis(2,7-dihexylbenzo[<i>lmn</i>][3,8]phenanthroline-1,3,6,8(2 <i>H</i> ,7 <i>H</i>)-tetraone) (6c)	24
Figure S20. 4,4'-(4-Dodecyl-4 <i>H</i> -pyrrolo[2,3- <i>d</i> :5,4- <i>d'</i>]bisthiazole-2,6-diyl)bis(2,7-dihexylbenzo[<i>lmn</i>][3,8]phenanthroline-1,3,6,8(2 <i>H</i> ,7 <i>H</i>)-tetraone) (6c): (a) CV analysis in 0.1 M Bu ₄ NPF ₆ in chloroform vs. Cp ₂ Fe ⁺⁰): $E_{1/2}^{0/2-} = -1.05$ V, $E_{1/2}^{2-/4-} = -1.43$ V; (b) DPV analysis in 0.1 M Bu ₄ NPF ₆ in chloroform vs. Cp ₂ Fe ⁺⁰): $E^{red1} = -1.05$ V; $E^{red2} = -1.42$ V.	25
Figure S21. 1 st cycle of the DSC analysis (10 °C/min heating-cooling rate) of 4,4'-(4-dodecyl-4 <i>H</i> -pyrrolo[2,3- <i>d</i> :5,4- <i>d'</i>]bisthiazole-2,6-diyl)bis(2,7-dihexylbenzo[<i>lmn</i>][3,8]phenanthroline-1,3,6,8(2 <i>H</i> ,7 <i>H</i>)-tetraone) (6c).	25
9,9'-(4-Hexyl-4 <i>H</i> -pyrrolo[2,3- <i>d</i> :5,4- <i>d'</i>]bisthiazole-2,6-diyl)bis(4-acetyl-2,7-dihexylbenzo[<i>lmn</i>][3,8]phenanthroline-1,3,6,8(2 <i>H</i> ,7 <i>H</i>)-tetraone) (6d)	26
Figure S22. 9,9'-(4-Hexyl-4 <i>H</i> -pyrrolo[2,3- <i>d</i> :5,4- <i>d'</i>]bisthiazole-2,6-diyl)bis(4-acetyl-2,7-dihexylbenzo[<i>lmn</i>][3,8]phenanthroline-1,3,6,8(2 <i>H</i> ,7 <i>H</i>)-tetraone) (6d) (0.1 M Bu ₄ NPF ₆ in chloroform vs. Cp ₂ Fe ⁺⁰ V): (left) CV, $E_{1/2}^{0/1-} = -0.88$ V, $E_{1/2}^{1-/2-} = -0.96$ V, (right) DPV, $E^{red1} = -0.90$ V, $E^{red2} = -1.00$ V, $E^{red3} = -1.44$ V.	27
Figure S23. 1 st heating of the DSC analysis (10 °C/min heating-cooling rate; endo down) of 9,9'-(4-hexyl-4 <i>H</i> -pyrrolo[2,3- <i>d</i> :5,4- <i>d'</i>]bisthiazole-2,6-diyl)bis(4-acetyl-2,7-dihexylbenzo[<i>lmn</i>][3,8]phenanthroline-1,3,6,8(2 <i>H</i> ,7 <i>H</i>)-tetraone) (6d).	27

9,9'-(4-Dodecyl-4 <i>H</i> -pyrrolo[2,3- <i>d</i> :5,4- <i>d'</i>]bisthiazole-2,6-diyl)bis(4-acetyl-2,7-dihexylbenzo[<i>lmn</i>][3,8]phenanthroline-1,3,6,8(2 <i>H</i> ,7 <i>H</i>)-tetraone) (6e)	27
Figure S24. DPV of 9,9'-(4-dodecyl-4 <i>H</i> -pyrrolo[2,3- <i>d</i> :5,4- <i>d'</i>]bisthiazole-2,6-diyl)bis(4-acetyl-2,7-dihexylbenzo[<i>lmn</i>][3,8]phenanthroline-1,3,6,8(2 <i>H</i> ,7 <i>H</i>)-tetraone) (6e) (0.1 M Bu ₄ NPF ₆ in chloroform vs. Cp ₂ Fe ⁺⁰ V): $E^{\text{red1}} = -0.89$ V, $E^{\text{red2}} = -0.96$ V, $E^{\text{red3}} = -1.36$ V.	28
Figure S25. 1 st cycle of the DSC analysis (10 °C/min heating-cooling rate) of 9,9'-(4-dodecyl-4 <i>H</i> -pyrrolo[2,3- <i>d</i> :5,4- <i>d'</i>]bisthiazole-2,6-diyl)bis(4-acetyl-2,7-dihexylbenzo[<i>lmn</i>][3,8]phenanthroline-1,3,6,8(2 <i>H</i> ,7 <i>H</i>)-tetraone) (6e).	29
2,2'-(4-Oxo-4 <i>H</i> -cyclopenta[1,2- <i>b</i> :5,4- <i>b'</i>]dithiazol-2,6-diyl)bis(2,7-dihexylnaphthalene-1,4:5,8-bis(dicarboximide) (8a)	29
Figure S26. 2,2'-(4-Oxo-4 <i>H</i> -cyclopenta[1,2- <i>b</i> :5,4- <i>b'</i>]dithiazol-2,6-diyl)bis(2,7-dihexylnaphthalene-1,4:5,8-bis(dicarboximide) (8a) in 0.1 M Bu ₄ NPF ₆ in chloroform vs. Cp ₂ Fe ⁺⁰ : (left) CV analysis $E_{1/2}^{0/2-} = -1.01$ V (there is a shoulder suggesting that there is another poorly resolved reduction), $E_{1/2}^{2-/4-} = -1.34$ V; (right) DPV analysis: $E^{\text{red1}} = -0.91$ V (appears as a shoulder); $E^{\text{red2}} = -0.96$ V, $E^{\text{red3}} = -1.34$ V.	30
Figure S27. 1 st cycle of the DSC analysis (10 °C/min heating-cooling rate) of 2,2'-(4-oxo-4 <i>H</i> -cyclopenta[1,2- <i>b</i> :5,4- <i>b'</i>]dithiazol-2,6-diyl)bis(2,7-dihexylnaphthalene-1,4:5,8-bis(dicarboximide) (8a).	30
9,9'-(7-Oxo-7 <i>H</i> -cyclopenta[1,2- <i>d</i> :4,3- <i>d'</i>]bisthiazole-2,5-diyl)bis(4-acetyl-2,7-dihexylbenzo[<i>lmn</i>][3,8]phenanthroline-1,3,6,8(2 <i>H</i> ,7 <i>H</i>)-tetraone) (8b)	31
Figure S28. 9,9'-(7-oxo-7 <i>H</i> -cyclopenta[1,2- <i>d</i> :4,3- <i>d'</i>]bisthiazole-2,5-diyl)bis(4-acetyl-2,7-dihexylbenzo[<i>lmn</i>][3,8]phenanthroline-1,3,6,8(2 <i>H</i> ,7 <i>H</i>)-tetraone) (8b) (0.1 M Bu ₄ NPF ₆ in tetrahydrofuran vs. Cp ₂ Fe ⁺⁰ V): (left) $E_{1/2}^{0/2-} = -0.86$ V, $E_{1/2}^{2-/4-} = -1.33$ V; $E_{1/2}^{4-/5-} = -1.83$ V; (right) DPV of $E^{\text{red1}} = -0.85$ V, $E^{\text{red2}} = -1.33$ V, $E^{\text{red3}} = -1.83$ V, $E^{\text{red4}} = -2.22$ V.	32
Figure S29. 9,9'-(7-oxo-7 <i>H</i> -cyclopenta[1,2- <i>d</i> :4,3- <i>d'</i>]bisthiazole-2,5-diyl)bis(4-acetyl-2,7-dihexylbenzo[<i>lmn</i>][3,8]phenanthroline-1,3,6,8(2 <i>H</i> ,7 <i>H</i>)-tetraone) (8b) (0.1 M Bu ₄ NPF ₆ in chloroform vs. Cp ₂ Fe ⁺⁰ V): (left) CV analysis, $E_{1/2}^{0/2-} = -0.84$ V, $E_{1/2}^{2-/4-} = -1.29$ V; DPV analysis, $E^{\text{red1}} = -0.84$ V, $E^{\text{red2}} = -1.28$ V.	32
Figure S30. 1 st cycle of the DSC analysis (10 °C/min heating-cooling rate) of 9,9'-(7-oxo-7 <i>H</i> -cyclopenta[1,2- <i>d</i> :4,3- <i>d'</i>]bisthiazole-2,5-diyl)bis(4-acetyl-2,7-dihexylbenzo[<i>lmn</i>][3,8]phenanthroline-1,3,6,8(2 <i>H</i> ,7 <i>H</i>)-tetraone) (8b).	33
Figure S31. Pictorial representations of the (a) HOMO (-5.76 eV) and (b) LUMO (-3.59 eV) for 4,4'-(4-methyl-4 <i>H</i> -pyrrolo[2,3- <i>d</i> :5,4- <i>d'</i>]bisthiazole-2,6-diyl)bis(2,7-dimethylbenzo[<i>lmn</i>][3,8]phenanthroline-1,3,6,8(2 <i>H</i> ,7 <i>H</i>)-tetraone) (IV) as determined at the B3LYP/6-31G** level of theory.	34
Table S2. Cartesian coordinates of I , II , III and IV for the optimized neutral state at the B3LYP/6-31G** level of theory.	34
Figure S32. ORTEP drawing of (a) 2a ; select bond lengths (Å): N(1)-C(1) 1.325(3), C(1)-Si(1) 1.885(2), C(12)-Si(2) 1.883(2), S(1)-C(1) 1.768(2), S(2)-C(4) 1.716(2), S(1)-C(3) 1.718(2), S(2)-C(12) 1.772(2), N(1)-C(2) 1.361(3), N(2)-C(2) 1.383(3), N(2)-C(5) 1.382(3), N(3)-C(5) 1.361(3), N(3)-C(12) 1.324(3); (b) 3a ; select bond lengths (Å): N(1)-C(1) 1.288(3), C(1)-Br(1) 1.875(3), C(12)-Br(2) 1.869(3), S(1)-C(1) 1.740(3), S(2)-C(4) 1.723(3), S(1)-C(3) 1.726(2), S(2)-C(12) 1.738(3), N(1)-C(2) 1.363(3), N(2)-C(2) 1.372(3), N(2)-C(5) 1.371(3), N(3)-C(5) 1.368(3), N(3)-C(12) 1.295(3). (50% Probability level, hydrogen atoms = drawn arbitrarily small)	39
Figure S33. ¹ H NMR spectrum of 2a	40
Figure S34. ¹ H NMR (400 MHz, CDCl ₃) spectrum (aliphatic region) of 2a	41

Figure S35. ^1H NMR (400 MHz, CDCl_3) spectrum of 2b	42
Figure S36. ^1H NMR (400 MHz, CDCl_3) spectrum (aliphatic region) of 2b	43
Figure S37. $^{13}\text{C}\{^1\text{H}\}$ NMR (100 MHz, CDCl_3) spectrum of 2b	44
Figure S38. $^{13}\text{C}\{^1\text{H}\}$ NMR (100 MHz, CDCl_3) spectrum (aliphatic region) of 2b	45
Figure S39. DEPT-135 NMR spectrum of 2b	46
Figure S40. DEPT-135 NMR spectrum (aliphatic region) of 2b	47
Figure S41. ^1H NMR (400 MHz, CDCl_3) spectrum of 3a	48
Figure S42. ^1H NMR (400 MHz, CDCl_3) spectrum (aliphatic region) of 3a	49
Figure S43. $^{13}\text{C}\{^1\text{H}\}$ NMR (100 MHz, CDCl_3) spectrum of 3a	50
Figure S44. DEPT-135 spectrum of 3a	51
Figure S45. ^1H NMR (400 MHz, CDCl_3) spectrum of 3b	52
Figure S46. ^1H NMR (400 MHz, CDCl_3) spectrum (aliphatic region) of 3b	53
Figure S47. $^{13}\text{C}\{^1\text{H}\}$ NMR (100 MHz, CDCl_3) spectrum of 3b	54
Figure S48. $^{13}\text{C}\{^1\text{H}\}$ NMR (100 MHz, CDCl_3) spectrum (aliphatic region) of 3b	55
Figure S49. $^{13}\text{C}\{^1\text{H}\}$ NMR (100 MHz, CDCl_3) spectrum (aliphatic region) of 3b	56
Figure S50. ^1H NMR (400 MHz, CDCl_3) spectrum of 5c (peak at 5.31 ppm belongs to residual CH_2Cl_2).	57
Figure S51. ^1H NMR (400 MHz, CDCl_3) spectrum (aliphatic region) of 5c	58
Figure S52. $^{13}\text{C}\{^1\text{H}\}$ NMR (100 MHz, CDCl_3) spectrum of 5c	59
Figure S53. $^{13}\text{C}\{^1\text{H}\}$ NMR (100 MHz, CDCl_3) spectrum (aromatic region) of 5c	60
Figure S54. $^{13}\text{C}\{^1\text{H}\}$ NMR (100 MHz, CDCl_3) spectrum (aliphatic region) of 5c	61
Figure S55. DEPT-135 spectrum of 5c	62
Figure S56. ^1H NMR (400 MHz, CDCl_3) spectrum of 5d (peak at 5.31 ppm belongs to residual CH_2Cl_2).	63
Figure S57. $^{13}\text{C}\{^1\text{H}\}$ NMR (100 MHz, CDCl_3) spectrum of 5d	64
Figure S58. $^{13}\text{C}\{^1\text{H}\}$ NMR (100 MHz, CDCl_3) spectrum (aromatic region) of 5d	65
Figure S59. $^{13}\text{C}\{^1\text{H}\}$ NMR (100 MHz, CDCl_3) spectrum (aliphatic region) of 5d	66
Figure S60. ^1H NMR (400 MHz, CDCl_3) spectrum of 6a	67
Figure S61. ^1H NMR (400 MHz, CDCl_3) spectrum (aromatic region) of 6a	68
Figure S62. ^1H NMR (400 MHz, CDCl_3) spectrum (aliphatic region) of 6a	69
Figure S63. ^1H NMR (400 MHz, CDCl_3) spectrum of 6b	71
Figure S64. ^1H NMR (400 MHz, CDCl_3) spectrum (aromatic region) of 6b	71
Figure S65. $^{13}\text{C}\{^1\text{H}\}$ NMR (100 MHz, CDCl_3) spectrum of 6b	72
Figure S66. ^1H NMR (400 MHz, CDCl_3) spectrum (340 K) of 6c	73
Figure S67. ^1H NMR (400 MHz, CDCl_3) spectrum (340 K; aliphatic region) of 6c	74
Figure S68. ^1H NMR (400 MHz, CDCl_3 , 340 K) spectrum of 6d	75
Figure S69. ^1H NMR (400 MHz, CDCl_3 , 340 K) spectrum of 6e	76
Figure S70. ^1H NMR (400 MHz, CDCl_3 , 340 K; aliphatic region) spectrum of 6e	77

Figure S71. ^1H NMR (400 MHz, CDCl_3) spectrum of 8a	78
Figure S72. ^1H NMR (400 MHz, CDCl_3) spectrum of 8b	79
Figure S73. ^1H NMR (400 MHz, CDCl_3) spectrum (aromatic region) of 8b	80
Figure S74. ^1H NMR (400 MHz, CDCl_3) spectrum (aliphatic region) of 8b	81
Figure S75. $^{13}\text{C}\{^1\text{H}\}$ NMR (100 MHz, CDCl_3) spectrum of 8b	82

General

Anhydrous tetrahydrofuran (THF) was obtained by the distillation from sodium benzophenone ketyl, anhydrous *N,N*-dimethylformamide (DMF) was purchased from EMD MILLIPORE, dichloromethane and toluene were dried by passing through columns of activated alumina (Brown solvent purification system), and chloroform was dried by the distillation from calcium hydride. 4,4'-Dibromo-2,2'-bis(triisopropylsilyl)-5,5'-bithiazole¹⁶ **1**, NID-tin reagents¹⁹ **4a**, **4b**, **5a**, **5b**, and 2,5-dibromo-7*H*-cyclopenta[1,2-*d*:4,3-*d'*]bis(thiazole)-7-one¹¹ **7** were prepared as described in the literature.

Characterization

Column chromatography purifications were performed using silica gel purchased from Sorbent Technologies (60 Å, 32–63 μm). ^1H and $^{13}\text{C}\{^1\text{H}\}$ NMR spectra were obtained on a Bruker AMX 400 MHz Spectrometer with chemical shifts referenced using the ^1H resonance of residual protonated solvent (CHCl_3 (7.27 ppm), 1,1,2,2-tetrachloroethane (6.00 ppm)); ^{13}C resonance of CDCl_3 at 77.00 ppm was used as a reference in $^{13}\text{C}\{^1\text{H}\}$ NMR spectra unless otherwise indicated. Electrochemical measurements were carried out under nitrogen in dry deoxygenated solution of 0.1 M tetrabutylammonium hexafluorophosphate in dichloromethane, tetrahydrofuran or chloroform using a CH Instrument Electrochemical Workstation #A2314 potentiostat and a conventional three-electrode cell with a glassy carbon working electrode, platinum wire counter electrode, and an Ag wire coated with AgCl as the pseudo-reference electrode. Potentials were referenced to ferrocenium/ferrocene by using ferrocene as an internal reference. Cyclic voltammograms were recorded at a scan rate of 50 mV s⁻¹. UV–vis spectra were recorded using a Varian Cary 5E spectrometer. Solution spectra were recorded in 1 cm cuvettes in dilute chloroform solution. DSC analysis was recorded using TA DSC Q200. Elemental analyses were performed by Atlantic Microlabs.

Device Fabrication

OFETs with bottom-contact and top-gate structure were fabricated on glass substrates (Eagle 2000 Corning). Au (50 nm) bottom contact source/drain electrodes were deposited by thermal evaporation through a shadow mask. Organic semiconductor layers were formed on the substrates by spin coating solution of **6a-c** (10 mg mL⁻¹), **6e** (2 mg mL⁻¹), **8a** (10 mg mL⁻¹) and **8b** (at 5 mg mL⁻¹) at 500 rpm for 10 s and at 2000 rpm for 20 s. These organic layers were annealed at 110 °C for 15 min (with exception of **6e**, which was annealed at 150 °C) on the hot plate inside a nitrogen glove box. CYTOP (45 nm)/Al₂O₃ (50 nm) bilayers was used as top gate dielectrics. CYTOP solution (CTL-809M) was purchased from Asahi Glass with a concentration of 9 wt%. To deposit the 45-nm-thick fluoropolymer layers, the original solution was diluted (CT-solv.180, Asahi glass) to give solution:solvent ratios of 1:3.5. CYTOP layers were deposited by spin coating at 3000 rpm for 60 s. Al₂O₃ (50 nm) films were deposited on fluoropolymer layers by atomic layer deposition at 110 °C using alternating exposures of AlMe₃ and H₂O vapor at a deposition rate of approximately 0.1 nm per cycle. All spin coating and

annealing processes were carried out in a N₂-filled dry box. Finally, Al (150 nm) gate electrodes were deposited by thermal evaporation through a shadow mask.

All current-voltage (I-V) characteristics of OFETs were measured with an Agilent E5272A source/monitor unit in a N₂-filled glove box (O₂, H₂O < 0.1 ppm).

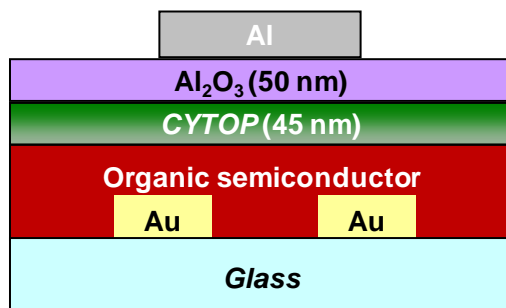


Figure S1. Device structure for top-gate bottom-contact organic field-effect transistor.

Device Characteristics

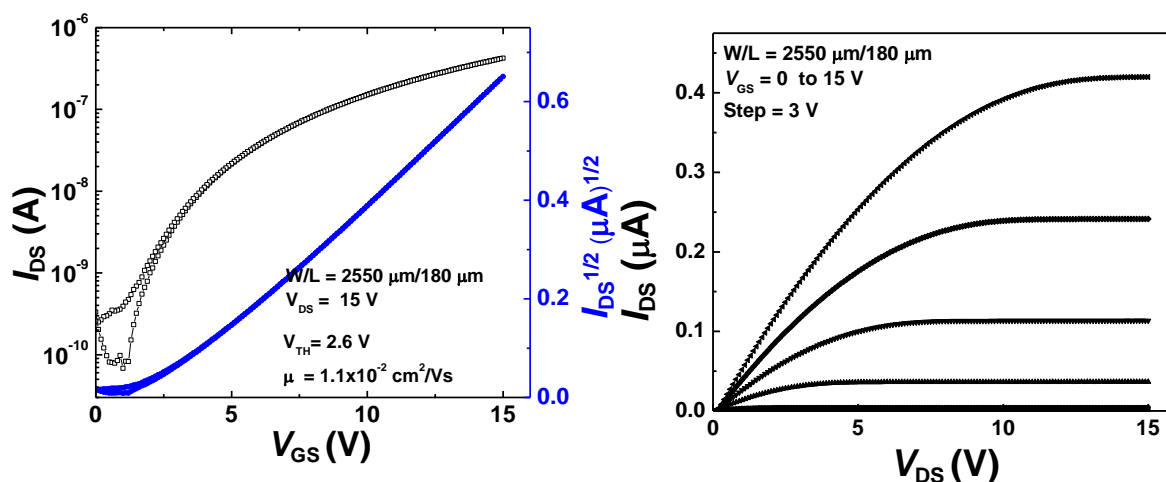


Figure S2. Transfer (*left*) and output (*right*) characteristics of a particular *n*-channel top-gate OFET with 6a semiconductor using chloroform solvent and CYTOP/Al₂O₃ gate dielectric layer with Au source / drain electrodes ($W/L = 2550 \mu m / 180 \mu m$).

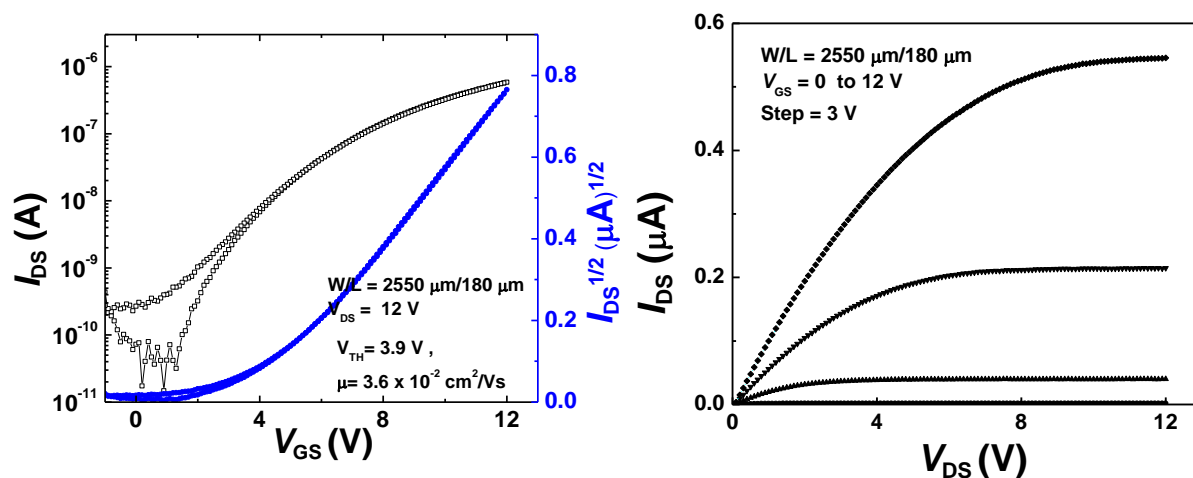


Figure S3. Transfer (*left*) and output (*right*) characteristics of a particular *n*-channel top-gate OFET with 6a semiconductor using chlorobenzene : chloroform (4:1) solvent and CYTOP/ Al_2O_3 gate dielectric layer with Au source / drain electrodes ($W/L = 2550 \mu\text{m} / 180 \mu\text{m}$).

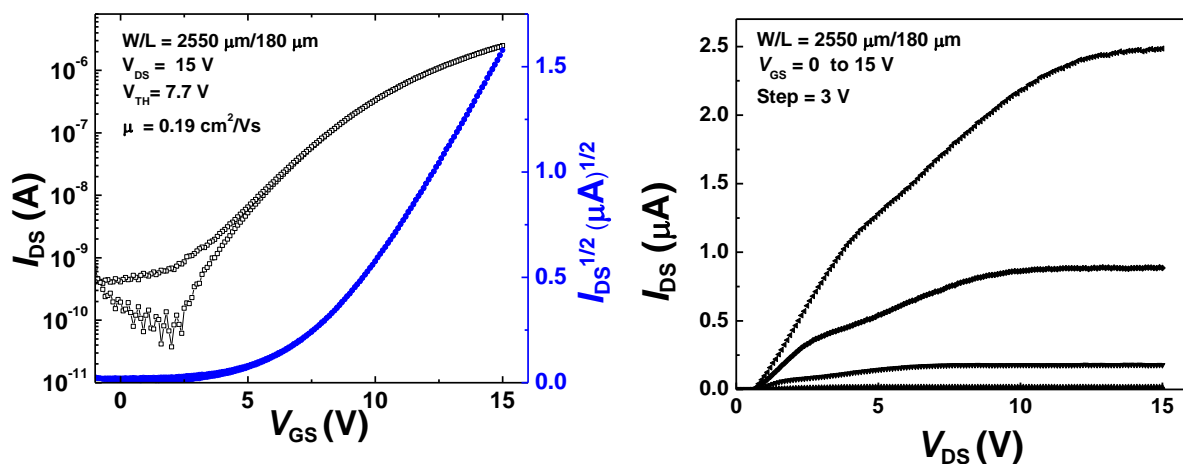


Figure S4. Transfer (*left*) and output (*right*) characteristics of a particular *n*-channel top-gate OFET with 6b semiconductor blended with PS using dichlorobenzene solvent and CYTOP/ Al_2O_3 gate dielectric layer with Au source / drain electrodes ($W/L = 2550 \mu\text{m} / 180 \mu\text{m}$).

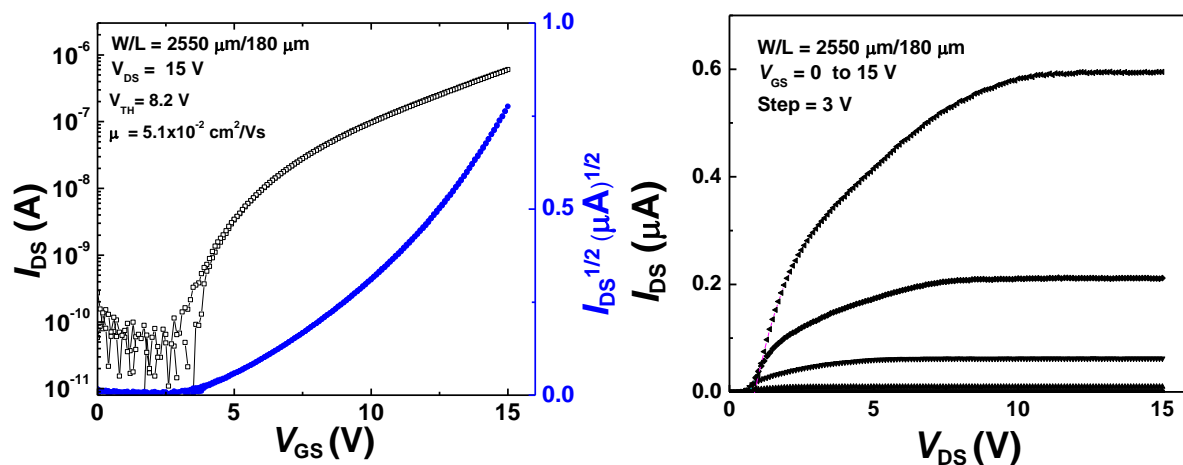


Figure S5. Transfer (*left*) and output (*right*) characteristics of a particular *n*-channel top-gate OFET with 6b semiconductor using 1,1,2,2-tetrachloroethane as a solvent and CYTOP/ Al_2O_3 gate dielectric layer with Au source / drain electrodes ($W/L = 2550 \mu\text{m} / 180 \mu\text{m}$).

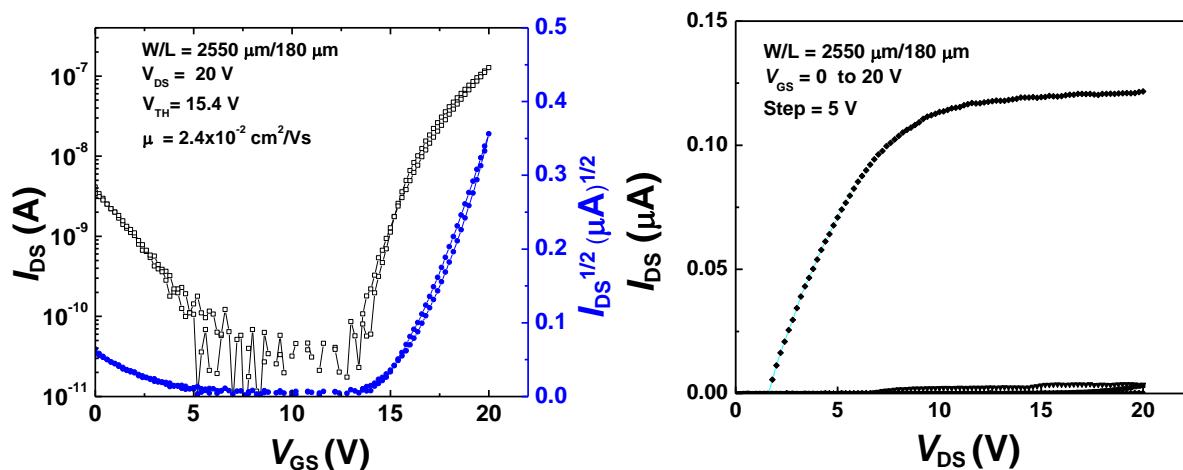


Figure S6. Transfer (*left*) and output (*right*) characteristics of a particular *n*-channel top-gate OFET with 6c semiconductor using 1,1,2,2-tetrachloroethane solvent and CYTOP/ Al_2O_3 gate dielectric layer with Au source / drain electrodes ($W/L = 2550 \mu\text{m} / 180 \mu\text{m}$).

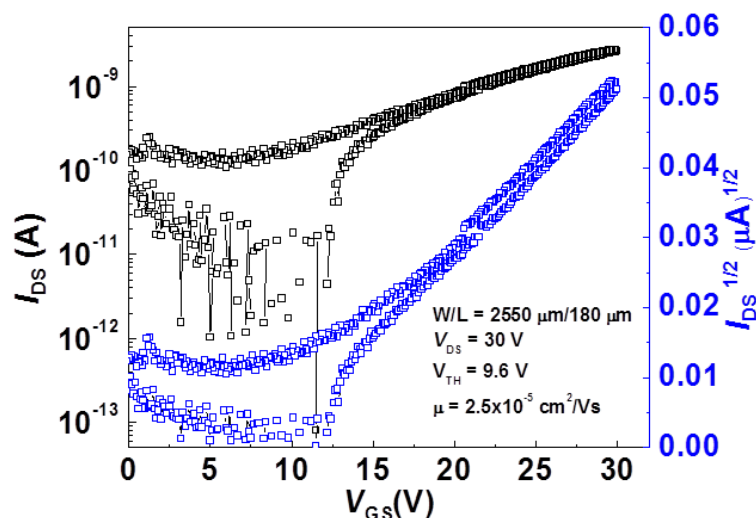


Figure S7. Transfer characteristics of a particular *n*-channel top-gate OFET with 6e semiconductor using chloroform solvent and CYTOP/Al₂O₃ gate dielectric layer with Au source / drain electrodes (*W/L*= 2550 μm / 180 μm).

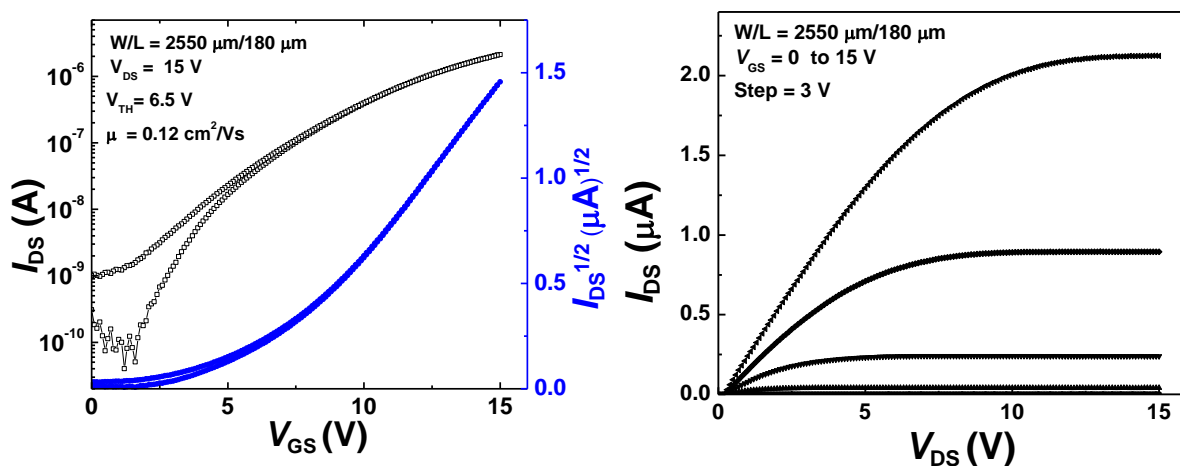


Figure S8. Transfer (*left*) and output (*right*) characteristics of a particular *n*-channel top-gate OFET with 8a semiconductor using 1,1,2,2-tetrachloroethane solvent and CYTOP/Al₂O₃ gate dielectric layer with Au source / drain electrodes (*W/L*= 2550 μm / 180 μm).

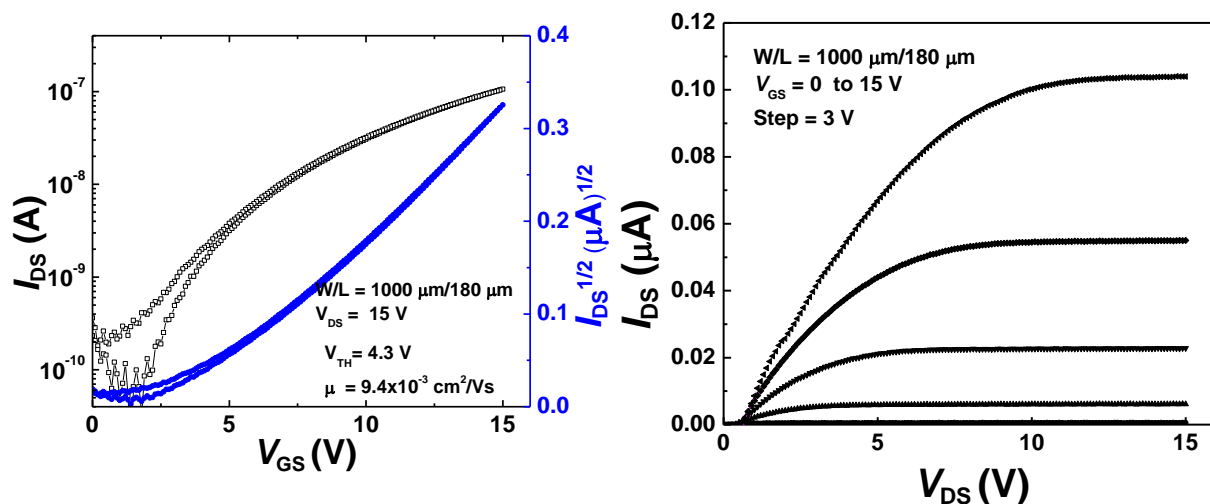


Figure S9. Transfer (*left*) and output (*right*) characteristics of a particular *n*-channel top-gate OFET with 8a semiconductor using dichlorobenzene as a solvent and CYTOP/ Al_2O_3 gate dielectric layer with Au source / drain electrodes ($W/L= 1000 \mu\text{m} / 180 \mu\text{m}$).

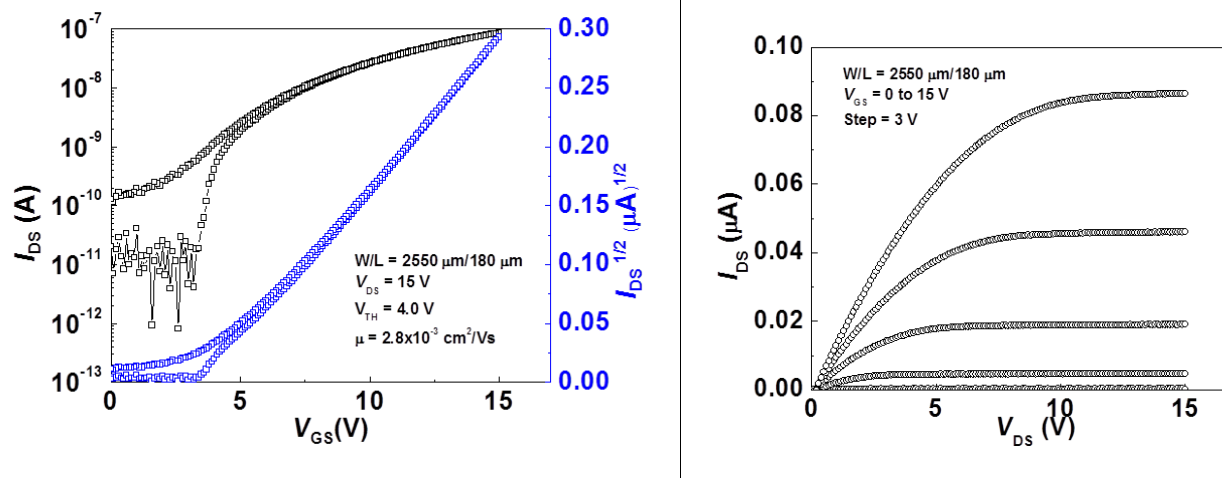


Figure S10. Transfer (*left*) and output (*right*) characteristics of a particular *n*-channel top-gate OFET with 8b semiconductor using 1,1,2,2-tetrachloroethane as a solvent and CYTOP/ Al_2O_3 gate dielectric layer with Au source / drain electrodes ($W/L= 1000 \mu\text{m} / 180 \mu\text{m}$).

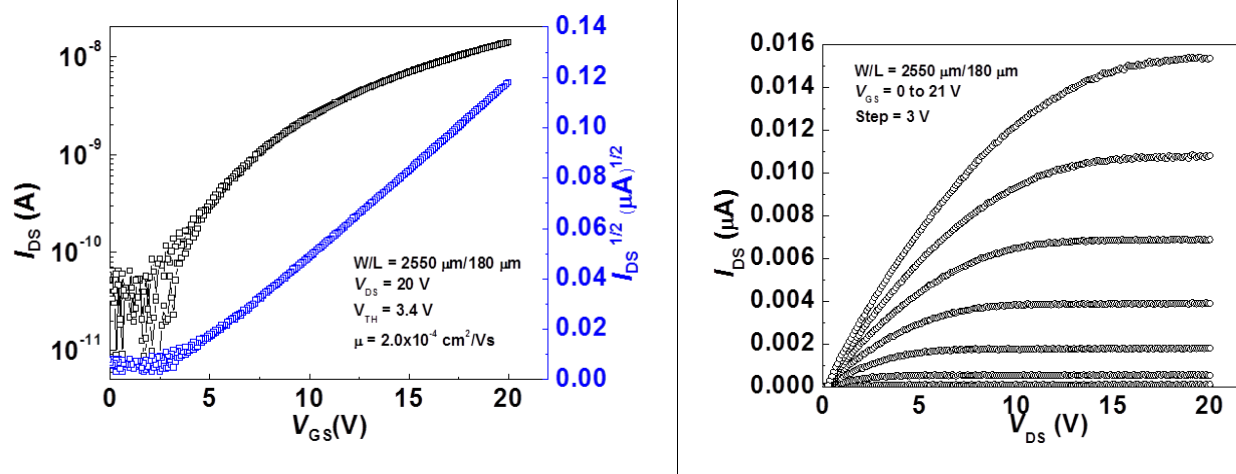


Figure S11. Transfer (left) and output (right) characteristics of a particular *n*-channel top-gate OFET with 8b semiconductor using 1,2-dichlorobenzene as a solvent and CYTOP/ Al_2O_3 gate dielectric layer with Au source / drain electrodes ($W/L= 1000 \mu\text{m} / 180 \mu\text{m}$).

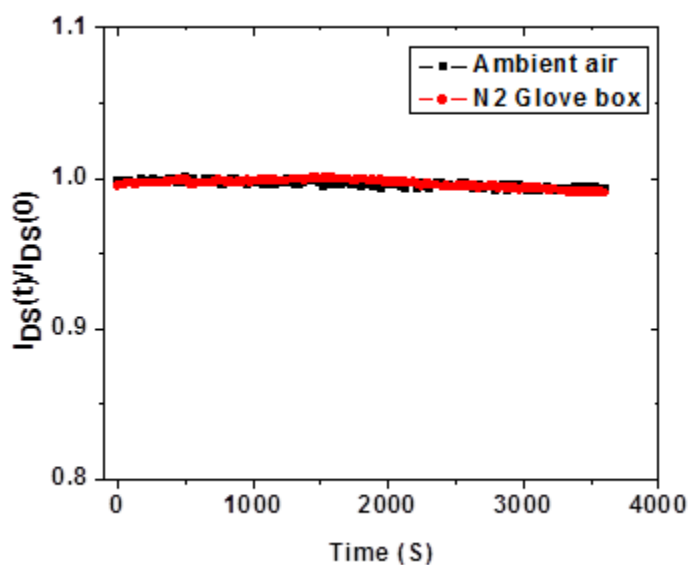


Figure S12. Continuous stress bias inside N_2 glove box and in ambient atmosphere for a particular *n*-channel top-gate OFET with 6a semiconductor.

Computational Methodology

Calculations for the (gas-phase) ground state neutral states were carried out at the density functional theory (DFT) level using generalized gradient approximation functional B3LYP in conjunction with a 6-31G** basis set (the *N*-alkyl group was replaced with methyl group to reduce the computational cost). All calculations were performed using the Spartan' 10 V1.1.0 software.

X-Ray Single Crystal Structural Analysis

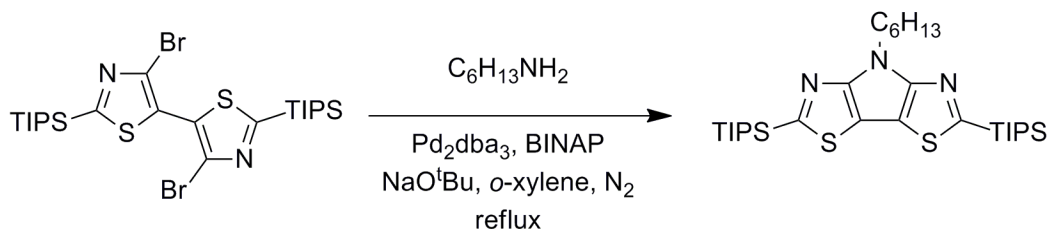
X-ray data collection for intermediates was performed with a Bruker-AXS SMART APEX CCD diffractometer using monochromatized Mo K α radiation ($\lambda = 0.71073$ Å) at 100K. Unit cell parameters were determined by least-squares analysis, and reflection data were integrated with the SAINT+ program using narrow-frame algorithm.¹ Lorentz and polarization corrections were applied. Absorption corrections were applied using the semiempirical method of the program SADABS.¹ The structures were solved by direct methods and refined using the Bruker SHELXTL programs suite² by full-matrix least-squares methods on F^2 with *SHELXL-97* in anisotropic approximation for all non-hydrogen atoms. Data reduction and further calculations were performed using the Bruker SAINT³ and SHELXTL NT⁴ program packages. All hydrogen atoms were placed in idealized positions and refined with constrained C-H distances and U_{iso} (H) values set to 1.2U_{eq} of the attached C atom. Selected refinement data and structure parameters, are shown in Table 1. Complete crystallographic data are also provided in CIF format.

Table S1. Crystallographic data for 4-hexyl-2,6-bis(triisopropylsilyl)-4*H*-pyrrolo[2,3-*d*:5,4-*d'*]bisthiazole (2a) and 2,6-dibromo-4-hexyl-4*H*-pyrrolo[2,3-*d*:5,4-*d'*]bisthiazole (3a)

	2a	3a
Empirical formula	C ₃₀ H ₅₅ N ₃ S ₂ Si ₂	C ₁₂ H ₁₃ Br ₂ N ₃ S ₂
FW	578.07	423.19
T, K	100(2) K	100(2) K
Crystal system	Triclinic	Monoclinic
Space group	P-1	P 21/n
<i>a</i> , Å	7.985(5)	8.318(6)
<i>b</i> , Å	11.898(7)	19.024(12)
<i>c</i> , Å	20.220(11)	10.557(7)
α , deg.	73.605(12)	90
β , deg.	78.698(12)	108.030(10)
γ , deg.	74.512(12)	90
<i>V</i> , Å ³	1760.70(17)	1588.57(19)
<i>Z</i>	2	4
<i>d</i> _c , g × cm ⁻³	1.090	1.769
<i>F</i> (000)	632	832
μ , mm ⁻¹	0.241	5.355
2 θ max, deg.	50	54
Index ranges	-9 ≤ <i>h</i> ≤ 9 -14 ≤ <i>k</i> ≤ 14 -24 ≤ <i>l</i> ≤ 24	-10 ≤ <i>h</i> ≤ 10 -24 ≤ <i>k</i> ≤ 24 -13 ≤ <i>l</i> ≤ 13
No. of Reflections collected	15576	16405
No. of Unique reflections	6192	3483
Data / restraints / parameters	6192 / 0 / 334	3483 / 0 / 172
GOF on F^2	1.015	1.027
<i>R</i> ₁ ; <i>wR</i> ₂ (<i>I</i> > 2 σ (<i>I</i>))	0.0428, 0.1059	0.0261, 0.0643
<i>R</i> ₁ ; <i>wR</i> ₂ (all data)	0.0687, 0.1166	0.0374, 0.0675
Largest diff. peak and hole e.Å ⁻³	0.278 and -0.178 e.Å ⁻³	0.433 and -0.378 e.Å ⁻³

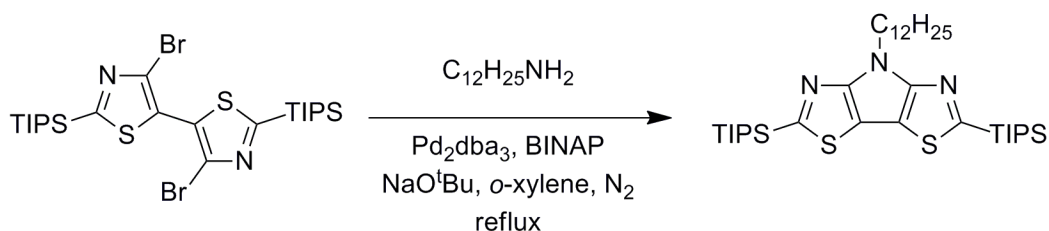
Synthetic Details

4-Hexyl-2,6-bis(triisopropylsilyl)-4*H*-pyrrolo[2,3-*d*:5,4-*d'*]bisthiazole (2a)



4,4'-Dibromo-2,2'-bis(triisopropylsilyl)-5,5'-bisthiazole (**1**) (4.00 mmol, 2.55 g), $Pd_2(dba)_3$ (10 mol%, 0.40 mmol, 0.37 g), BINAP (0.80 mmol, 0.50 g), and NaO^tBu (19.2 mmol, 1.85 g) were mixed in an oven-dried flask under nitrogen atmosphere, mesitylene (dried over molecular sieves, 20 mL) was added, followed by the addition of hexylamine (4.00 mmol, 0.40 g). The reaction mixture was heated to reflux for 3 h, cooled to room temperature, treated with water, and organic phase was extracted with diethyl ether and hexanes. The combined organic phases were dried over anhydrous $MgSO_4$, volatile solvents were removed by rotary evaporation, and the dark brown solution was applied to the silica gel column (silica gel, hexanes:dichloromethane (4:1) as eluent). The first fractions containing pure product were combined, the solvents were removed, and product was obtained as yellowish oil (~50-100 mg). A later fraction containing majority of the product (slightly contaminated) was subjected to rotary evaporation, and solid was obtained (0.30 g, 13% yield; this material was used in the next step without further purification; analytically pure compound can be obtained by recrystallization from ethanol). A few mgs of this material left on the sides of the flask were dissolved in ethanol under reflux, and yellowish solution was cooled on a cork ring. Yellowish crystals suitable for the single crystal X-ray structural analysis were obtained. This material was obtained in slightly better yield of 30.7% (0.55 g) during the 2nd run (3.1 mmol of **1**). 1H NMR (400 MHz, $CDCl_3$): δ 4.62 (t, $J = 6.7$ Hz, 2H), 2.05 (m, 2H), 1.48 (heptet, $J = 7.6$ Hz, 6H), 1.31 (m, 4H), 1.25 (m, 2H), 1.18 (d, $J = 7.4$ Hz, 34H observed; 36H expected; this peak overlaps with signal at 1.25 ppm), 0.83 (t, $J = 7.1$ Hz, 3H). HRMS (EI) calculated for $C_{30}H_{55}N_3S_2Si_2$ 577.3376; found 577.3362. Anal. Calcd. for $C_{30}H_{55}N_3S_2Si_2$: C, 62.33; H, 9.59; N, 7.27. Found: C, 62.34; H, 9.49; N, 7.16.

4-Dodecyl-2,6-bis(triisopropylsilyl)-4*H*-pyrrolo[2,3-*d*:5,4-*d'*]bisthiazole (2b)



4,4'-Dibromo-2,2'-bis(triisopropylsilyl)-5,5'-bisthiazole (**1**) (5.00 mmol, 3.19 g), $Pd_2(dba)_3$ (10 mol%, 0.5 mmol, 0.46 g), BINAP (1.00 mmol, 0.62 g), and NaO^tBu (4.8 eq., 24.0 mmol, 2.31 g) were mixed in an oven-dried flask under nitrogen atmosphere, mesitylene (dried over molecular sieves, 20 mL) was added, followed by the addition of dodecylamine (5.00 mmol, 0.93 g). The reaction mixture was heated to reflux overnight, cooled to room temperature, treated with water, and the organic phase was extracted

with diethyl ether and hexanes. The combined organic phases were dried over anhydrous magnesium sulfate, the volatile solvents were removed by rotary evaporation, and the residue was applied to the silica gel column (hexanes:dichloromethane (1:4) as eluant). Fractions containing the product were combined, the solvents were removed, and the residue was dried under vacuum with heating. The product was obtained as very thick yellow-orange oil (1.76 g, 53.2% yield). This material solidified after being transferred to the vial. ^1H NMR (400 MHz, CDCl_3): δ 4.63 (t, $J = 6.7$ Hz, 2H), 2.06 (m, 2H), 1.55-1.42 (m, 6H), 1.39-1.26 (m, 6H), 1.26-1.13 (m, 48H), 0.88 (t, $J = 6.9$ Hz, 3H); $^{13}\text{C}\{^1\text{H}\}$ NMR (100 MHz, CDCl_3): δ 166.40, 158.50, 106.66, 45.32 (CH_2), 31.92 (CH_2), 29.81 (CH_2), 29.68 (CH_2), 29.65 (CH_2), 29.63 (CH_2), 29.47 (CH_2), 29.36 (CH_2), 29.14 (CH_2), 26.77 (CH_2), 22.69 (CH_2), 18.57 (CH_3), 14.12 (CH), 11.77 (CH_3). HRMS (EI) calculated for $\text{C}_{36}\text{H}_{67}\text{N}_3\text{S}_2\text{Si}_2$ 661.4315; found 661.4330. Anal. Calcd. for $\text{C}_{36}\text{H}_{67}\text{N}_3\text{S}_2\text{Si}_2$: C, 65.29; H, 10.20; N, 6.35. Found: C, 65.53; H, 10.02; N, 6.22.

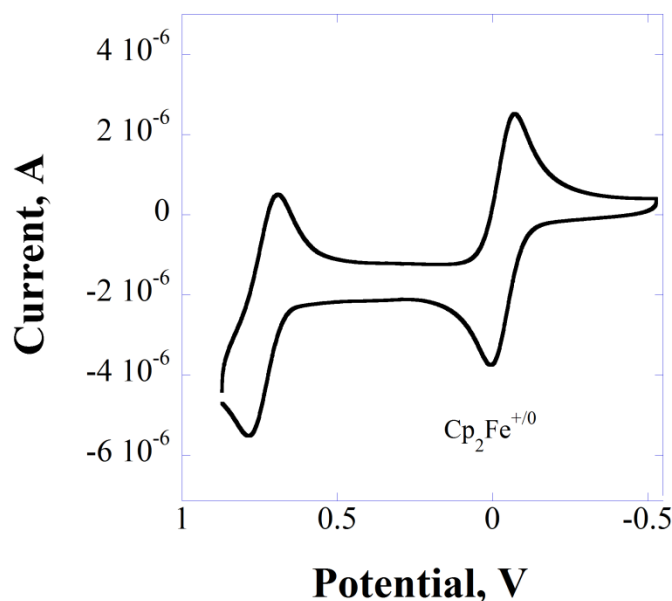
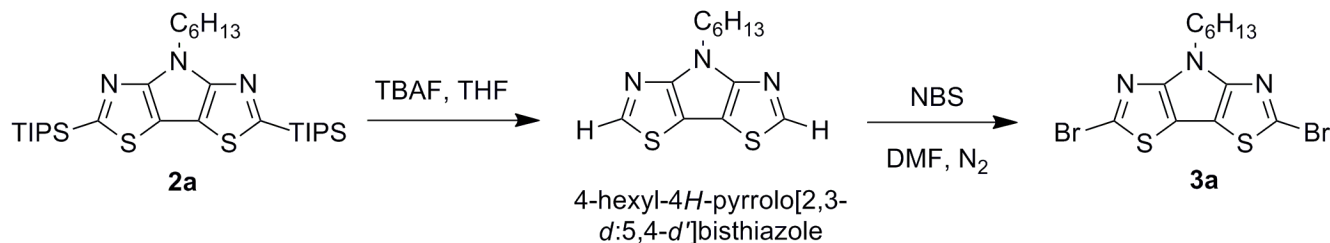


Figure S13. CV of 4-dodecyl-2,6-bis(triisopropylsilyl)-4H-pyrrolo[2,3-d:5,4-d']bisthiazole (**2b**) in 0.1 M Bu_4PF_6 in dichloromethane: $E_{1/2}^{0/+} = +0.77$ V.

2,6-Dibromo-4-hexyl-4H-pyrrolo[2,3-d:5,4-d']bisthiazole (**3a**)



4-Hexyl-2,6-bis(triisopropylsilyl)-4H-pyrrolo[2,3-d:5,4-d']bisthiazole (**2a**) (0.52 mmol, 0.30 g) was dissolved in anhydrous THF under nitrogen atmosphere, and TBAF (1.0 M in THF, 2.1 eq., 1.09 mmol, 1.1 mL) was added to a yellowish solution. The yellow reaction mixture was stirred for ~1-2 h, analyzed by TLC, and a more polar spot was detected. The reaction mixture was treated with water, diethyl ether was added, and organic phase (yellow) was removed. The aqueous phase was extracted with diethyl

ether, the combined organic phases were dried over anhydrous MgSO_4 , the drying agent was filtered off, and the solvents were removed by rotary evaporation. The residue was dried under vacuum, and then used in the next step without further purification (4-hexyl-4*H*-pyrrolo[2,3-*d*:5,4-*d'*]bisthiazole: ^1H NMR (400 MHz, CDCl_3): δ 8.61 (s, 2H), 4.58 (t, $J = 7.3$ Hz, 2H), 2.03 (m, 2H), 1.43-1.23 (m, 6H), 0.84 (t, 3H); HRMS (EI) calculated for $\text{C}_{12}\text{H}_{15}\text{N}_3\text{S}_2$ 265.0707; found 265.0709).

4-Hexyl-4*H*-pyrrolo[2,3-*d*:5,4-*d'*]bisthiazole ([0.50] mmol) was mixed with anhydrous dimethylformamide (5 mL), and *N*-bromosuccinimide (1.025 mmol, 0.182 g) was added to yellow solution. The reaction mixture was stirred for ~1 h, and reddish reaction mixture was treated with water. The organic matter was extracted with hexanes several times, combined organic phases were dried over anhydrous magnesium sulfate, the drying agent was filtered off, and the solvents were removed by rotary evaporation. The residue (pinkish solid) was heated to reflux with ~10-15 mL of ethanol, and the resulting yellowish solution was cooled to room temperature. Yellowish crystals were separated by vacuum filtration (0.135 g, 64.3% yield for two steps). ^1H NMR (400 MHz, CDCl_3): δ 4.45 (t, $J = 7.4$ Hz, 2H), 1.95 (m, 2H), 1.40-1.25 (m, 6H), 0.88 (t, $J = 7.0$ Hz, 3H); $^{13}\text{C}\{^1\text{H}\}$ NMR (100 MHz, CDCl_3): δ 150.06, 132.03, 106.54, 45.65 (CH_2), 31.26, 29.95 (CH_2), 26.29 (CH_2), 22.50 (CH_2), 13.95 (CH_3). HRMS (EI) calculated for $\text{C}_{12}\text{H}_{13}\text{Br}_2\text{N}_3\text{S}_2$ 420.8918; found 420.8908. Anal. Calcd. for $\text{C}_{12}\text{H}_{13}\text{Br}_2\text{N}_3\text{S}_2$: C, 34.06; H, 3.10; N, 9.93. Found: C, 34.31; H, 3.14; N, 10.05.

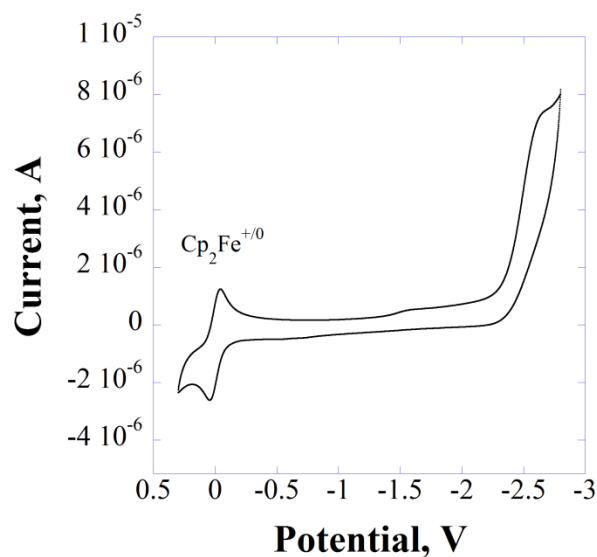
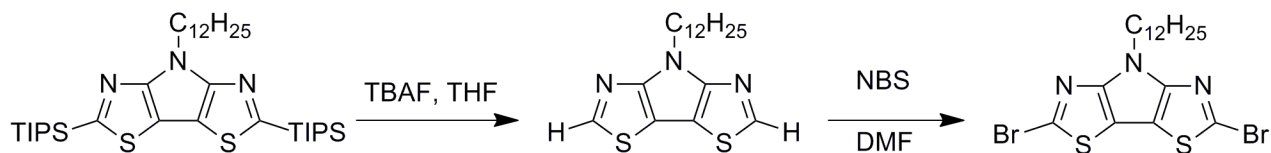


Figure S14. Cyclic voltammetry of 2,6-dibromo-4-hexyl-4*H*-pyrrolo[2,3-*d*:5,4-*d'*]bisthiazole (3a) in 0.1 M Bu_4NPF_6 in tetrahydrofuran vs. $\text{Cp}_2\text{Fe}^{+/0}$: $E_{pc} = -2.5$ V.

DSC analysis (10 $^\circ\text{C}/\text{min}$ heating-cooling rate): 92.4 $^\circ\text{C}$ (m.p.) (1st cycle). Endothermic peak at 30.6 $^\circ\text{C}$ (crystallization) was observed during the 2nd heating, followed by the endothermic peak at 103.0 $^\circ\text{C}$ (melting).

2,6-Dibromo-4-dodecyl-4*H*-pyrrolo[2,3-*d*:5,4-*d'*]bisthiazole (3b)



4-Dodecyl-2,6-bis(triisopropylsilyl)-4*H*-pyrrolo[2,3-*d*:5,4-*d'*]bisthiazole (**2b**) (2.66 mmol, 1.76 g) was dissolved in anhydrous THF (30 mL) under nitrogen atmosphere. TBAF (1.0 M in THF, 2.1 eq., 5.59 mmol, 5.6 mL) was added dropwise, and the yellowish solution became orange-yellow. The mixture was stirred for 5 minutes, water was added, and the solvent was removed by rotary evaporation. The organic matter was extracted with hexanes, dried over anhydrous magnesium sulfate, the drying agent was filtered off, and the solvent was removed by rotary evaporation. The crude product was obtained as yellow-orange oil and was used in the next step without purification (1.7 g, contains some residual solvent; HRMS (EI) calculated for 4-dodecyl-4*H*-pyrrolo[2,3-*d*:5,4-*d'*]bisthiazole C₁₈H₂₇N₃S₂ 349.1646; found: 349.1642). This material was dissolved in anhydrous DMF (10 mL), and *N*-bromosuccinimide (2.1 eq., 5.59 mmol, 0.99 g) was added at room temperature (nitrogen atmosphere). The reaction mixture became red, and after stirring for ~1-2 hours it was treated with water. The organic matter was extracted with hexanes several times, the combined organic phases were dried over anhydrous magnesium sulfate, the drying agent was filtered off, and the solvent was removed by rotary evaporation. The crude product (pink-red oil) was purified by column chromatography (silica gel, hexanes:dichloromethane (1:1) as eluant). The solvents were removed from combined barely yellowish fractions, the residue (yellowish thick oil) was dried under vacuum, and after storage in the freezer (-20 °C) the product was obtained as yellowish solid (0.98 g, 75.6% yield for two steps). ¹H NMR (400 MHz, CDCl₃): δ 4.45 (t, *J* = 7.3 Hz, 2H), 1.96 (m, 2H), 1.40-1.20 (m, 18H), 0.89 (t, *J* = 6.9 Hz, 3H); ¹³C{¹H} NMR (100 MHz, CDCl₃): δ 150.09, 132.03, 106.55, 45.65 (CH₂), 31.95 (CH₂), 29.95 (CH₂), 29.61 (two overlapping signals, CH₂), 29.52 (CH₂), 29.46 (CH₂), 29.33 (CH₂), 29.07 (CH₂), 26.61 (CH₂), 22.68 (CH₂), 14.15 (CH₃). HRMS (EI) calculated for C₁₈H₂₅Br₂N₃S₂ 504.9857; found 504.9848. Anal. Calcd. for C₁₈H₂₅Br₂N₃S₂: C, 42.61; H, 4.97; N, 8.28. Found: C, 42.62; H, 4.95; N, 8.27.

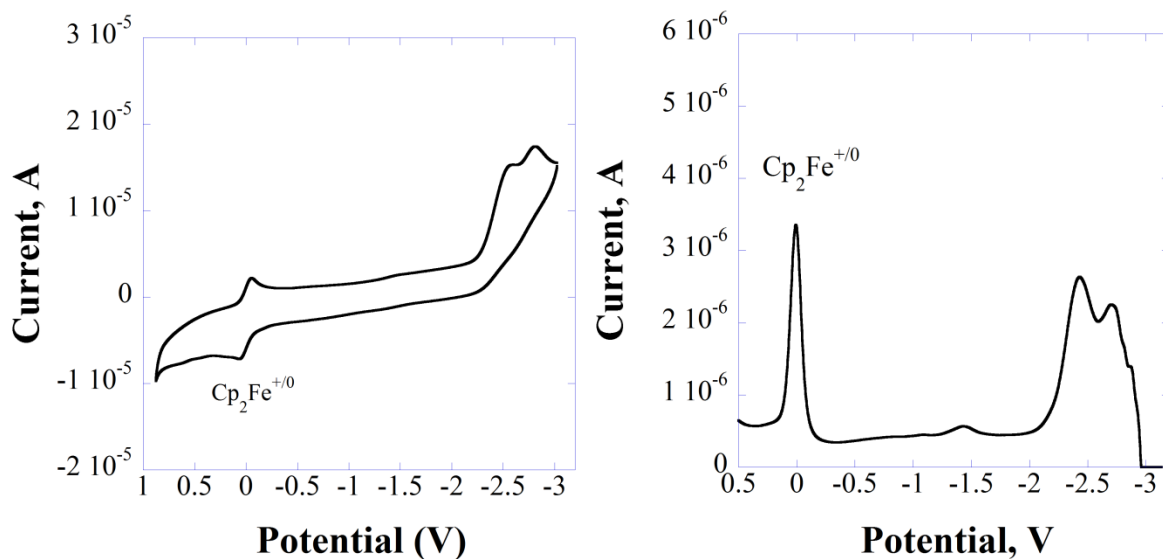
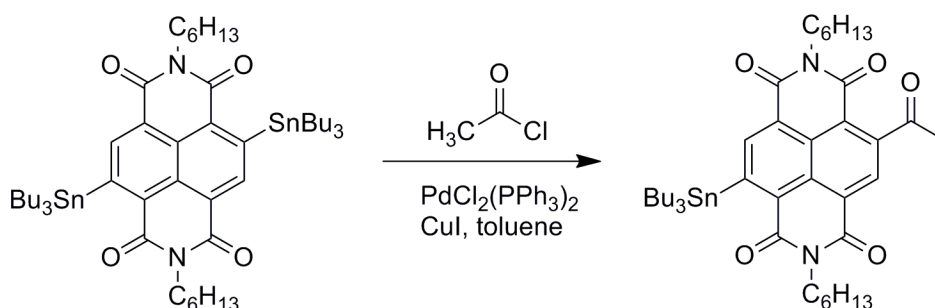


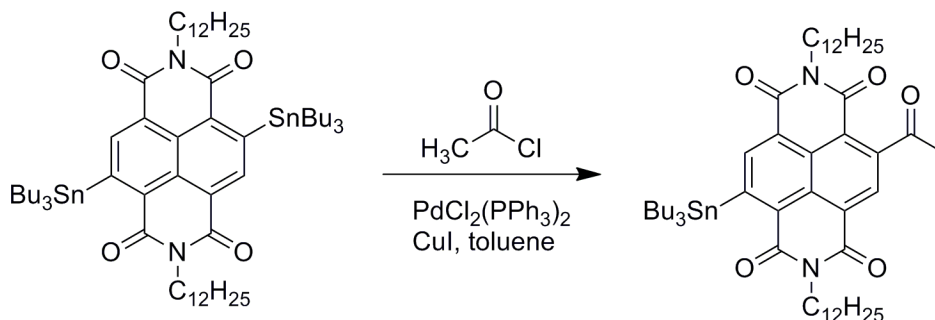
Figure S15. 2,6-Dibromo-4-dodecyl-4*H*-pyrrolo[2,3-*d*:5,4-*d'*]bisthiazole (**3b**) (0.1 M Bu₄NPF₆ in tetrahydrofuran vs. Cp₂Fe⁺⁰): (left) CV : *E*_{pc} = -2.4 V; one more peak was observed with *E*_{pc} = -2.8 V; (right) DPV (0.1 M Bu₄NPF₆ in tetrahydrofuran vs. Cp₂Fe⁺⁰): *E*_{1/2}^{0/-} = -2.44 V, *E*_{1/2}⁻²⁻ = -2.71 V.

4-Acetyl-2,7-dihexyl-9-(tributylstannyl)benzo[*lmn*][3,8]phenanthroline-1,3,6,8(2*H*,7*H*)-tetraone (5c)



2,7-Dihexyl-4,9-bis(tributylstannyl)benzo[*lmn*][3,8]phenanthroline-1,3,6,8(2*H*,7*H*)-tetraone (**4a**) (3.00 mmol, 3.04 g), PdCl₂(PPh₃)₂ (5 mol%, 0.150 mmol, 0.105 g), CuI (0.025 mol%, 0.075 mmol, 14 mg), and anhydrous toluene (30 mL) were mixed in the oven-dried flask under nitrogen atmosphere, acetyl chloride (1.0 eq., 3.00 mmol, 0.24 g) was added, and the mixture was stirred at mild reflux for ~ 1 h. The orange-yellow solution became greenish, the reaction mixture was cooled to room temperature, and applied to the top of the chromatographic column (~150 mL of silica gel, dichloromethane as eluant). Some unreacted starting material eluted first, followed by the desired product **5c** (slightly contaminated), which was further purified (~100 mL of silica gel treated with triethylamine (~0.5 mL), dichloromethane as eluant). The solvent was removed from the combined fractions, and the residue (yellow-orange oil) was dried under vacuum (the material solidified on standing, 0.93 g, 40.4%). More polar byproduct (presumably the diacetyl derivative) was also observed. ¹H NMR (400 MHz, CDCl₃): δ 9.04 (s with satellites, 1H), 8.46 (s, 1H), 4.22 (t, *J* = 7.4 Hz, 2H), 4.15 (t, *J* = 7.8 Hz, 2H), 2.69 (s, 3H), 1.72 (m, 4H), 1.64 (m, 2H), 1.58-1.49 (m, 6H), 1.48-1.28 (m, 16H expected, 25H observed) 1.28-1.21 (m, 6H), 0.93 (t, *J* = 7.3 Hz, 6H), 0.88 (t, *J* = 7.3 Hz, 13H observed, 15H expected). ¹³C{¹H} NMR (100 MHz, CDCl₃): δ 202.99, 164.64, 163.13, 162.8, 162.38, 157.00, 145.71, 139.68 (CH), 131.65, 127.37 (CH), 12.78, 126.38, 126.30, 123.62, 122.19, 41.10 (CH₂), 31.46 (CH₂), 30.71 (CH₃), 29.19 (CH₂), 27.98 (CH₂), 27.83 (CH₂), 27.38 (CH₂), 26.84 (CH₂), 26.75 (CH₂), 26.60 (CH₂), 22.55 (CH₂), 22.47 (CH₂), 17.50 (CH₂), 14.01 (CH₃), 13.69 (CH₃), 13.60 (CH₃), 11.61 (CH₂). HRMS (MALDI-TOF) calculated for (C₄₀H₅₈N₂O₅Sn+1H) 767.3446; found 767.3414. Anal. Calcd. for C₄₀H₅₈N₂O₅Sn: C, 62.75; H, 7.64; N, 3.66. Found: 62.93; H, 7.58; N, 3.70.

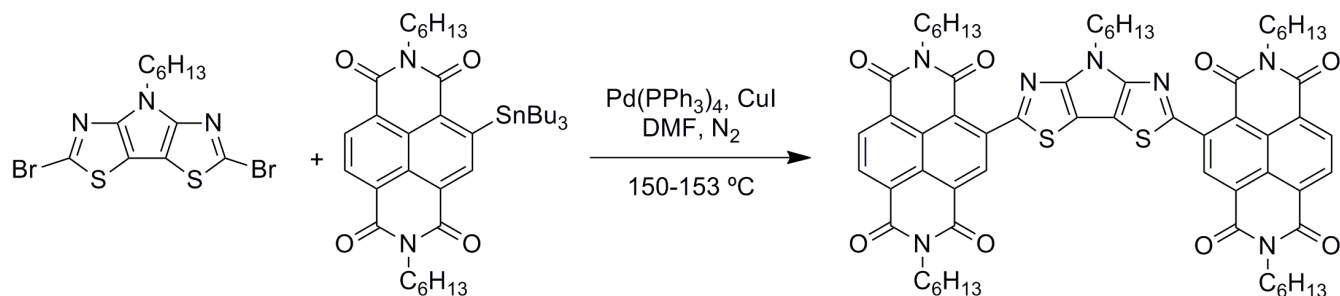
4-Acetyl-2,7-didodecyl-9-(tributylstannyl)benzo[*lmn*][3,8]phenanthroline-1,3,6,8(2*H*,7*H*)-tetraone (5d)



2,7-Didodecyl-4,9-bis(tributylstannyl)benzo[*lmn*][3,8]phenanthroline-1,3,6,8(2*H*,7*H*)-tetraone (**4b**) (1.78 mmol, 2.10 g), PdCl₂(PPh₃)₂ (5 mol%, 0.089 mmol, 0.065 g), CuI (0.025 mol%, 0.045 mmol, 8 mg), and anhydrous toluene (20 mL) were mixed in the oven-dried flask under nitrogen atmosphere, acetyl chloride (1.1 eq., 1.96 mmol, 0.16 g) was added, and the mixture was stirred at mild reflux for ~ 1 h. The brown-yellow mixture became yellowish-greenish in color, and it was cooled to room temperature and applied to the top of the chromatographic column (~100 mL of silica gel treated with triethylamine, dichloromethane as eluant). The fractions with the desired product were combined, the

solvent was removed by rotary evaporation, and the residue yellow-orange oil) was further purified by column chromatography twice (silica gel treated with triethylamine, dichloromethane:hexanes (1:1) as eluent). The product was obtained as yellow-orange thick oil (0.42 g, 25%), which solidified on standing. ^1H NMR (400 MHz, CDCl_3): δ 9.04 (s with satellites, 1H), 8.46 (s, 1H), 4.22 (t, $J = 7.3$ Hz, 2H), 4.15 (t, $J = 7.6$ Hz, 2H), 2.69 (s, 3H), 1.72 (m, 4H), 1.54 (m, 6H), 1.45-1.20 (m, 48H), 0.88 (t, $J = 7.2$ Hz, 15H). $^{13}\text{C}\{^1\text{H}\}$ NMR (100 MHz, CDCl_3): δ 202.98, 164.64, 163.13, 162.78, 162.38, 157.00, 145.71, 139.68 (CH), 131.65, 127.37 (CH), 126.78, 126.38, 126.38, 126.30, 123.62, 122.19, 41.10 (CH_2), 31.90 (CH_2), 30.71 (CH_3), 29.61 (CH_2), 29.56(CH_2), 29.53 (CH_2), 29.47 (CH_2), 29.33 (CH_2), 29.30 (CH_2), 29.19 (CH_2), 28.03 (CH_2), 27.38 (CH_2), 27.11 (CH_2), 26.96 (CH_2), 22.67 (CH_2), 14.10 (CH_3), 13.70 (CH_2), 11.61 (CH_2). HRMS (MALDI-TOF) calculated for ($\text{C}_{52}\text{H}_{82}\text{N}_2\text{O}_5\text{Sn}+1\text{H}$) 935.5324; found 935.5330. Anal. Calcd. for $\text{C}_{52}\text{H}_{82}\text{N}_2\text{O}_5\text{Sn}$: C, 66.87; H, 8.85; N, 3.00. Found: 67.07; H, 8.94; N, 3.02.

4,4'-(4-Hexyl-4H-pyrrolo[2,3-d:5,4-d']bis(thiazole)-2,6-diyl)bis(2,7-dihexylbenzo[lmn][3,8]phenanthroline-1,3,6,8(2H,7H)-tetraone) (6a)



2,6-Dibromo-4-hexyl-4H-pyrrolo[2,3-d:5,4-d']bisthiazole (**3a**) (0.270 mmol, 0.114 g), 2,7-dihexyl-4-(tributylstannyl)benzo[lmn][3,8]phenanthroline-1,3,6,8(2H,7H)-tetraone (0.820 mmol, 0.593 g), $\text{Pd}(\text{PPh}_3)_4$ (20 mol%, 0.080 mmol, 0.092 g) and CuI (10 mol%, 0.040 mmol, 0.008 g) were mixed in an oven-dried flask under nitrogen atmosphere. Anhydrous DMF (10 mL) was added, and the orange mixture was heated to reflux. A blue precipitate formed, and after a few minutes the reaction mixture was cooled to room temperature, treated with water, a dark precipitate was separated by vacuum filtration, washed with water, ethanol, and dried (236 mg, 77.4% crude yield). This crude product was purified by column chromatography (~100 mL of silica gel, dichloromethane as eluant first, then dichloromethane:ethyl acetate, then chloroform:ethyl acetate (20:1) to elute the product. All fractions containing the product were combined (some impurities were still evident by TLC), the solvents were removed by rotary evaporation, and the residue was purified by column chromatography (silica gel treated with triethylamine, chloroform as eluant). Very dilute blue fractions containing product eluted first. Chloroform:ethyl acetate (~10:1) eluted the product, the fractions were combined, the solvents were removed, and the purified material was obtained (120 mg, 26.5% purified yield). This product was further purified (silica gel treated with triethylamine, chloroform first, then chloroform:ethyl acetate (100:1, then 30:1)). Elution with chloroform led to separation of a pinkish impurity. A small amount of a less polar green impurity was also separated, but some of the product was still contaminated with it. The fractions containing the product were combined, the solvents were removed by rotary evaporation, and the residue was purified (silica gel treated with triethylamine, chloroform to pack the column and load the sample, chloroform:ethyl acetate (30:1, then 20:1) to elute the product). The first two fractions containing the product contaminated with less polar impurity were kept separately, fractions containing the pure product were combined, the solvents were removed, and the residue was heated to reflux with ethyl acetate (~25 mL, HPLC grade). The mixture was cooled to room temperature, and the dark solid was separated by vacuum filtration, and then dried under vacuum (106 mg, 45% recovery, 35% purified yield). ^1H NMR (400 MHz, CDCl_3): δ 9.12 (s, 2H), 8.86 (d, $J = 7.6$ Hz, 2H), 8.81 (d, $J = 7.6$ Hz, 2H),

4.65 (t, $J = 7.2$ Hz, 2H), 4.24 (t, $J = 7.6$ Hz, 4H), 4.15 (t, $J = 7.7$ Hz, 4H), 2.12 (m, 2H), 1.82-1.66 (m, 8H), 1.51-1.28 (m, 30H), 0.95-0.83 (m, 15H). $^{13}\text{C}\{^1\text{H}\}$ NMR (100 MHz, 1,2-dichloroethane- d_4 , 300 K) was attempted, but the material is not sufficiently soluble to record a spectrum with acceptable signal to noise. HRMS (EI) calculated for ($\text{C}_{64}\text{H}_{71}\text{N}_7\text{O}_8\text{S}_2+\text{H}$) 1130.4884; found 1130.4867. Anal. Calcd. for $\text{C}_{64}\text{H}_{71}\text{N}_7\text{O}_8\text{S}_2$: C, 68.00; H, 6.33; N, 8.67. Found: C, 68.06; H, 6.28; N, 8.72.

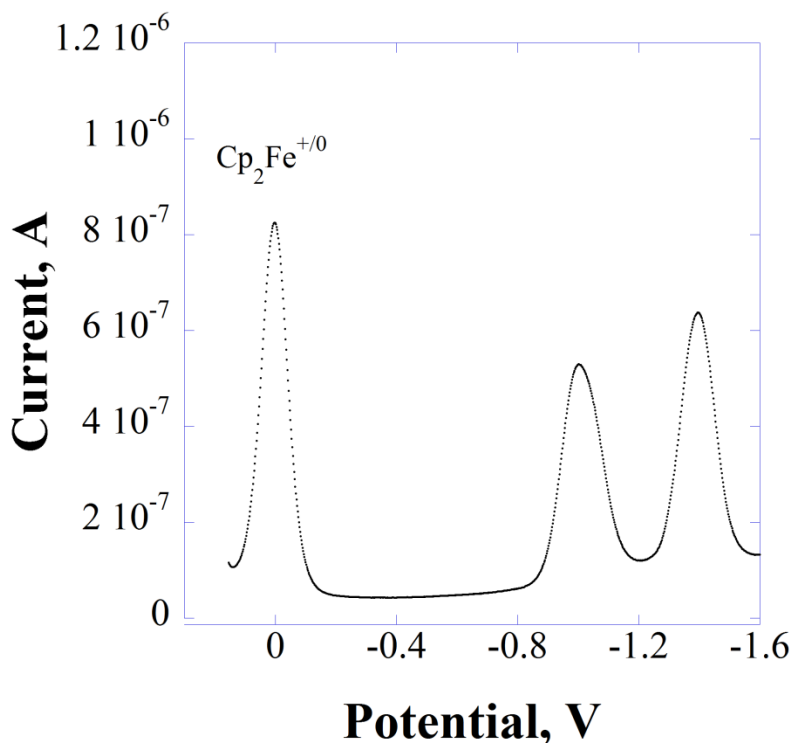


Figure S16. DPV analysis of 4,4'-(4-hexyl-4*H*-pyrrolo[2,3-*d*:5,4-*d'*]bisthiazole-2,6-diyl)bis(2,7-dihexylbenzo[*lmn*][3,8]phenanthroline-1,3,6,8(2*H*,7*H*)-tetraone) (6a) (0.1 M Bu_4NPF_6 in chloroform vs. $\text{Cp}_2\text{Fe}^{+/0}$): $E^{\text{red1}} = -1.00$ V, $E^{\text{red2}} = -1.40$ V.

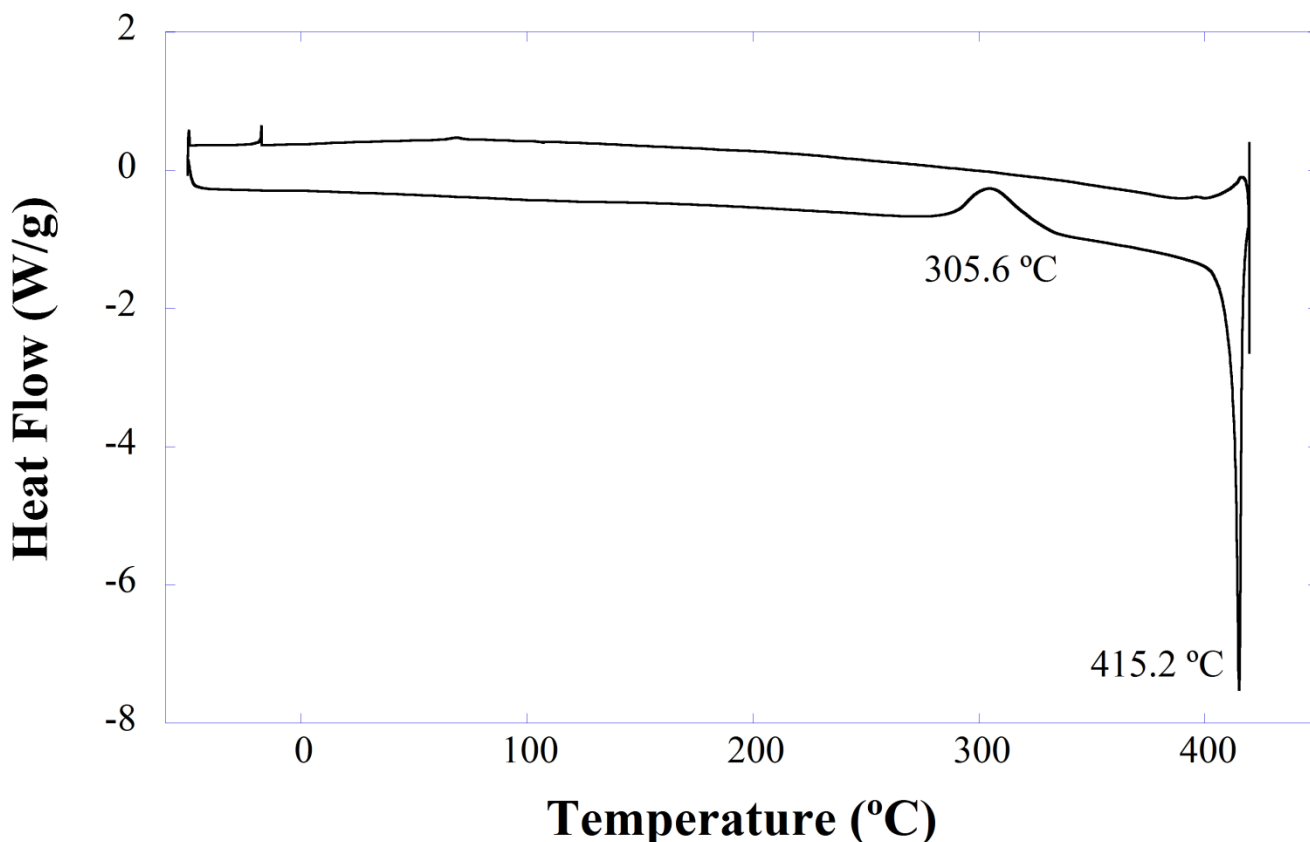
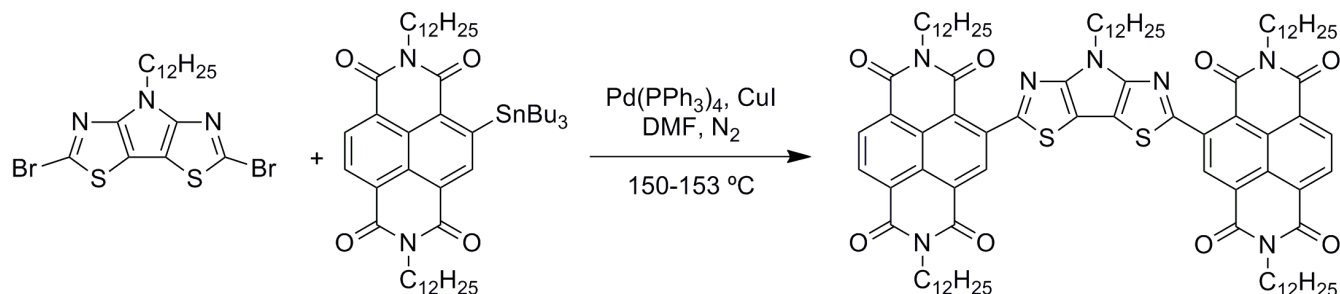


Figure S17. 1st cycle of the DSC analysis (10 °C/min heating-cooling rate, endo down) of 4,4'-(4-hexyl-4*H*-pyrrolo[2,3-*d*:5,4-*d'*]bis(thiazole)-2,6-diyl)bis(2,7-dihexylbenzo[*lmn*][3,8]phenanthroline-1,3,6,8(2*H*,7*H*)-tetraone) (6a).

4,4'-(4-Dodecyl-4*H*-pyrrolo[2,3-*d*:5,4-*d'*]bis(thiazole)-2,6-diyl)bis(2,7-didodecylbenzo[*lmn*][3,8]phenanthroline-1,3,6,8(2*H*,7*H*)-tetraone) (6b)



2,6-Dibromo-4-dodecyl-4*H*-pyrrolo[2,3-*d*:5,4-*d'*]bisthiazole (**3b**) (0.60 mmol, 0.30 g), 2,7-didodecyl-4-(tributylstannyl)benzo[*lmn*][3,8]phenanthroline-1,3,6,8(2*H*,7*H*)-tetraone (**5b**) (2.1 eq., 1.26 mmol, 1.12 g), Pd(PPh₃)₄ (20 mol%, 0.12 mmol, 0.14 g) and CuI (10 mol%, 0.06 mmol, 11 mg) were mixed in an oven-dried flask under nitrogen atmosphere. Anhydrous DMF (15 mL) was added, and the orange-brown mixture was heated to reflux for a few minutes, analyzed by TLC, and the mono-substituted byproduct (purple) was detected. Additional amount of **5b** (68 mg, 0.08 mmol) was added, the mixture was heated to reflux for a few more minutes, and the blue mixture with a precipitate was cooled to room temperature, and then treated with water. A dark solid was separated by vacuum filtration, washed with water, ethanol, and then dried (1.1 g, 118% crude yield, probably contains solvent or water). This crude product was purified by column chromatography (silica gel treated with triethylamine, chloroform to

elute impurities, chloroform:diethyl ether (100:1) to elute the product). The fractions (blue) containing the product were combined, the solvents were removed, and the material was further purified by column chromatography as described earlier four more times, and the product was obtained as dark solid (0.41 g, 44% purified yield). ^1H NMR (400 MHz, CDCl_3): δ 9.13 (s, 2H), 8.85 (d, $J = 7.6$ Hz, 2H), 8.80 (d, $J = 7.7$ Hz, 2H), 4.64 (t, $J = 7.2$ Hz, 2H), 4.23 (t, $J = 7.6$ Hz, 4H), 4.15 (t, $J = 7.3$ Hz, 4H), 2.11 (m, 2H), 1.82-1.65 (m, 8H), 1.50-1.10 (m, 90H expected, 100H observed), 0.92-0.78 (m, 15H). $^{13}\text{C}\{^1\text{H}\}$ NMR (100 MHz, CDCl_3): δ 162.69, 162.39, 162.34, 161.98, 160.64, 154.62, 139.04, 135.10 (CH), 131.62 (CH), 131.19 (CH), 127.64, 126.95, 126.72, 126.59, 125.36, 124.07, 108.54, 45.79 (CH_2), 41.33 (CH_2), 41.11 (CH_2), 31.91 (CH_2), 30.20 (CH_2), 29.64 (CH_2), 29.62 (CH_2), 29.59 (CH_2), 29.53 (CH_2), 29.38 (CH_2), 29.34 (CH_2), 29.29 (CH_2), 28.08 (CH_2), 28.06 (CH_2), 27.13 (CH_2), 27.09 (CH_2), 26.90 (CH_2), 22.68 (CH_2), 14.11 (CH_3) (28 aliphatic carbons are expected; 18 are observed; 10 signals are missing presumably due to overlap). HRMS (MALDI-TOF) calculated for $\text{C}_{94}\text{H}_{131}\text{N}_7\text{O}_8\text{S}_2$ 1549.9501; found 1549.9479. Anal. Calcd. for $\text{C}_{94}\text{H}_{131}\text{N}_7\text{O}_8\text{S}_2$: C, 72.78; H, 8.51; N, 6.32. Found: 72.73; H, 8.49; N, 6.25.

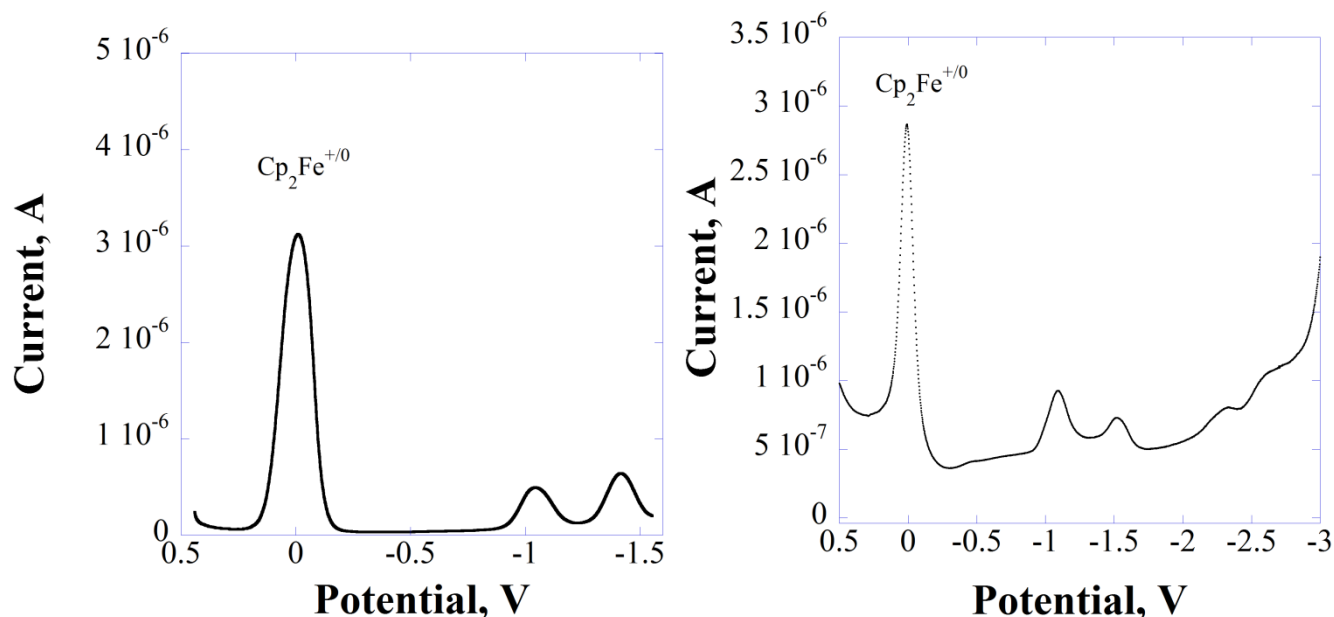


Figure S18. DPV analysis of 4,4'-(4-dodecyl-4*H*-pyrrolo[2,3-*d*:5,4-*d'*]bisthiazole-2,6-diyl)bis(2,7-didodecylbenzo[*lmn*][3,8]phenanthroline-1,3,6,8(2*H*,7*H*)-tetraone) (6b): (*left*) (0.1 M Bu_4NPF_6 in chloroform vs. $\text{Cp}_2\text{Fe}^{+/0}$): $E^{\text{red1}} = -1.04$ V, $E^{\text{red2}} = -1.42$ V; (*right*) 0.1 M Bu_4NPF_6 in tetrahydrofuran vs. $\text{Cp}_2\text{Fe}^{+/0}$): $E^{\text{red1}} = -1.09$ V, $E^{\text{red2}} = -1.52$ V, $E^{\text{red3}} = -2.33$ V, $E^{\text{red4}} = -2.63$ V.

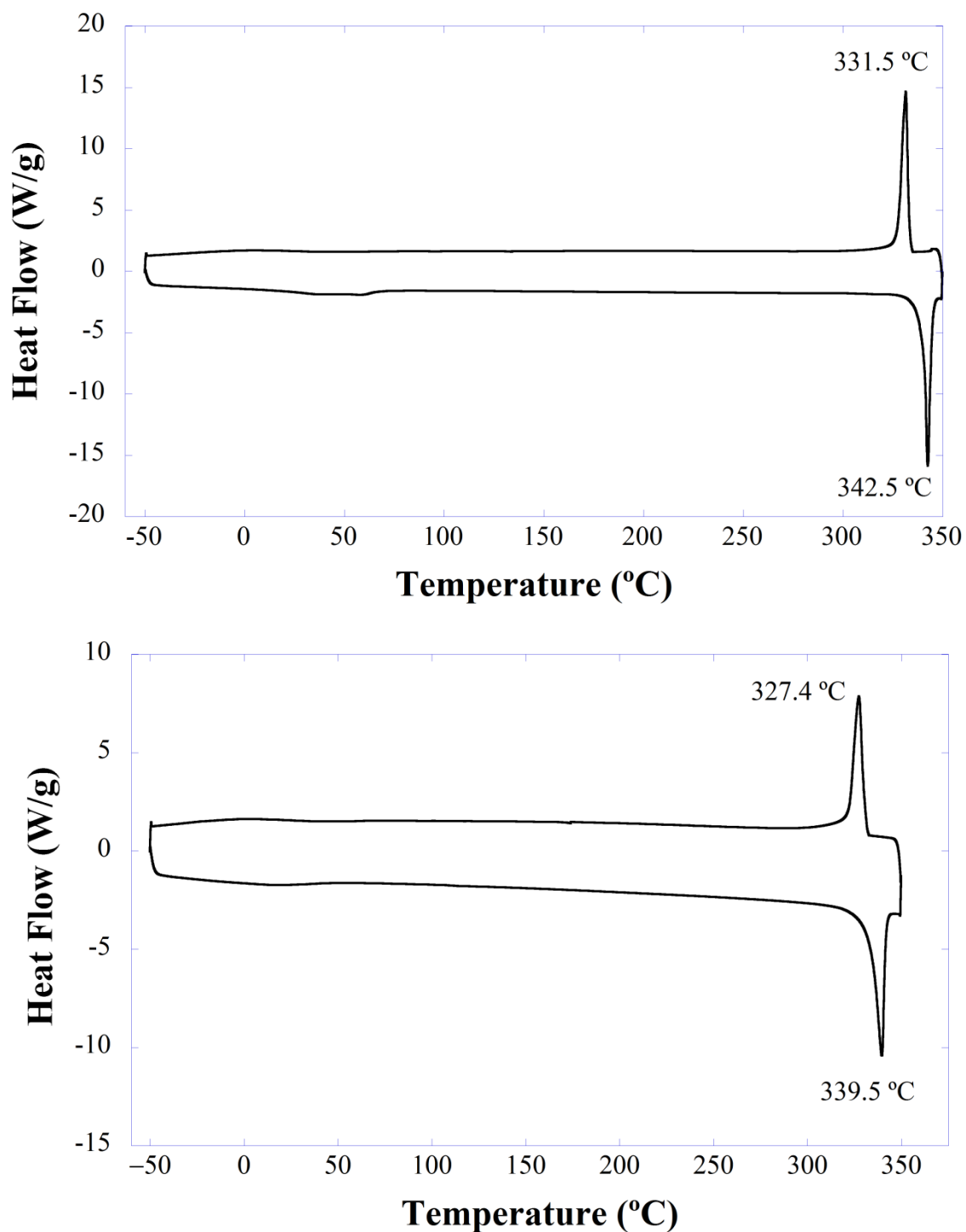
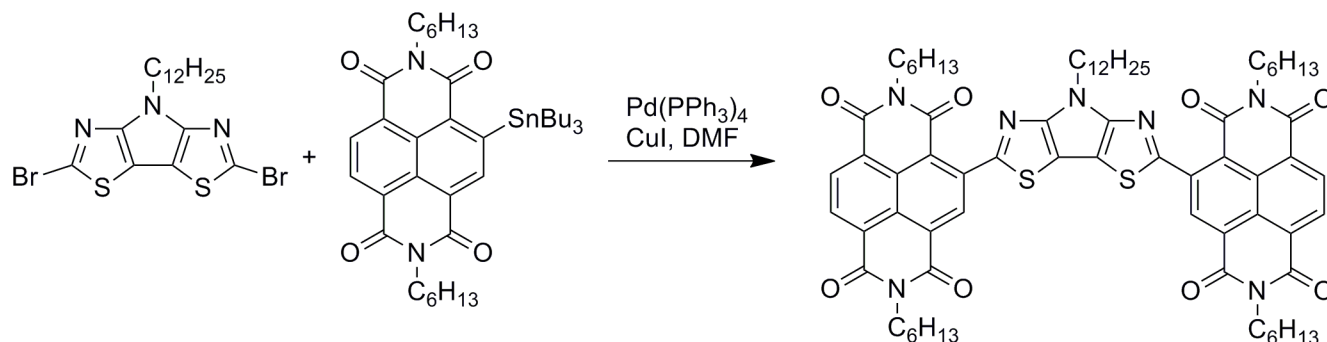


Figure S19. DSC analysis (10 °C/min heating-cooling rate, endo down) of 4,4'-(4-dodecyl-4*H*-pyrrolo[2,3-*d*:5,4-*d'*]bisthiazole-2,6-diyl)bis(2,7-didodecylbenzo[*lmn*][3,8]phenanthroline-1,3,6,8(2*H*,7*H*)-tetraone) (6b): 1st cycle (top); 2nd cycle (bottom).

4,4'-(4-Dodecyl-4*H*-pyrrolo[2,3-*d*:5,4-*d'*]bisthiazole-2,6-diyl)bis(2,7-dihexylbenzo[*lmn*][3,8]phenanthroline-1,3,6,8(2*H*,7*H*)-tetraone) (6c)



2,6-Dibromo-4-dodecyl-4*H*-pyrrolo[2,3-*d*:5,4-*d'*]bisthiazole (**3b**) (0.66 mmol, 0.34 g), 2,7-dihexyl-4-(tributylstannyl)benzo[*lmn*][3,8]phenanthroline-1,3,6,8(2*H*,7*H*)-tetraone (**5a**) (2.1 eq., 1.38 mmol, 1.00 g), Pd(PPh₃)₄ (20 mol%, 0.13 mmol, 0.15 g) and CuI (10 mol%, 0.066 mmol, 0.013 g) were mixed in the oven-dried flask under nitrogen atmosphere, anhydrous DMF (15 mL) was added, and the resulting mixture was heated to reflux for a few minutes, cooled to room temperature, treated with water, and the precipitate was separated by vacuum filtration. A dark solid was washed with water, ethanol, and then dried (0.81 g). This crude material was purified by column chromatography (silica gel, chloroform to elute byproducts, chloroform-ethyl acetate (20:1) to elute the product). The fractions containing the product (still slightly impure) were combined, the solvents were removed, the residue was heated to reflux with 2-propanol, cooled, and the dark solid was separated by vacuum filtration (0.41 g, 51.4% purified yield). This material was further purified by column chromatography (200 mL of silica gel treated with triethylamine (~4 mL), chloroform to elute majority of impurities, chloroform:diethyl ether (20:1) to elute the product (the material has low solubility which required that a large amount of solvent be used to elute the compound). The blue fractions containing the product were combined the solvents were removed, and the residue (0.33 g) was purified two times using silica gel columns as described above, then using basic Al₂O₃ column (~200 mL, chloroform, then chloroform:diethyl ether (100:1), and then silica gel column (~300 mL of silica gel treated with triethylamine (6 mL), chloroform, then chloroform:ethyl ether (100:1)). The fractions with the pure material were combined, the solvents were removed, and the residue was recrystallized from chlorobenzene twice (~50 mL). The product (0.18 g, 22.6% purified yield) was dried under vacuum with heating (40-120 °C). ¹H NMR (400 MHz, CDCl₃, 340 K): δ 9.21 (s, 2H), 8.86 (d, *J* = 7.6 Hz, 2H), 8.81 (d, *J* = 7.7 Hz, 2H), 4.69 (t, *J* = 7.3 Hz, 2H), 4.27 (t, *J* = 7.5 Hz, 4H), 4.21 (t, *J* = 7.5 Hz, 4H), 2.19 (m, 2H), 1.90-1.70 (m, 8H), 1.55-1.30 (m, 28H), 1.30-1.20 (m, 14H), 1.00-0.70 (multiplet overlapping with triplet, 12H+3H); DEPT-135 (1,1,2,2-tetrachloroethane-*d*₂, 100 MHz, 400 K): 135.31 (CH), 131.38 (CH), 130.84 (CH), 46.09 (CH₂), 45.03 (CH₂, due to low solubility of the sample the peak-to-noise ratio is low, and it is not clear if it is actual peak or noise), 41.38 (CH₂), 41.23 (CH₂), 31.5 (two CH₂), 29.87 (CH₂), 29.58 (CH₂), 29.53 (CH₂), 28.22 (CH₂), 27.05 (CH₂), 26.82 (CH₂), 26.77 (CH₂), 22.45 (CH₂), 22.42 (CH₂), 13.73 (CH₃; weak). HRMS (MALDI-TOF) calculated for (C₇₀H₈₃N₇O₈S₂+H) 1214.5823; found 1214.5822. Anal. Calcd. for C₇₀H₈₃N₇O₈S₂: C, 69.22; H, 6.89; N, 8.07. Found: C, 69.38; H, 6.83; N, 8.04.

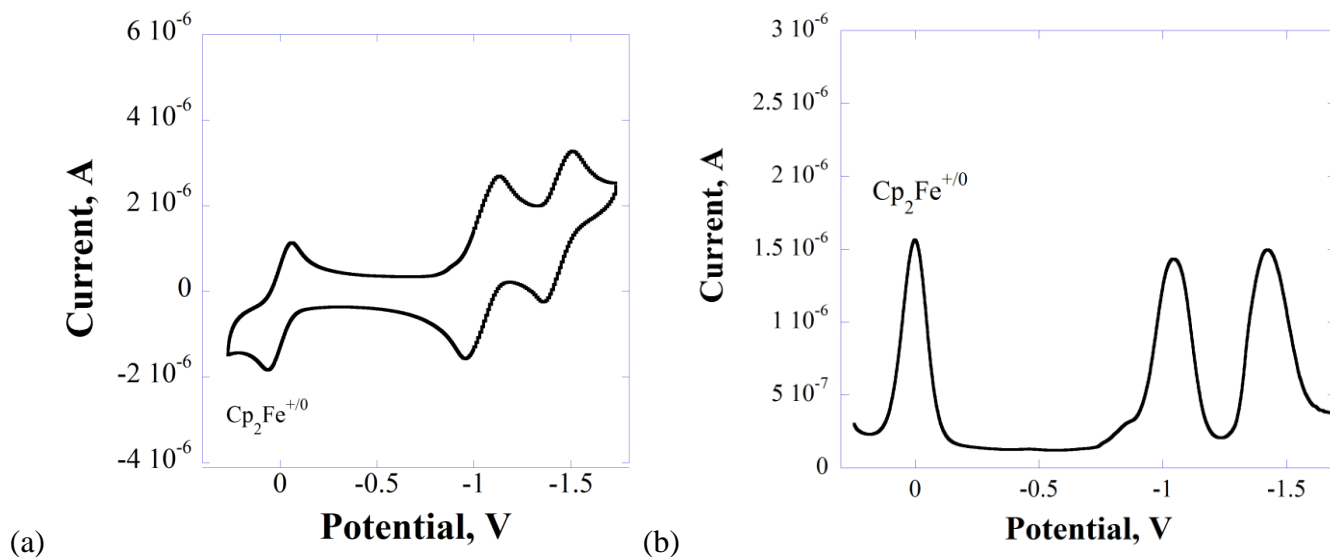


Figure S20. 4,4'-(4-Dodecyl-4*H*-pyrrolo[2,3-*d*:5,4-*d'*]bisthiazole-2,6-diyl)bis(2,7-dihexylbenzo[*lmn*][3,8]phenanthroline-1,3,6,8(2*H*,7*H*)-tetraone) (6c): (a) CV analysis in 0.1 M Bu₄NPF₆ in chloroform vs. Cp₂Fe⁺⁰: $E_{1/2}^{0/2-} = -1.05$ V, $E_{1/2}^{2-/4-} = -1.43$ V; (b) DPV analysis in 0.1 M Bu₄NPF₆ in chloroform vs. Cp₂Fe⁺⁰: $E^{\text{red}1} = -1.05$ V; $E^{\text{red}2} = -1.42$ V.

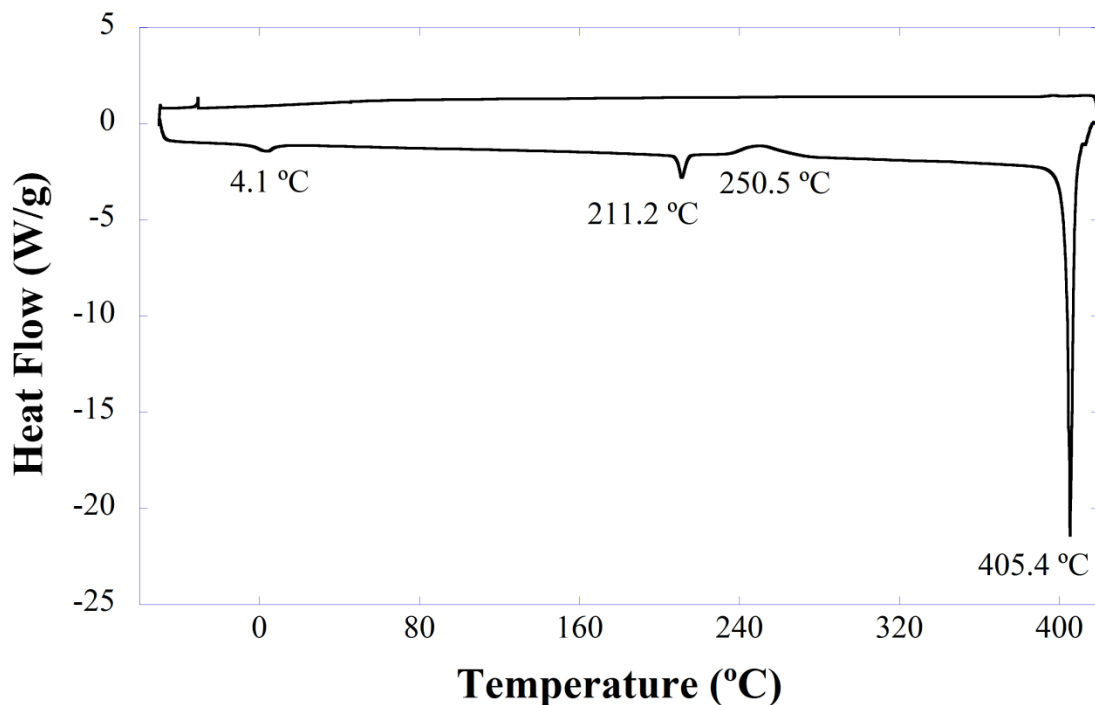
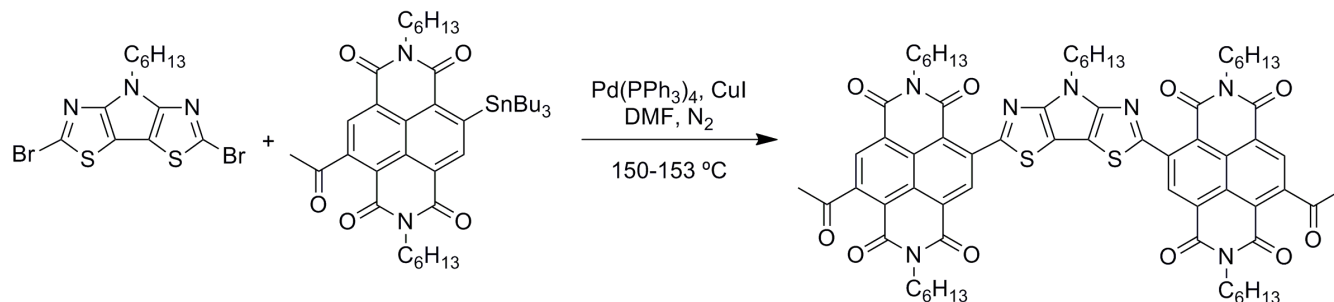


Figure S21. 1st cycle of the DSC analysis (10 °C/min heating-cooling rate) of 4,4'-(4-dodecyl-4*H*-pyrrolo[2,3-*d*:5,4-*d'*]bisthiazole-2,6-diyl)bis(2,7-dihexylbenzo[*lmn*][3,8]phenanthroline-1,3,6,8(2*H*,7*H*)-tetraone) (6c).

9,9'-(4-Hexyl-4*H*-pyrrolo[2,3-*d*:5,4-*d'*]bisthiazole-2,6-diyl)bis(4-acetyl-2,7-dihexylbenzo[*lmn*][3,8]phenanthroline-1,3,6,8(2*H*,7*H*)-tetraone) (6d)



2,6-Dibromo-4-hexyl-4*H*-pyrrolo[2,3-*d*:5,4-*d'*]bisthiazole (**3a**) (0.240 mmol, 102 mg) was mixed with 4-acetyl-2,7-di-hexyl-9-(tributylstannyl)benzo[*lmn*][3,8]phenanthroline-1,3,6,8(2*H*,7*H*)-tetraone (**5c**) (2.05 eq., 0.49 mmol, 377 mg) in an oven-dried flask (nitrogen atmosphere). The catalyst, Pd(PPh₃)₄ (10 mol% based on **3a**, 0.024 mmol, 28 mg), CuI (5 mol% based on **3a**, 0.012 mmol, 2.3 mg), and anhydrous DMF (40 mL) were added, and a yellow-brownish mixture was heated to reflux. Within a few minutes it became purple, then blue with a precipitate. The mixture was cooled to room temperature, and then treated with water. The dark solid was separated by vacuum filtration, washed with water, ethanol, dried, and then purified by column chromatography (silica gel treated with triethylamine, chloroform to elute less polar byproducts, chloroform:ethyl ether (30:1) to elute the product. Fractions containing the product (blue) were combined, the solvents were removed, and the purified product was obtained as dark solid (130 mg, 44.7% yield). This material combined with a product obtained on a previous batch (~30-40 mg) was further purified by column chromatography several times for mobility measurements (silica gel treated with triethylamine, chloroform, to elute less polar impurities, chloroform:diethyl ether (30:1, then 10:1) to elute the product). ¹H NMR (400 MHz, CDCl₃, 340 K): δ 9.31 (s, 2H), 8.58 (s, 2H), 4.69 (t, *J* = 6.4 Hz, 2H), 4.20 (m, 8H expected, 7H observed), 2.73 (s, 6H), 2.17 (2H expected, 3.6H observed), 1.78 (m, 8H), 1.70-1.23 (m, 30H), 0.90 (m, 15H expected, 12.4 H observed) (concentration of the material in CDCl₃ (340 K) or in 1,1,2,2-tetrachloroethane (420 K) was too low to record ¹³C{¹H} NMR or DEPT-135). HRMS (MALDI-TOF) calculated for C₆₈H₇₅N₇O₁₀S₂ 1213.5017; found 1213.4992. Anal. Calcd. for C₆₈H₇₅N₇O₁₀S₂: C, 67.25; H, 6.22; N, 8.07. Found: 67.36; H, 6.11; N, 7.96.

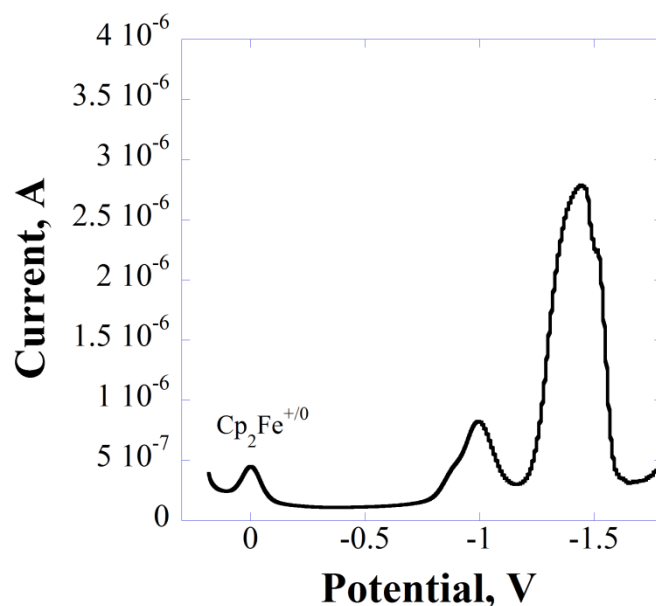
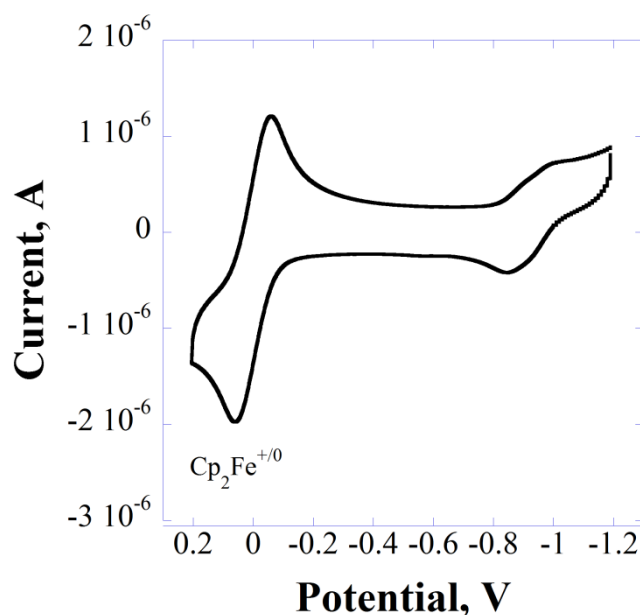


Figure S22. 9,9'-(4-Hexyl-4*H*-pyrrolo[2,3-*d*:5,4-*d'*]bisthiazole-2,6-diyl)bis(4-acetyl-2,7-dihexylbenzo[*lmn*][3,8]phenanthroline-1,3,6,8(2*H*,7*H*)-tetraone) (**6d**) (0.1 M Bu₄NPF₆ in chloroform vs. Cp₂Fe⁺⁰ V): (left) CV, $E_{1/2}^{0/1-} = -0.88$ V, $E_{1/2}^{1-/2-} = -0.96$ V, (right) DPV, $E^{\text{red1}} = -0.90$ V, $E^{\text{red2}} = -1.00$ V, $E^{\text{red3}} = -1.44$ V.

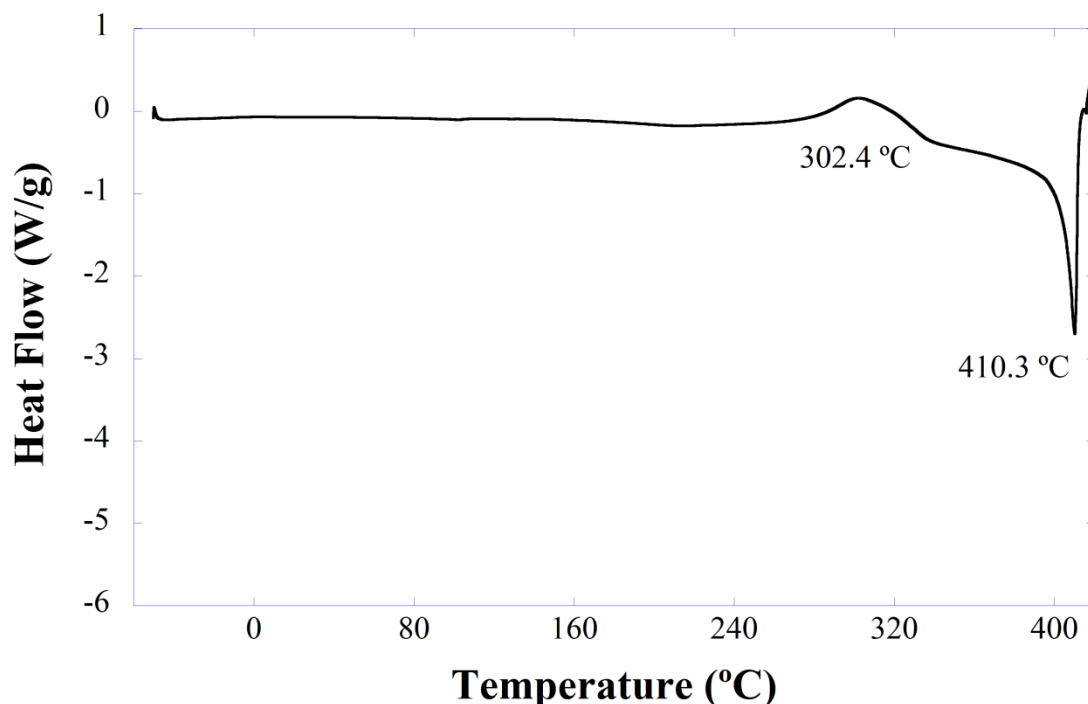
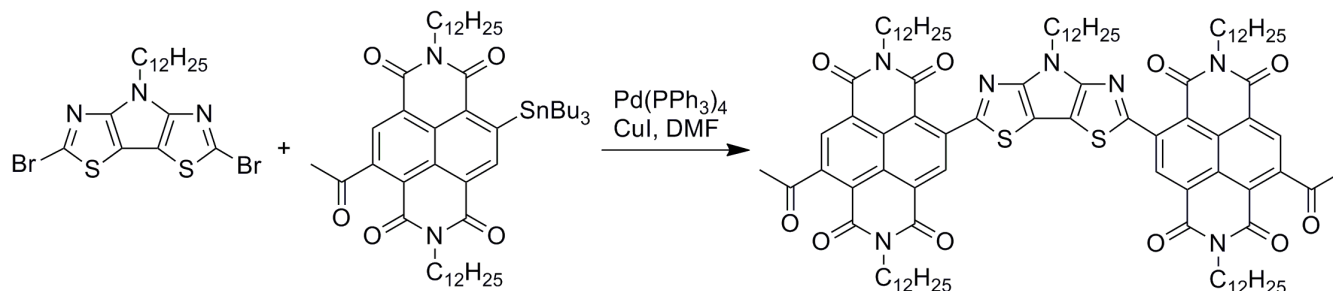


Figure S23. 1st heating of the DSC analysis (10 °C/min heating-cooling rate; endo down) of 9,9'-(4-hexyl-4*H*-pyrrolo[2,3-*d*:5,4-*d'*]bisthiazole-2,6-diyl)bis(4-acetyl-2,7-dihexylbenzo[*lmn*][3,8]phenanthroline-1,3,6,8(2*H*,7*H*)-tetraone) (**6d**).

9,9'-(4-Dodecyl-4*H*-pyrrolo[2,3-*d*:5,4-*d'*]bisthiazole-2,6-diyl)bis(4-acetyl-2,7-dihexylbenzo[*lmn*][3,8]phenanthroline-1,3,6,8(2*H*,7*H*)-tetraone) (**6e**)



2,6-Dibromo-4-dodecyl-4*H*-pyrrolo[2,3-*d*:5,4-*d'*]bisthiazole (**3b**) (0.15 mmol, 76.0 mg) was mixed with 4-acetyl-2,7-didodecyl-9-(tributylstannyl)benzo[*lmn*][3,8]phenanthroline-1,3,6,8(2*H*,7*H*)-tetraone (**5d**) (2.1 eq., 0.315 mmol, 294 mg) in an oven-dried flask (nitrogen atmosphere). The catalyst, Pd(PPh₃)₄ (10 mol% based on **3b**, 0.015 mmol, 17 mg), CuI (5 mol% based on **3b**, 0.075 mmol, 1.4 mg), and anhydrous DMF (30 mL) were added, and the yellow-brownish mixture was heated to reflux for ~ 5 minutes. The reaction mixture became blue with a precipitate, and it was cooled to room temperature and treated with water. The dark solid was separated by the vacuum filtration, washed with water, ethanol, and then dried (110 mg, 44.9% crude yield). This crude product was purified by column

chromatography (silica gel treated with triethylamine, chloroform to elute less polar byproducts, chloroform:diethyl ether (30:1) to elute the product). The solvents were removed from the combined fractions, and the residue was purified by column chromatography four times (silica gel treated with triethylamine, chloroform:diethyl ether (40:1 or 50:1) as eluant). The material was obtained as blue solid (56 mg, 50.9% recovery, 22.9% purified yield). $^1\text{H NMR}$ (400 MHz, CDCl_3 , 340 K): δ 9.27 (s, 2H), 8.56 (s, 2H), 4.66 (t, $J = 7.1$ Hz, 2H), 4.17 (m, 8H), 2.74 (s, 6H), 2.13 (m, 2H), 1.74 (m, 8H), 1.50-1.18 (m, 84H), 0.89 (m, 15H). DEPT-135 (CDCl_3) was attempted (the signal to noise was still very low): 136.26 (CH), 128.81 (CH), 41.49 (CH_2), 41.32 (CH), 31.97 (CH_2), 29.65 (CH_2), 29.60 (CH_2), 29.36 (CH_2), 29.31 (CH_2), 28.02 (CH_2), 27.10 (CH_2), 22.68 (CH_2), 14.12 (CH_3) (recording of the spectra in 1,1,2,2-tetrachloroethane- d_2 at 420 K was attempted without success due to low solubility). HRMS (MALDI-TOF) calculated for ($\text{C}_{98}\text{H}_{135}\text{N}_7\text{O}_{10}\text{S}_2+1\text{H}$) 1634.9790; found 1634.9739. Anal. Calcd. for $\text{C}_{98}\text{H}_{135}\text{N}_7\text{O}_{10}\text{S}_2$: C, 71.98; H, 8.32; N, 6.00. Found: 71.70; H, 8.23; N, 5.86.

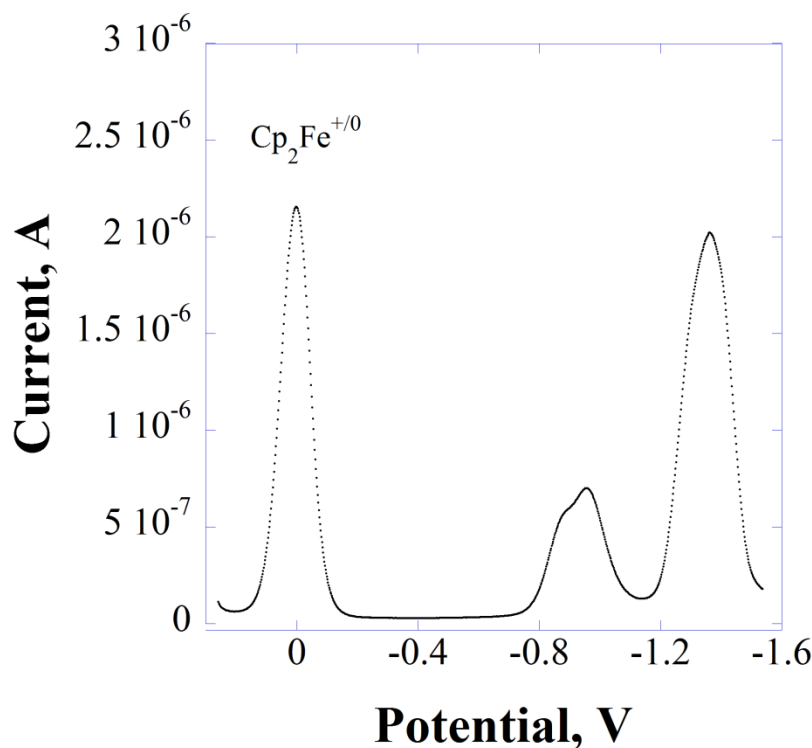


Figure S24. DPV of 9,9'-(4-dodecyl-4*H*-pyrrolo[2,3-*d*:5,4-*d'*]bisthiazole-2,6-diyl)bis(4-acetyl-2,7-dihexylbenzo[*lmn*][3,8]phenanthroline-1,3,6,8(2*H*,7*H*)-tetraone) (6e) (0.1 M Bu_4NPF_6 in chloroform vs. $\text{Cp}_2\text{Fe}^{+/0}$ V): $E^{\text{red1}} = -0.89$ V, $E^{\text{red2}} = -0.96$ V, $E^{\text{red3}} = -1.36$ V.

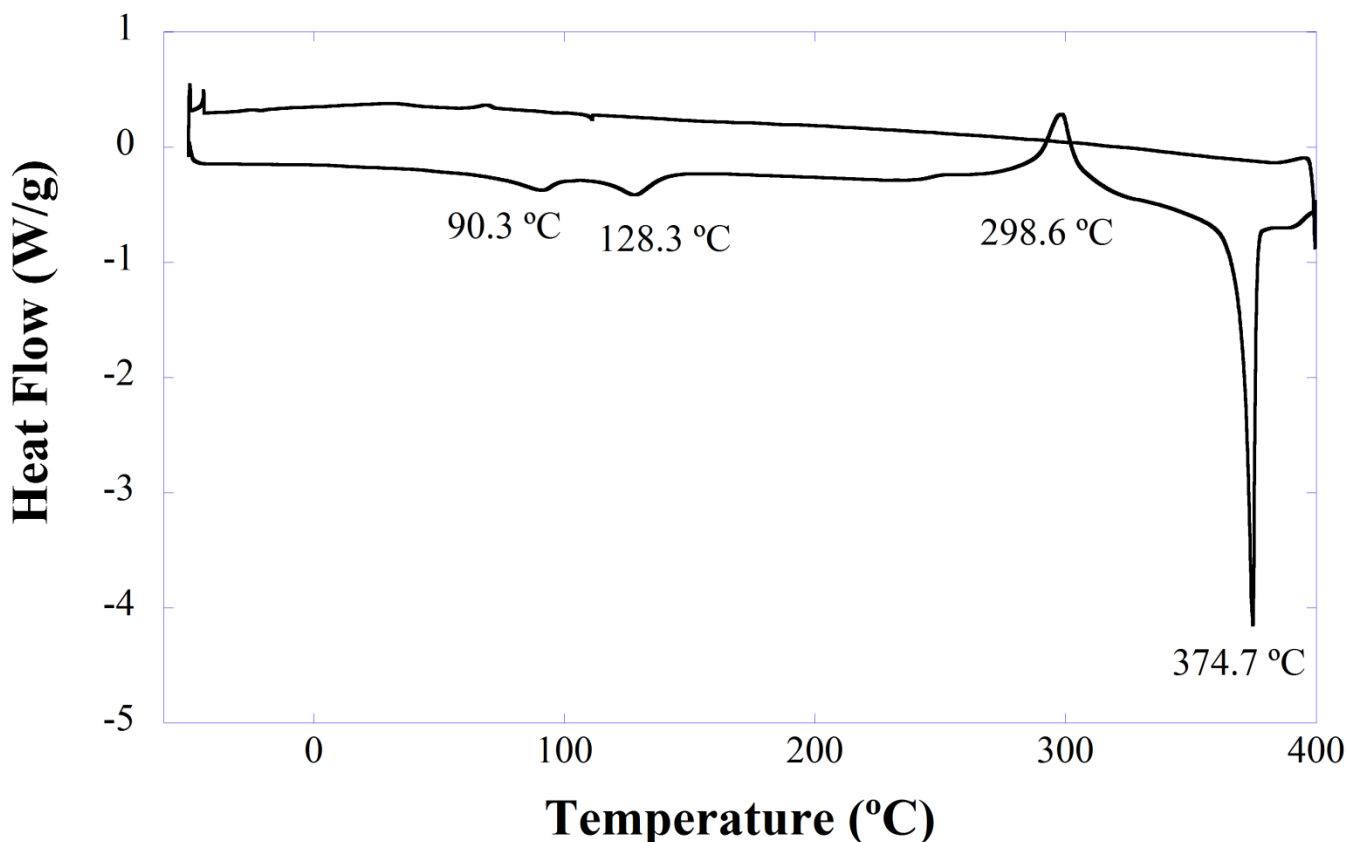


Figure S25. 1st cycle of the DSC analysis (10 °C/min heating-cooling rate) of 9,9'-(4-dodecyl-4*H*-pyrrolo[2,3-*d*:5,4-*d'*]bisthiazole-2,6-diyl)bis(4-acetyl-2,7-dihexylbenzo[*lmn*][3,8]phenanthroline-1,3,6,8(2*H*,7*H*)-tetraone) (6e).

2,2'-(4-Oxo-4*H*-cyclopenta[1,2-*b*:5,4-*b'*]dithiazol-2,6-diyl)bis(2,7-dihexylnaphthalene-1,4:5,8-bis(dicarboximide) (8a)

This material was prepared as described previously.¹¹ The material was extensively purified by the column chromatography (silica gel treated with triethylamine, dichloromethane:diethyl ether (100:1, then 30:1) as eluant (1st column); chloroform:diethyl ether (30:1) as eluant (2nd column), dichloromethane:ethyl ether (50:1) as eluant (3rd column); chloroform:diethyl ether (30:1) (4th column)) until analytically pure compound was obtained. Anal. Calcd. for C₅₉H₅₈N₆O₉S₂: 66.90; H, 5.52; N, 7.93. Found: C, 66.80; H, 5.62; N, 7.94.

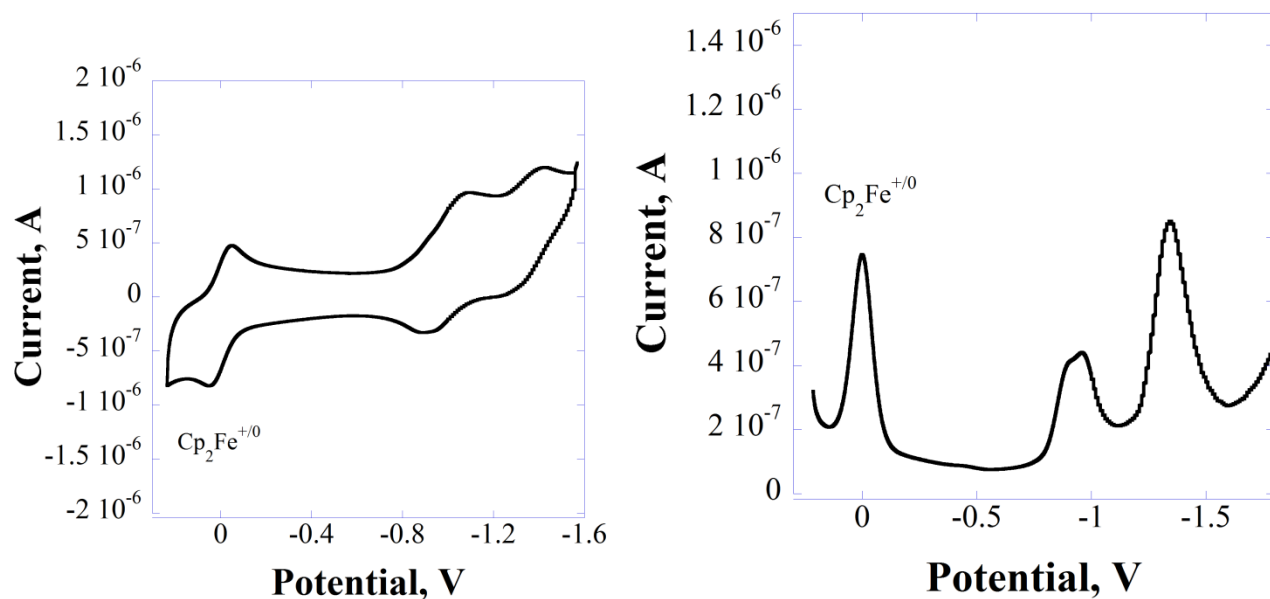


Figure S26. 2,2'-(4-Oxo-4H-cyclopenta[1,2-b:5,4-b']dithiazol-2,6-diyl)bis(2,7-dihexylnaphthalene-1,4:5,8-bis(dicarboximide) (8a) in 0.1 M Bu_4NPF_6 in chloroform vs. $\text{Cp}_2\text{Fe}^{+/0}$: (left) CV analysis $E_{1/2}^{0/2-} = -1.01$ V (there is a shoulder suggesting that there is another poorly resolved reduction), $E_{1/2}^{2-/4-} = -1.34$ V; (right) DPV analysis: $E^{\text{red1}} = -0.91$ V (appears as a shoulder); $E^{\text{red2}} = -0.96$ V, $E^{\text{red3}} = -1.34$ V.

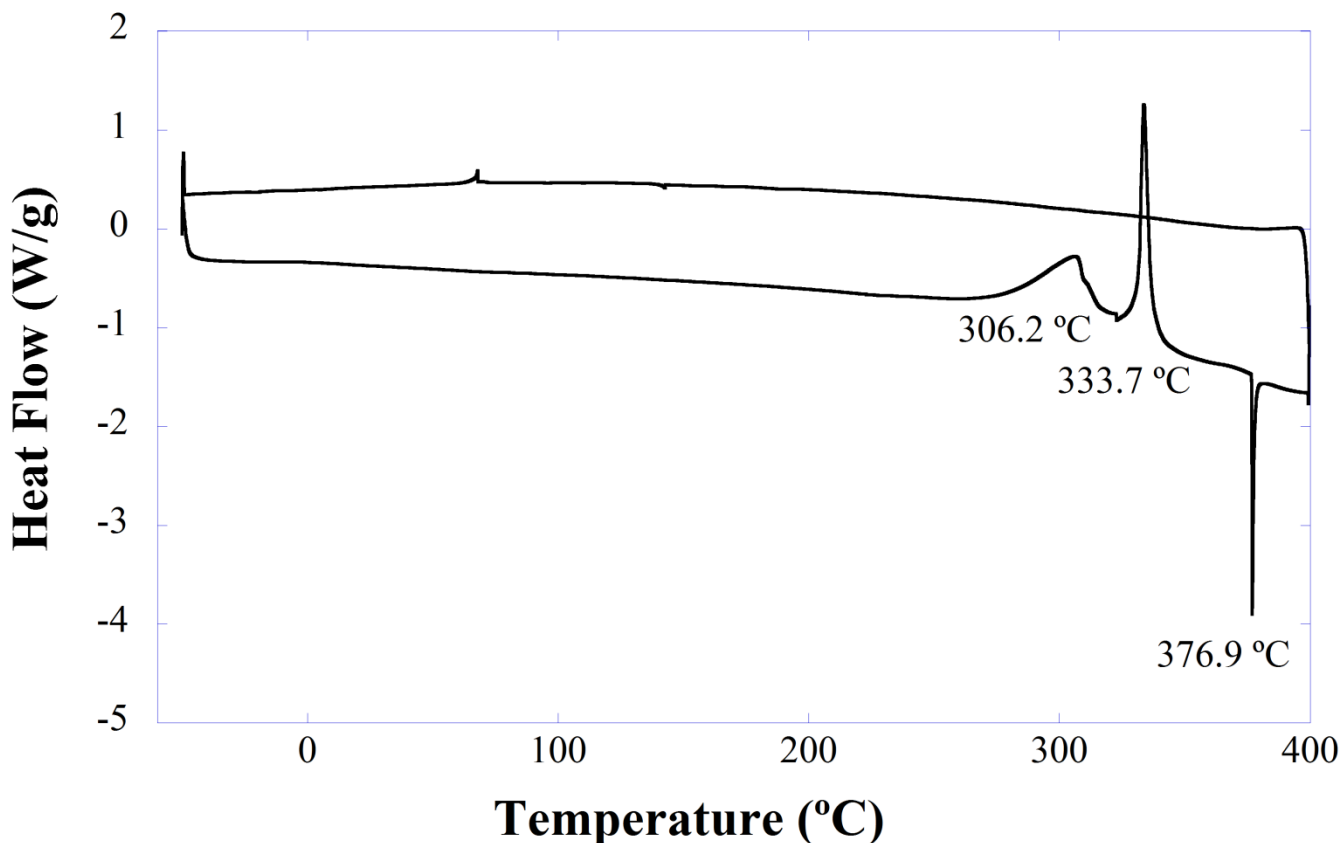
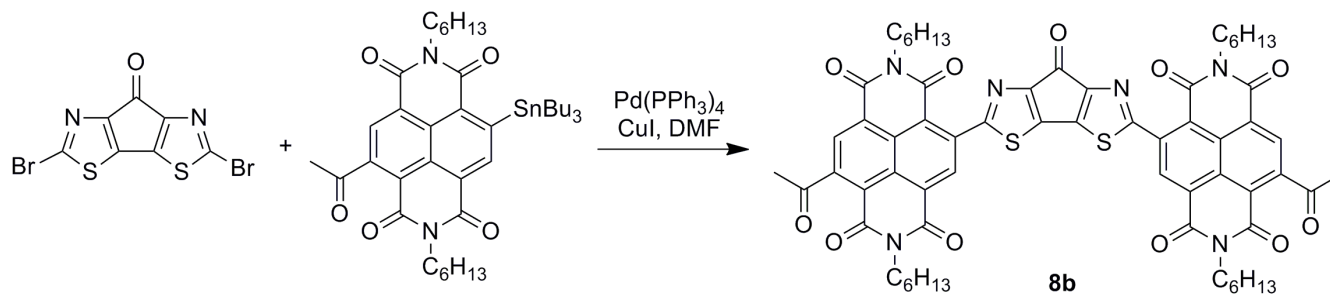


Figure S27. 1st cycle of the DSC analysis (10 $^{\circ}\text{C}/\text{min}$ heating-cooling rate) of 2,2'-(4-oxo-4H-cyclopenta[1,2-b:5,4-b']dithiazol-2,6-diyl)bis(2,7-dihexylnaphthalene-1,4:5,8-bis(dicarboximide) (8a).

9,9'-(7-Oxo-7H-cyclopenta[1,2-d:4,3-d']bisthiazole-2,5-diyl)bis(4-acetyl-2,7-dihexylbenzo[lmn][3,8]phenanthroline-1,3,6,8(2H,7H)-tetraone) (8b)



2,5-Dibromo-7H-cyclopenta[1,2-d:4,3-d']bis(thiazole)-7-one (**7**) (0.320 mmol, 112 mg) was mixed with 4-acetyl-2,7-dihexyl-9-(tributylstannyl)benzo[lmn][3,8]phenanthroline-1,3,6,8(2H,7H)-tetraone (**5c**) (2.1 eq., 0.67 mmol, 511 mg) in an oven-dried flask (nitrogen atmosphere). The catalyst, Pd(PPh₃)₄ (10 mol% based on **7**, 0.032 mmol, 37 mg), CuI (5 mol% based on **7**, 0.016 mmol, 3 mg), and anhydrous DMF (30 mL) were added, and the reddish-purple mixture was heated to reflux for about 10 minutes. The mixture (purple-reddish) was cooled to room temperature, treated with water, the precipitate was separated by vacuum filtration, washed with water, ethanol, and then dried. This crude material was purified by column chromatography (~100 mL of silica gel treated triethylamine, dichloromethane to elute less polar byproducts, dichloromethane:diethyl ether (30:1, then 20:1) to elute the product). The desired material still contained a minor more polar impurity, and was further purified by column chromatography (~100 mL of silica gel treated with triethylamine (~0.5 mL), chloroform to pack the column, chloroform:diethyl ether (40:1 (very slow elution), then 30:1). Fractions containing the purified product **8b** were combined, the solvents were removed, and the material was purified by column chromatography three more times (silica gel treated with triethylamine, dichloromethane:ethyl ether (30:1) as eluant). Product **8b** was obtained as red-purple solid (97 mg, 26.5% purified yield). Formation of a more polar unidentified purple byproduct was observed (MS (MALDI-TOF) found 1337.3, which can correspond to C₇₀H₆₂N₈O₁₂S₄+1H).

8b: ¹H NMR (400 MHz, CDCl₃): δ 9.22 (s, 2H), 8.58 (s, 2H), 4.17 (m, 8H), 2.73 (s, 6H), 1.73 (m, 8H), 1.50-1.20 (m, 24H), 0.91 (m, 12H). ¹³C{¹H} NMR (100 MHz, CDCl₃): δ 202.33, 177.28, 165.93, 162.26, 161.52, 161.41, 154.31, 146.87, 145.64, 137.50, 135.80 (CH), 129.18 (CH), 127.19, 127.17, 127.01, 126.10, 123.59, 122.18, 41.54 (CH₂), 41.31 (CH₂), 31.46 (CH₂), 31.44 (CH₂), 30.61 (CH₃), 27.91 (CH₂), 26.72 (CH₂), 26.68 (CH₂), 22.54 (CH₂), 14.01 (CH₃) (13 aliphatic carbons are expected, 10 are observed; 3 aliphatic carbon signals are missing due to overlap; one aromatic signal is missing possibly due to overlap). HRMS (MALDI-TOF) calculated for (C₆₃H₆₂N₆O₁₁S₂+H) 1143.3996; found 1143.3944. Anal. Calcd. for C₆₃H₆₂N₆O₁₁S₂: C, 66.18; H, 5.47; N, 7.35. Found: 66.17; H, 5.51; N, 7.22.

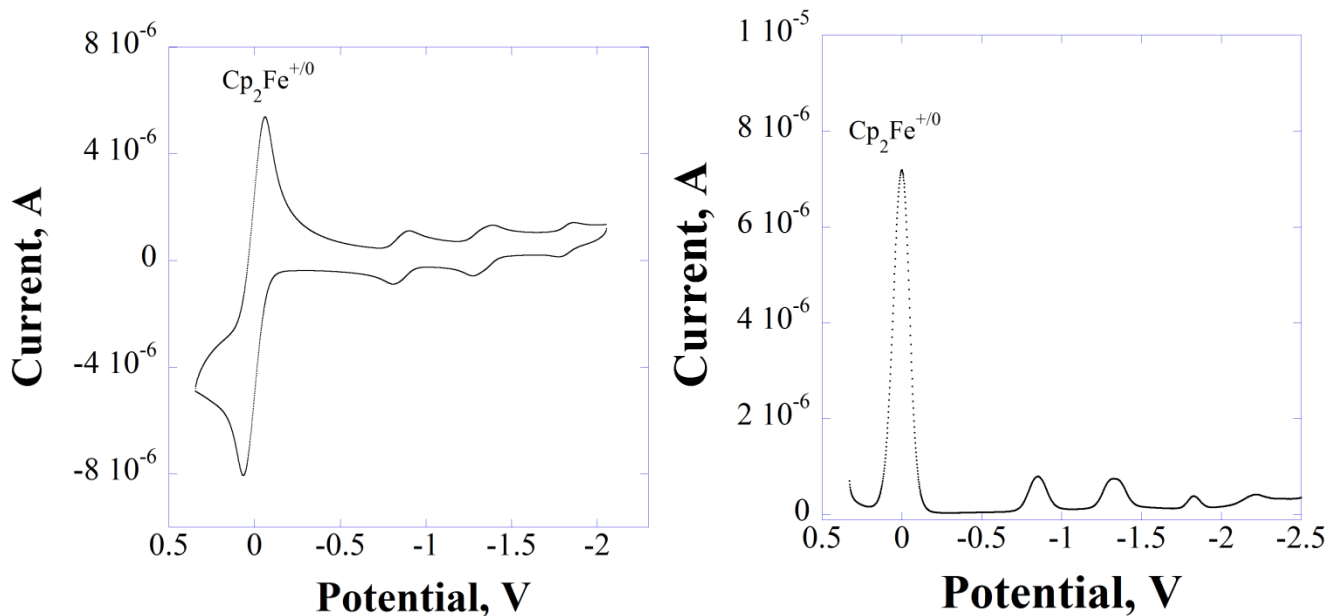


Figure S28. 9,9'-(7-oxo-7*H*-cyclopenta[1,2-*d*:4,3-*d'*]bisthiazole-2,5-diyl)bis(4-acetyl-2,7-dihexylbenzo[*lmn*][3,8]phenanthroline-1,3,6,8(2*H*,7*H*)-tetraone) (**8b**) (0.1 M Bu₄NPF₆ in tetrahydrofuran vs. Cp₂Fe⁺⁰ V): (left) $E_{1/2}^{0/2-} = -0.86$ V, $E_{1/2}^{2-/4-} = -1.33$ V; $E_{1/2}^{4-/5-} = -1.83$ V; (right) DPV of $E^{\text{red}1} = -0.85$ V, $E^{\text{red}2} = -1.33$ V, $E^{\text{red}3} = -1.83$ V, $E^{\text{red}4} = -2.22$ V.

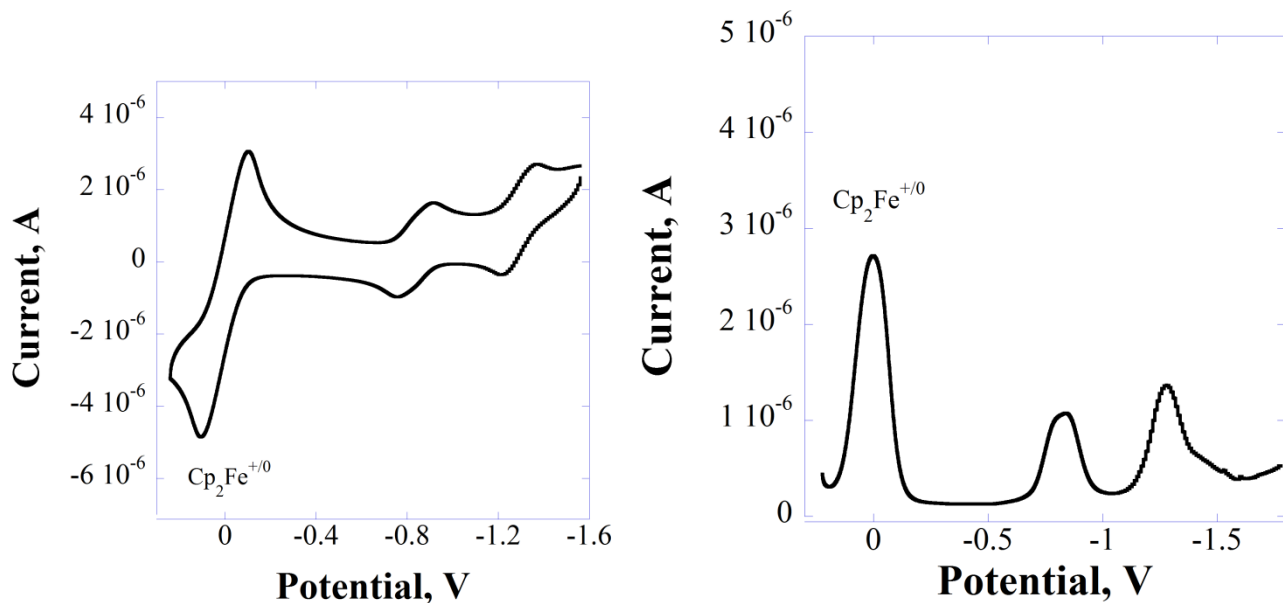


Figure S29. 9,9'-(7-oxo-7*H*-cyclopenta[1,2-*d*:4,3-*d'*]bisthiazole-2,5-diyl)bis(4-acetyl-2,7-dihexylbenzo[*lmn*][3,8]phenanthroline-1,3,6,8(2*H*,7*H*)-tetraone) (**8b**) (0.1 M Bu₄NPF₆ in chloroform vs. Cp₂Fe⁺⁰ V): (left) CV analysis, $E_{1/2}^{0/2-} = -0.84$ V, $E_{1/2}^{2-/4-} = -1.29$ V; DPV analysis, $E^{\text{red}1} = -0.84$ V, $E^{\text{red}2} = -1.28$ V

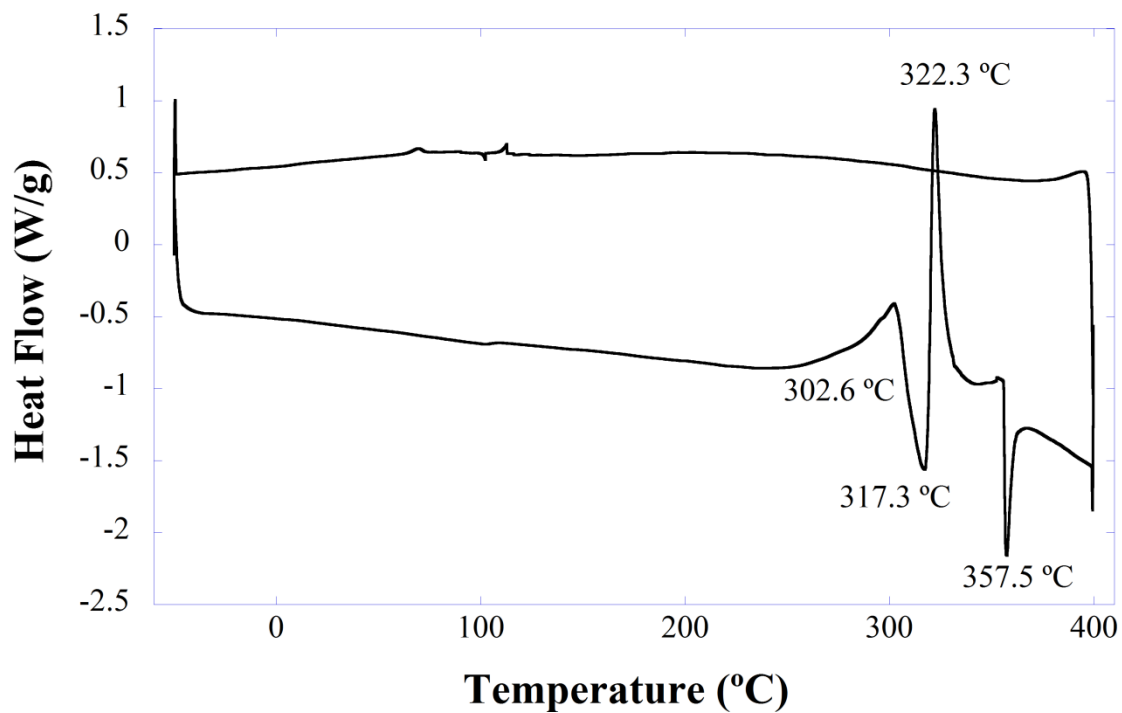


Figure S30. 1st cycle of the DSC analysis (10 °C/min heating-cooling rate) of 9,9'-(7-oxo-7*H*-cyclopenta[1,2-*d*:4,3-*d'*]bisthiazole-2,5-diyl)bis(4-acetyl-2,7-dihexylbenzo[*lmn*][3,8]phenanthroline-1,3,6,8(2*H*,7*H*)-tetraone) (8b).

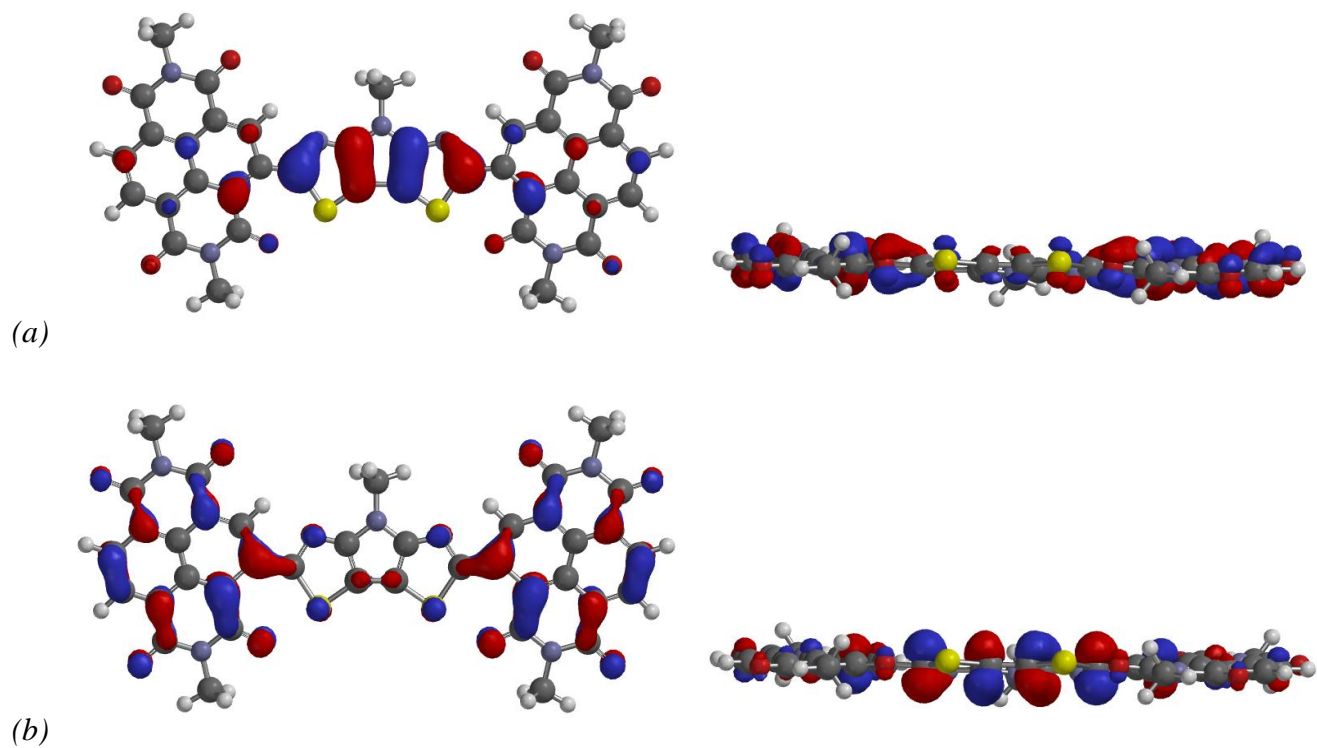


Figure S31. Pictorial representations of the (a) HOMO (-5.76 eV) and (b) LUMO (-3.59 eV) for 4,4'-(4-methyl-4*H*-pyrrolo[2,3-*d*:5,4-*d'*]bisthiazole-2,6-diyl)bis(2,7-dimethylbenzo[*lmn*][3,8]phenanthroline-1,3,6,8(2*H*,7*H*)-tetraone) (IV) as determined at the B3LYP/6-31G level of theory.**

Table S2. Cartesian coordinates of I, II, III and IV for the optimized neutral state at the B3LYP/6-31G level of theory.**

	X	Y	Z
I			
C	1.095883	-0.7121	-0.00728
C	0.701325	0.642595	0.00161
C	-0.70551	0.639468	-0.01523
C	-1.09601	-0.71665	-0.02725
S	-2.12549	1.625732	0.028299
S	2.120038	1.630832	-0.01782
N	-2.40183	-0.98859	-0.02604
N	0.00202	-1.55492	-0.03511
C	0.013656	-3.01511	0.036454
H	0.766064	-3.37572	-0.67248
H	-0.96537	-3.3559	-0.31077
N	2.401249	-0.98133	0.00908
C	3.123369	0.138076	0.016269
C	-3.1236	0.130102	0.003261
H	4.210693	0.032996	0.105168
H	-4.21412	0.02227	-0.01546
H	0.225134	-3.39311	1.043234
II			
C	2.524117	0.941676	0.06221
H	3.041101	1.893539	0.081452
C	3.167449	-0.26597	0.051387
C	1.110947	0.764176	0.039612

C	0.701184	-0.57621	0.004062
S	2.077142	-1.64233	0.01085
C	-1.11695	0.770306	0.003228
C	-0.71394	-0.57227	-0.01897
C	-2.52898	0.955979	-0.021
H	-3.04059	1.910922	-0.0183
C	-3.1786	-0.248	-0.05321
S	-2.09544	-1.63036	-0.05785
N	-0.00134	1.590873	0.056701
H	4.233306	-0.44454	0.060956
C	0.003328	3.036916	-0.02535
H	-0.8826	3.434332	0.475828
H	0.011244	3.392427	-1.06322
H	0.884787	3.428842	0.487631
H	-4.24522	-0.42082	-0.07792

III

C	3.139076	-0.14502	0.013955
C	1.183014	0.821751	-0.01959
C	0.727489	-0.48548	-0.02556
S	2.053326	-1.57043	0.002384
C	-0.72749	-0.48547	-0.02558
C	-1.18299	0.821751	-0.01969
C	-3.13903	-0.145	0.013846
S	-2.05335	-1.57042	0.002559
C	0.000001	1.767871	-0.0102
O	0.00001	2.976286	0.011217
N	-2.52415	1.006957	0.005984
N	2.524128	1.006948	0.006107

H	4.224171	-0.27816	0.091793
H	-4.22413	-0.27819	0.09161
IV			
C	9.714856	0.210987	-0.03193
H	10.74217	0.557114	-0.0421
C	9.400864	-1.1531	-0.00919
H	10.17858	-1.90841	0.003143
C	8.079134	-1.58179	-0.00011
C	8.69115	1.146634	-0.03799
C	7.344174	0.729087	-0.02336
C	7.00682	-0.65108	-0.01198
C	5.637907	-1.07529	-0.00775
C	6.296544	1.679752	-0.01734
C	4.596281	-0.11219	0.017521
C	4.991568	1.267148	0.011323
H	4.218204	2.020333	0.026296
C	7.824274	-3.03838	0.029322
C	5.391872	-2.53265	-0.03484
O	4.267666	-3.02153	-0.10416
O	8.72187	-3.86849	0.058174
N	6.477661	-3.41207	0.016625
C	6.150109	-4.84409	0.013306
H	7.08642	-5.39266	0.071725
H	5.610292	-5.09977	-0.90052
H	5.510519	-5.07756	0.866171
C	9.02111	2.596008	-0.05652
C	6.591448	3.140289	-0.0422
O	10.17158	3.007689	-0.06888

O	5.708612	3.985522	-0.04624
N	7.947655	3.498104	-0.06068
C	8.297992	4.923745	-0.08471
H	7.371821	5.491954	-0.10782
H	8.904687	5.138246	-0.96639
H	8.881083	5.176707	0.80318
C	1.096408	0.571635	0.195099
C	0.703066	-0.76374	-0.03588
C	-0.70349	-0.76103	-0.04256
C	-1.0956	0.575851	0.183635
S	-2.12214	-1.73798	-0.18729
C	-4.59578	-0.10754	-0.0073
C	-4.99314	1.270933	-0.02694
H	-4.22155	2.026641	-0.02976
C	-5.63558	-1.07329	-0.01514
C	-7.00541	-0.65228	-0.00838
C	-6.29992	1.67981	-0.04558
C	-7.34536	0.727024	-0.03028
C	-8.69366	1.141626	-0.0354
C	-8.07554	-1.5849	0.026757
C	-9.39821	-1.159	0.02758
H	-10.1744	-1.91543	0.057973
C	-9.71509	0.204124	-0.00806
H	-10.7431	0.548158	-0.01119
C	-6.59883	3.139456	-0.08016
C	-9.02758	2.589968	-0.06679
N	-7.95687	3.493835	-0.09
O	-10.1796	2.997897	-0.07312
O	-5.71835	3.985821	-0.099

C	-8.31038	4.918543	-0.12463
H	-8.91531	5.12656	-1.00927
H	-7.38525	5.488414	-0.14988
H	-8.89626	5.175606	0.760154
C	-5.38777	-2.53066	-0.03824
C	-7.81768	-3.04028	0.072091
N	-6.47053	-3.4115	0.044414
O	-8.71302	-3.87168	0.124845
O	-4.26493	-3.01854	-0.13192
C	-6.14033	-4.84311	0.049228
H	-5.48004	-5.06598	0.889092
H	-5.62203	-5.10834	-0.87432
H	-7.07401	-5.39235	0.13599
S	2.12161	-1.74292	-0.16932
N	-2.4006	0.843595	0.219238
N	0.001456	1.400806	0.340621
C	0.011391	2.848872	0.540741
H	0.73475	3.069393	1.332712
H	-0.98143	3.122122	0.907855
N	2.401476	0.837461	0.240733
C	3.125407	-0.26684	0.062078
C	-3.12445	-0.26039	0.03731
H	0.259128	3.409381	-0.36792

Compound	State	B3LYP/6-31G**
I	Neutral	-1230.36166 (a. u.)
II	Neutral	-1198.27925 (a. u.)
III	Neutral	-1249.00074 (a. u.)
IV	Neutral	-3280.44996 (a. u.)

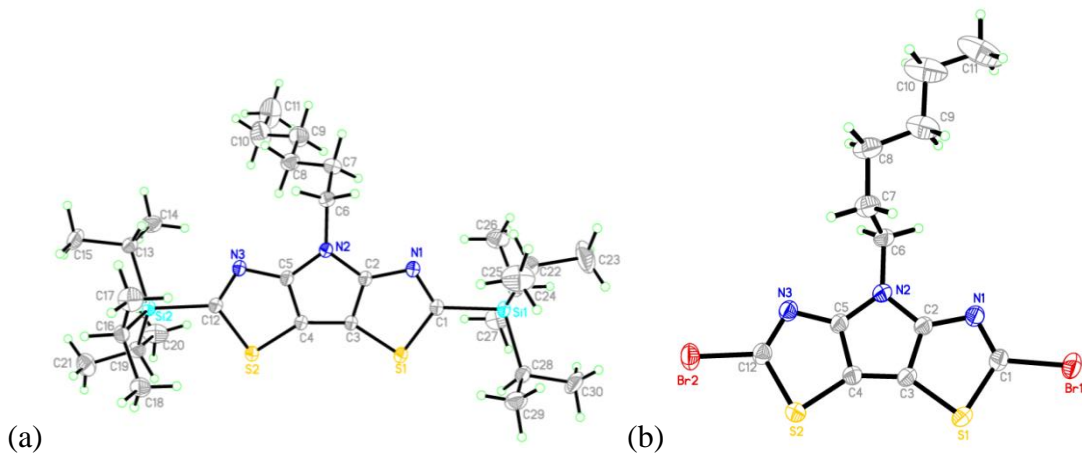


Figure S32. ORTEP drawing of (a) 2a; select bond lengths (Å): N(1)-C(1) 1.325(3), C(1)-Si(1) 1.885(2), C(12)-Si(2) 1.883(2), S(1)-C(1) 1.768(2), S(2)-C(4) 1.716(2), S(1)-C(3) 1.718(2), S(2)-C(12) 1.772(2), N(1)-C(2) 1.361(3), N(2)-C(2) 1.383(3), N(2)-C(5) 1.382(3), N(3)-C(5) 1.361(3), N(3)-C(12) 1.324(3); (b) 3a; select bond lengths (Å): N(1)-C(1) 1.288(3), C(1)-Br1(1) 1.875(3), C(12)-Br(2) 1.869(3), S(1)-C(1) 1.740(3), S(2)-C(4) 1.723(3), S(1)-C(3) 1.726(2), S(2)-C(12) 1.738(3), N(1)-C(2) 1.363(3), N(2)-C(2) 1.372(3), N(2)-C(5) 1.371(3), N(3)-C(5) 1.368(3), N(3)-C(12) 1.295(3). (50% Probability level, hydrogen atoms drawn arbitrarily small)

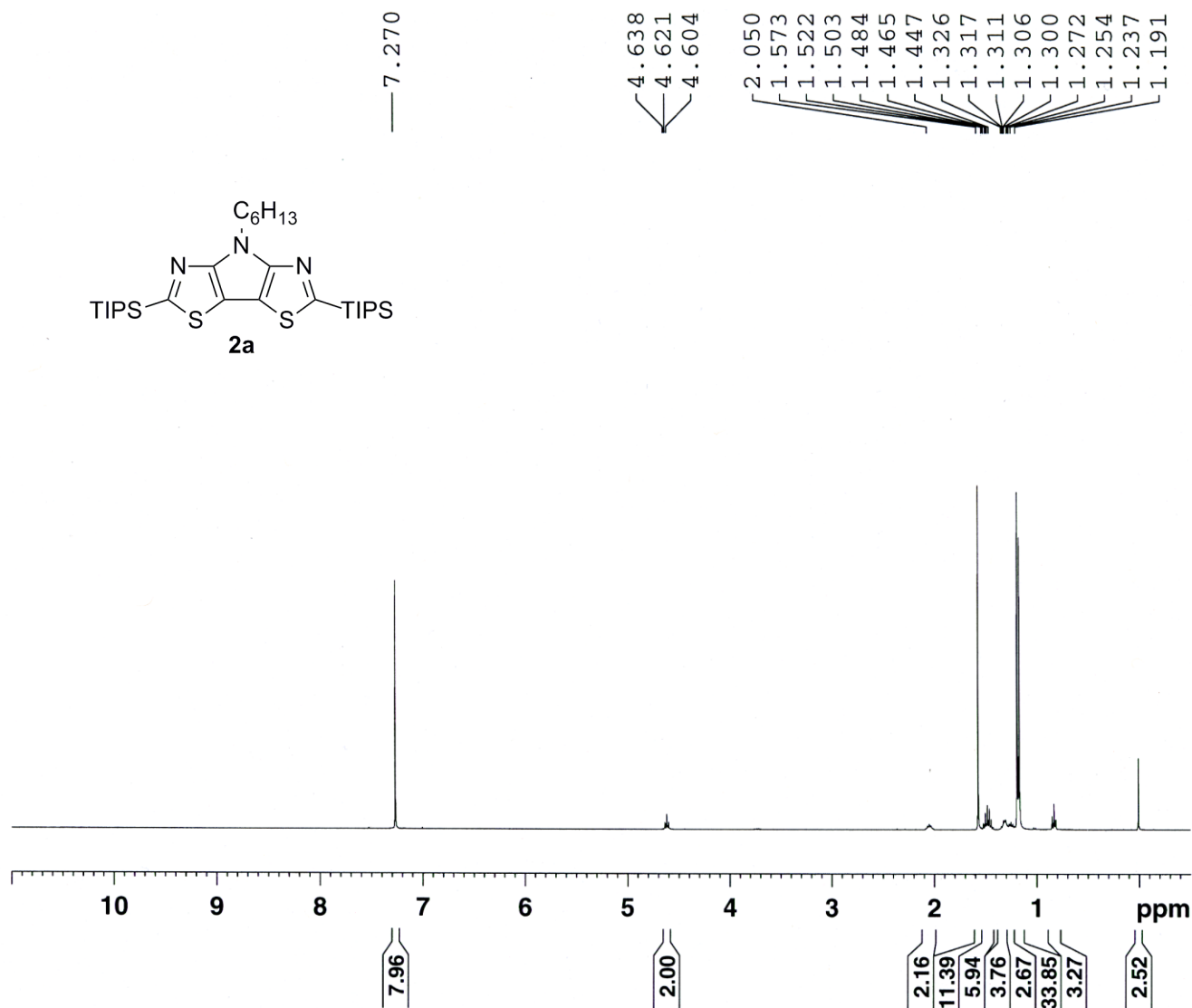


Figure S33. ^1H NMR spectrum of **2a**.

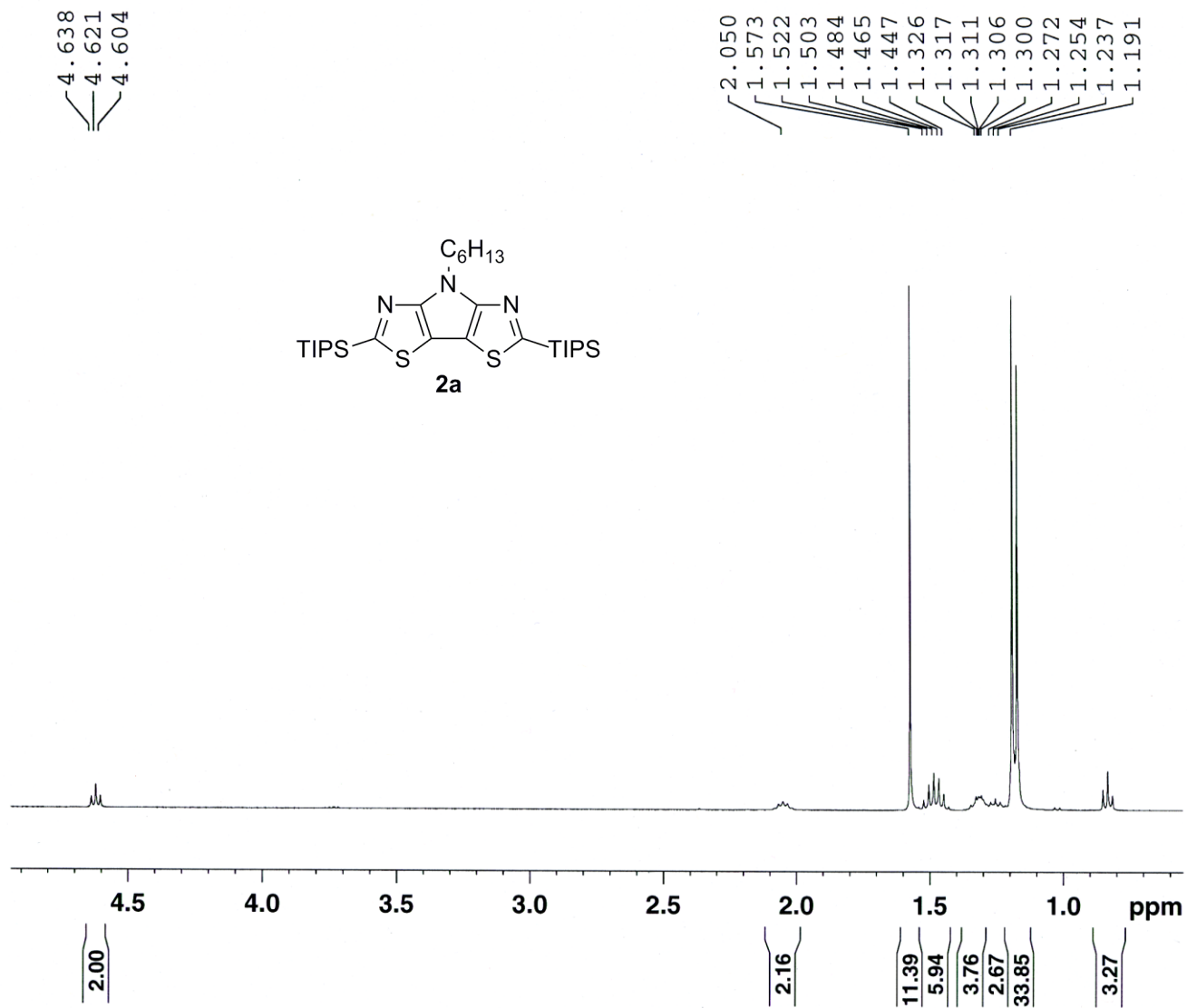


Figure S34. ^1H NMR (400 MHz, CDCl_3) spectrum (aliphatic region) of 2a.

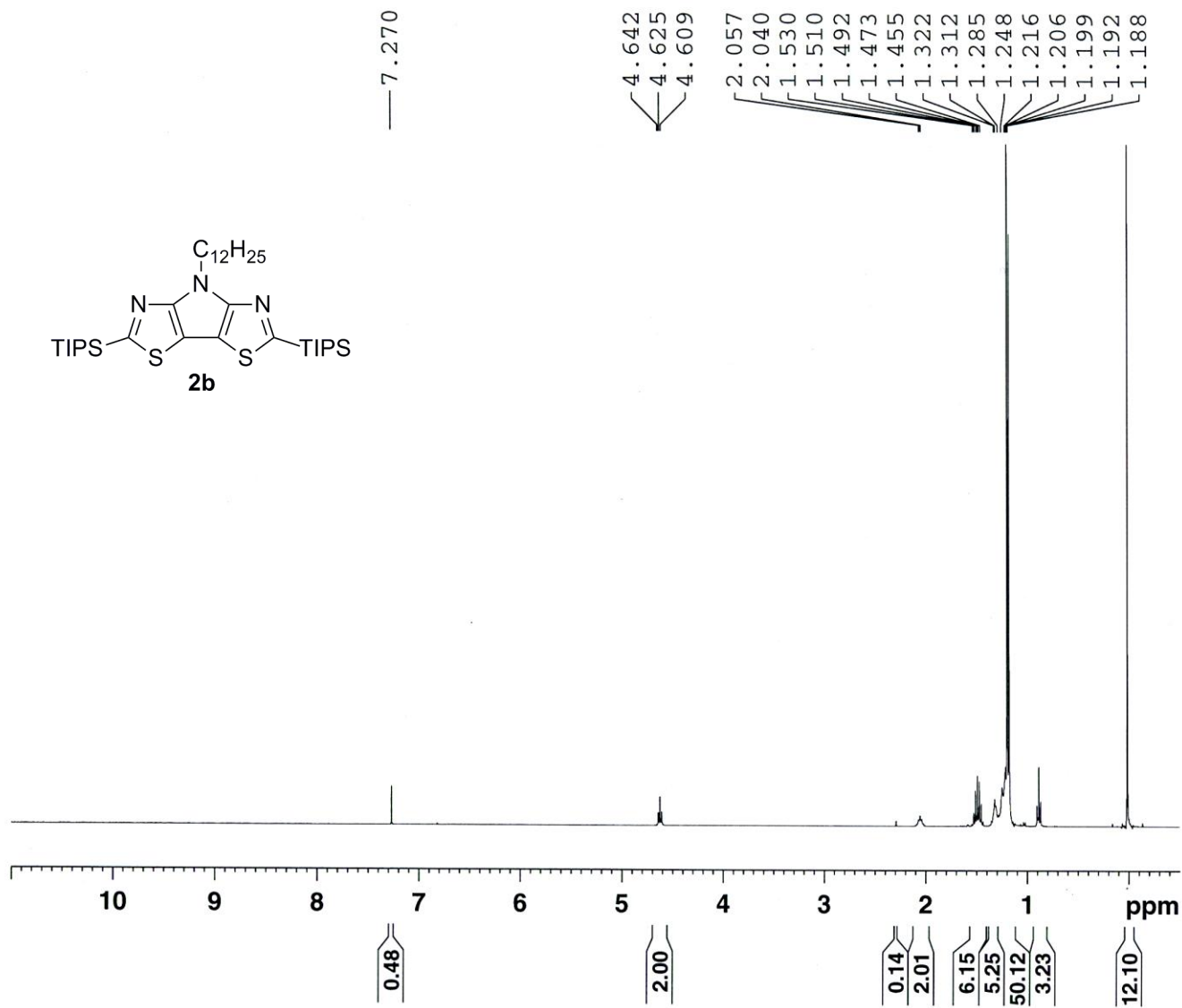


Figure S35. ¹H NMR (400 MHz, CDCl₃) spectrum of **2b**.

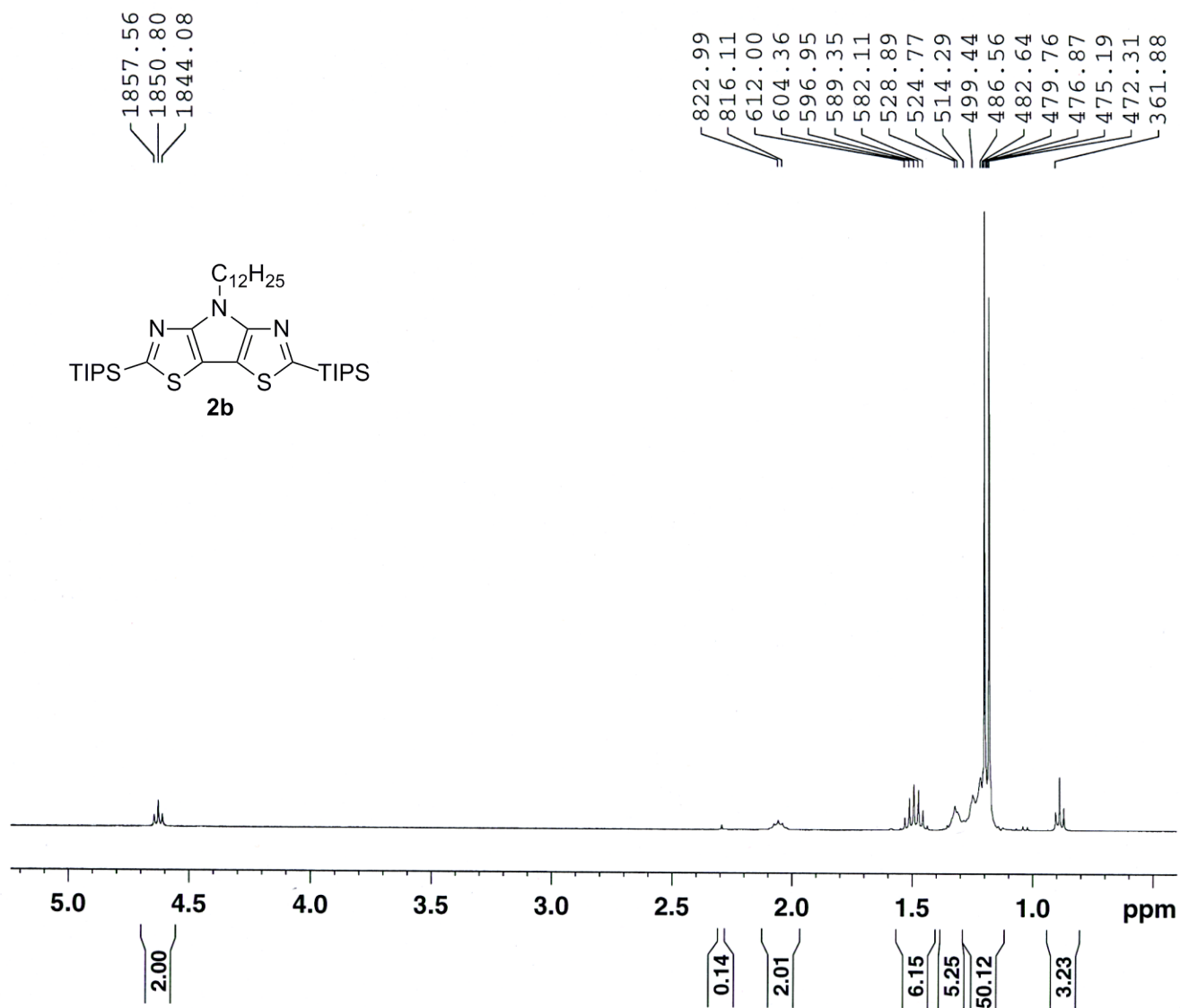


Figure S36. ¹H NMR (400 MHz, CDCl₃) spectrum (aliphatic region) of **2b**.

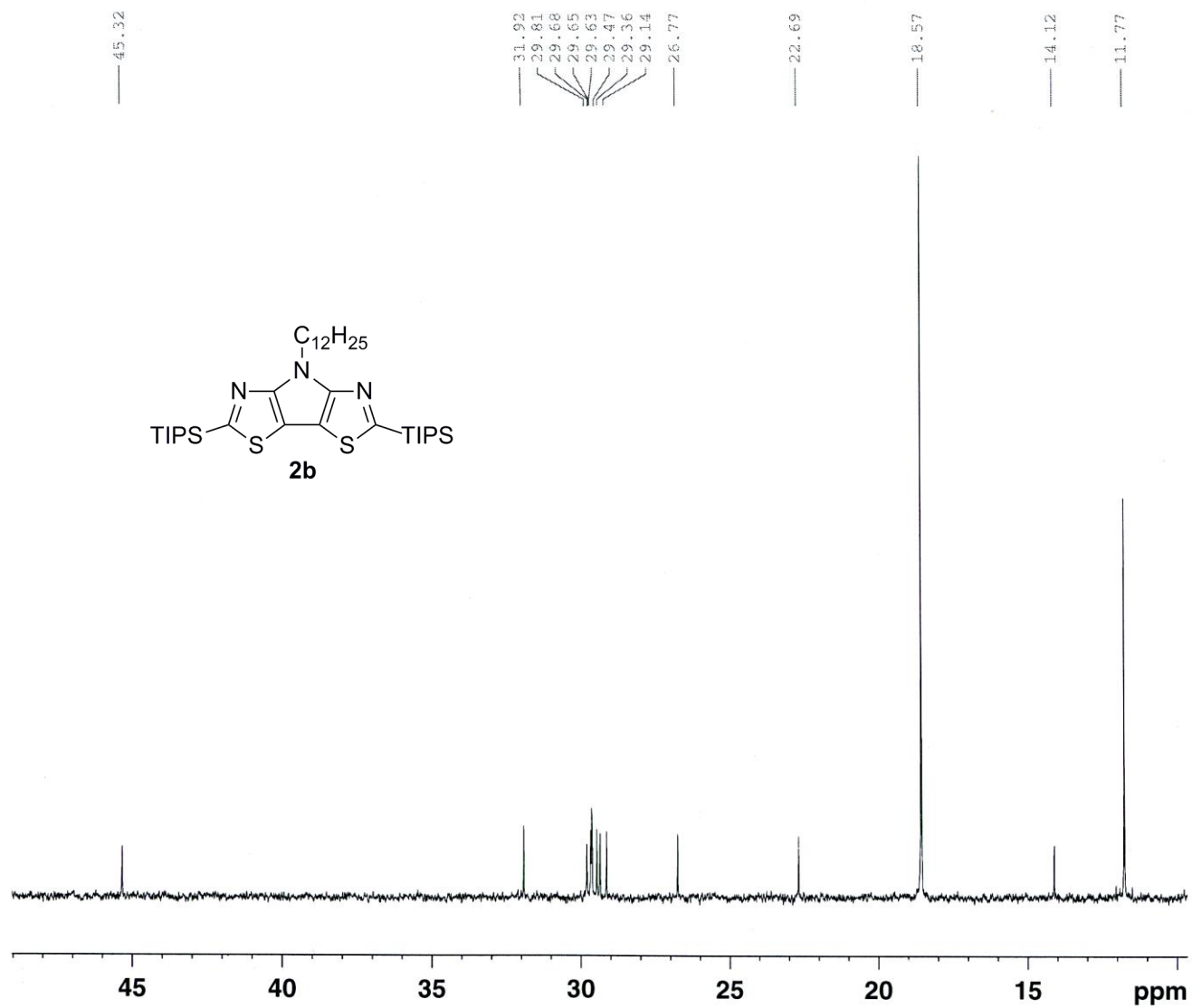


Figure S38. $^{13}C\{^1H\}$ NMR (100 MHz, $CDCl_3$) spectrum (aliphatic region) of **2b**.

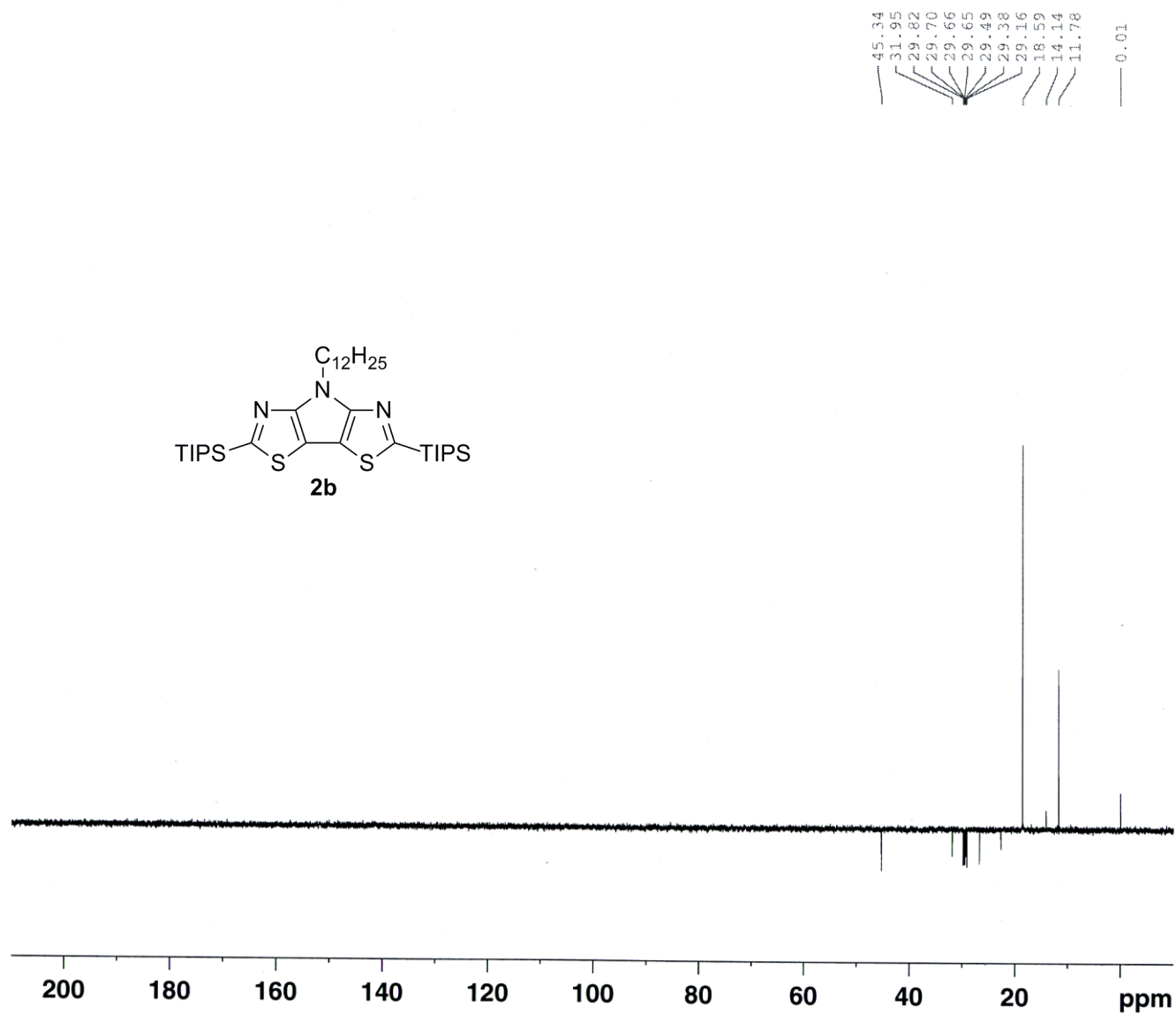


Figure S39. DEPT-135 NMR spectrum of **2b**.

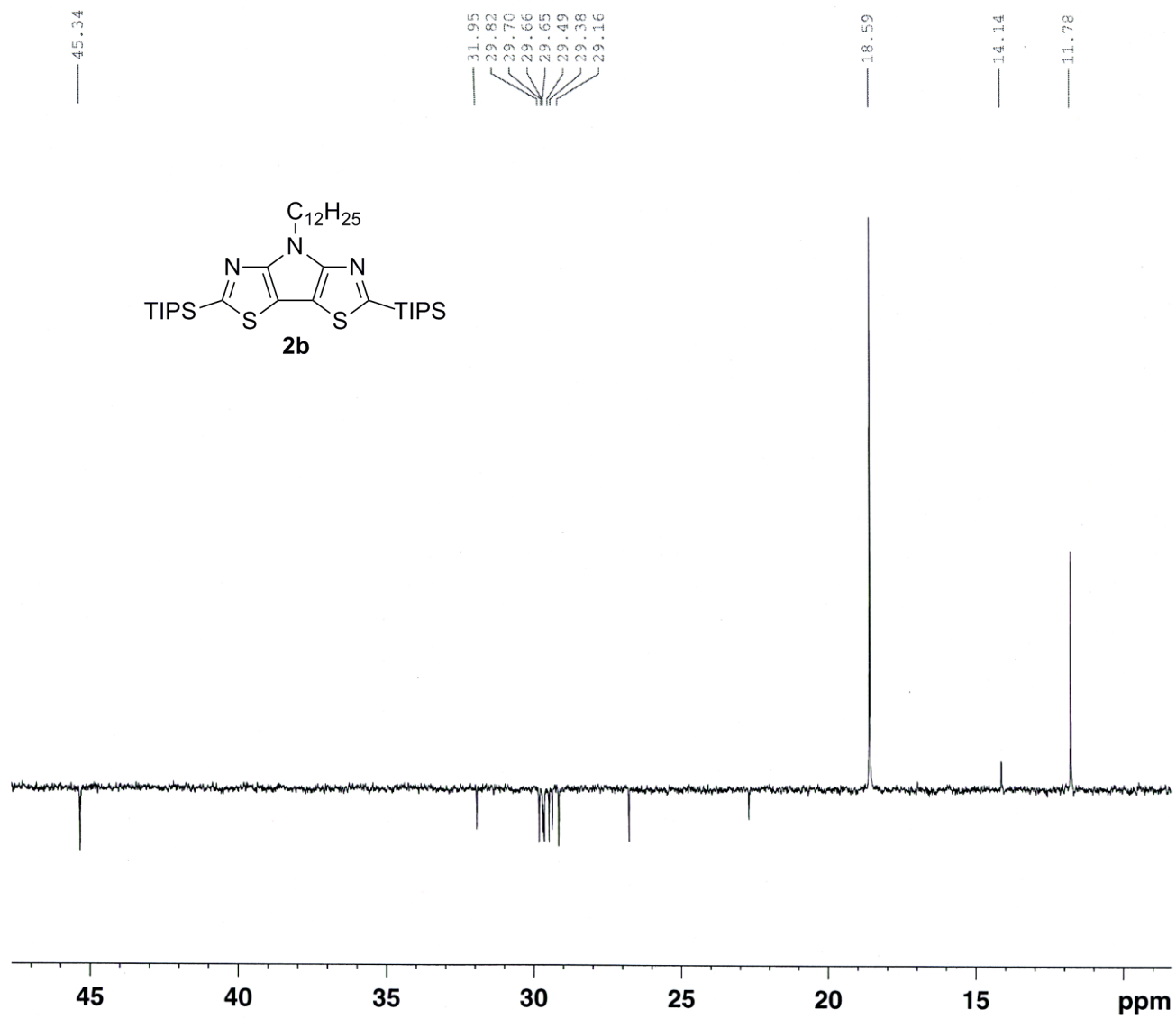


Figure S40. DEPT-135 NMR spectrum (aliphatic region) of 2b.

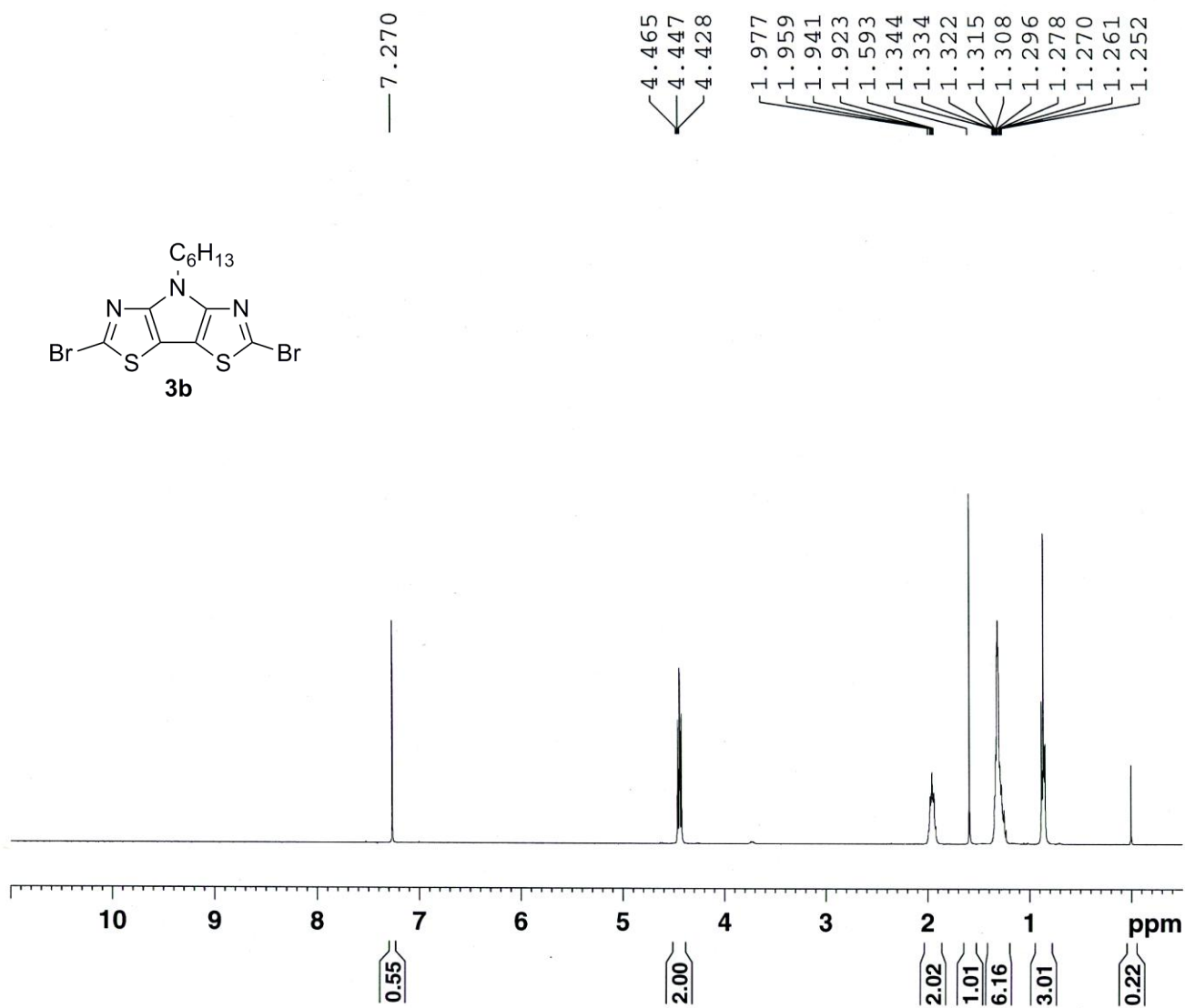


Figure S41. ^1H NMR (400 MHz, CDCl_3) spectrum of **3a**.

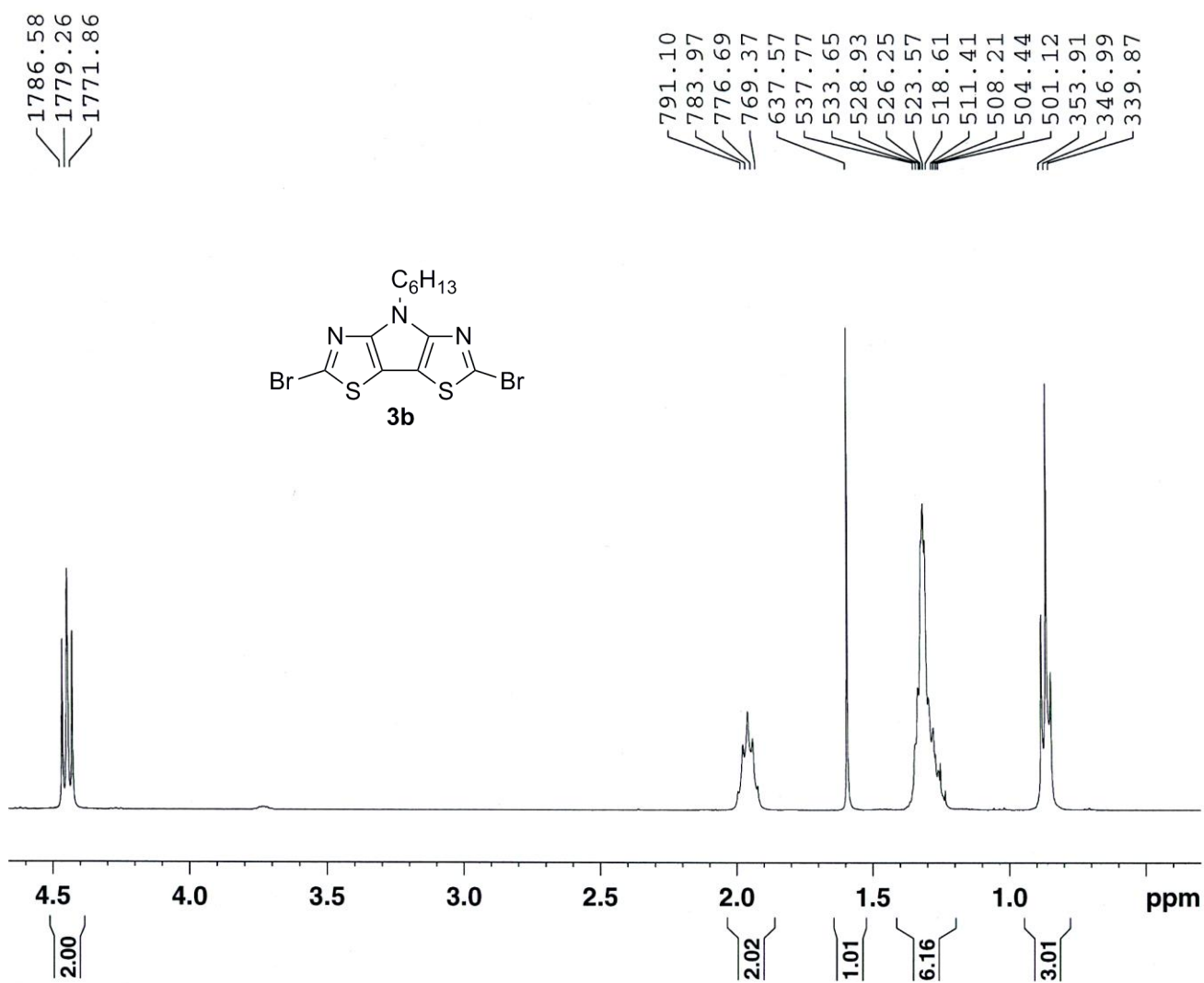


Figure S42. ¹H NMR (400 MHz, CDCl₃) spectrum (aliphatic region) of **3a**.

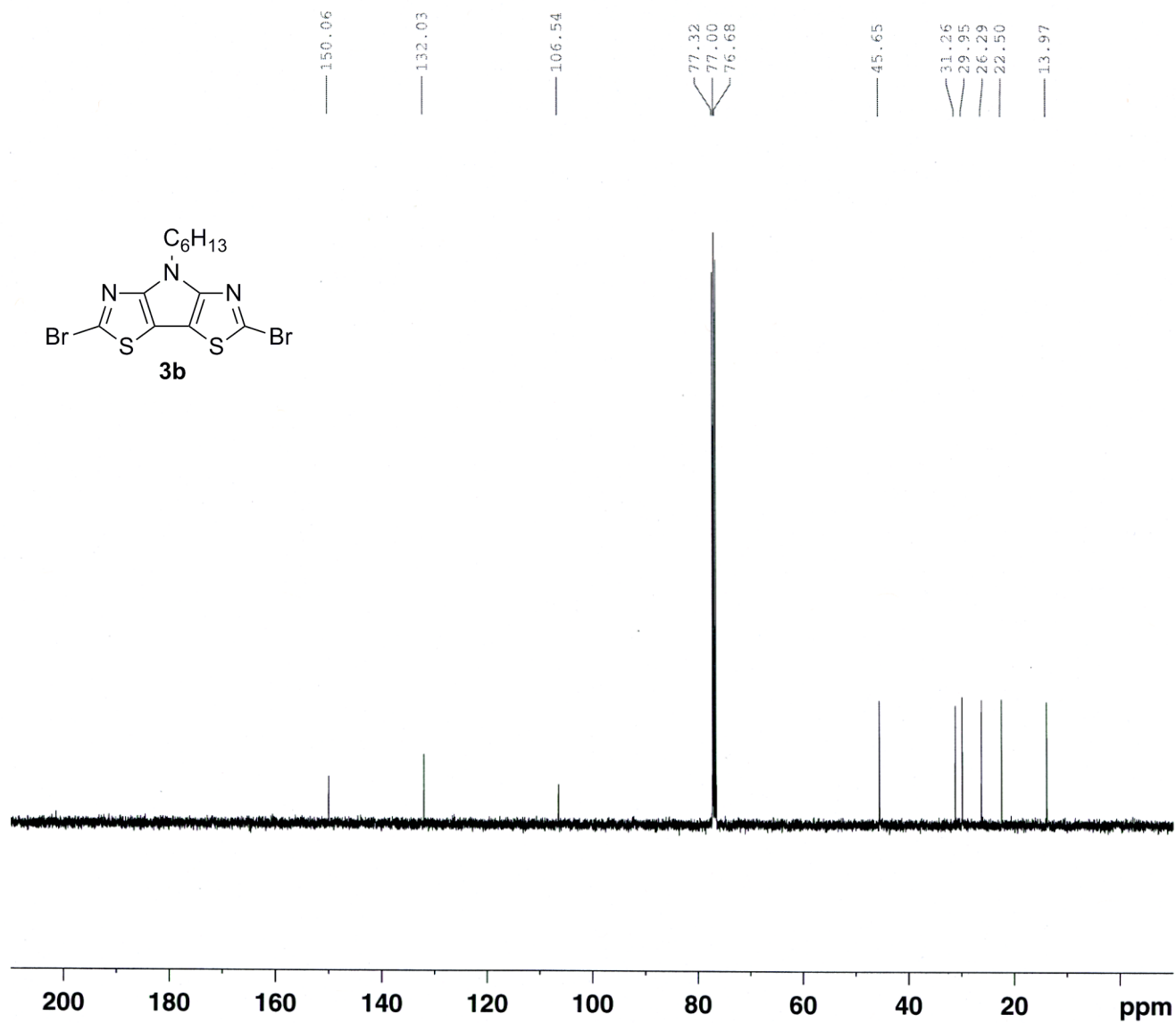


Figure S43. $^{13}\text{C}\{^1\text{H}\}$ NMR (100 MHz, CDCl_3) spectrum of **3a**.

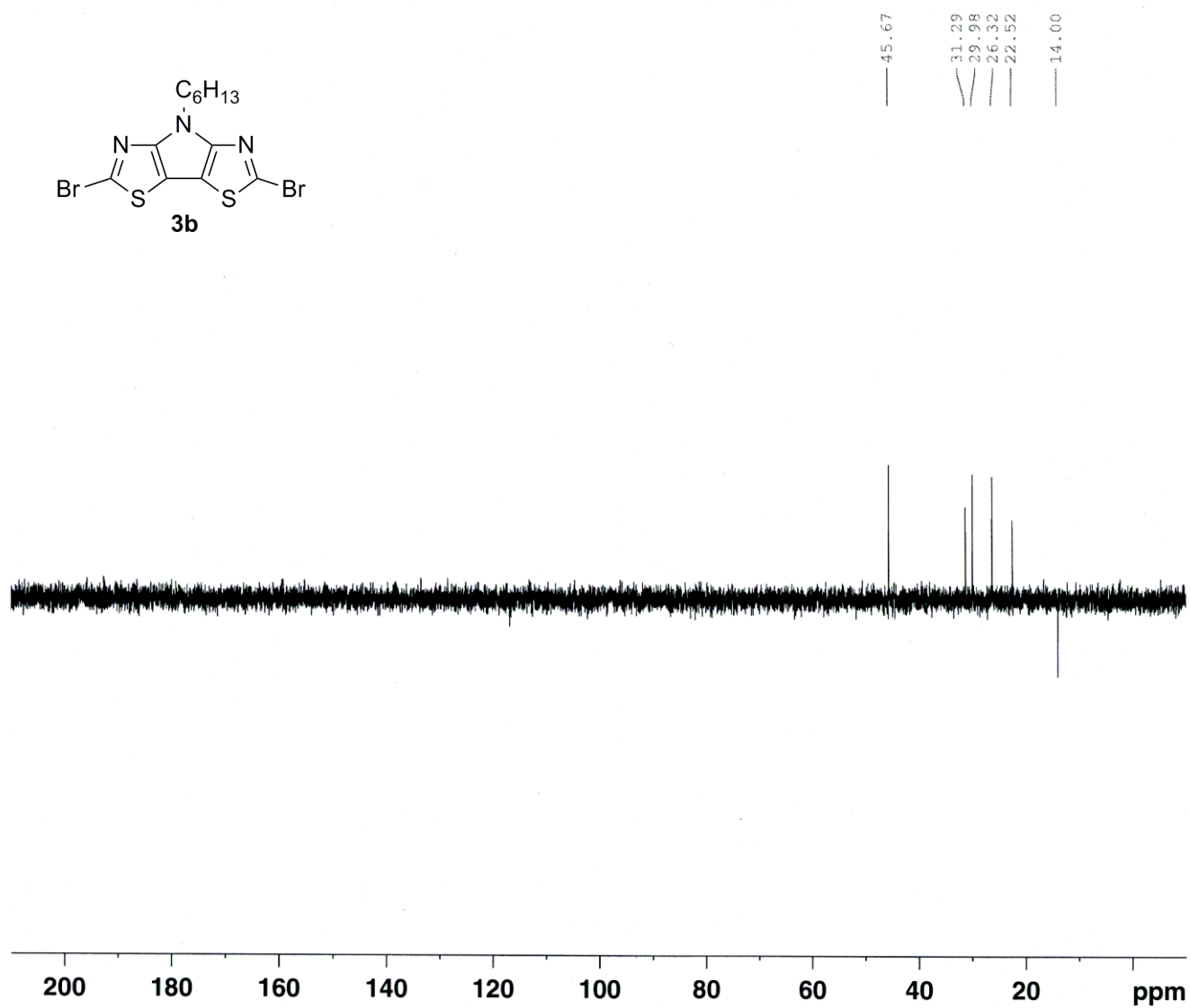


Figure S44. DEPT-135 spectrum of 3a.

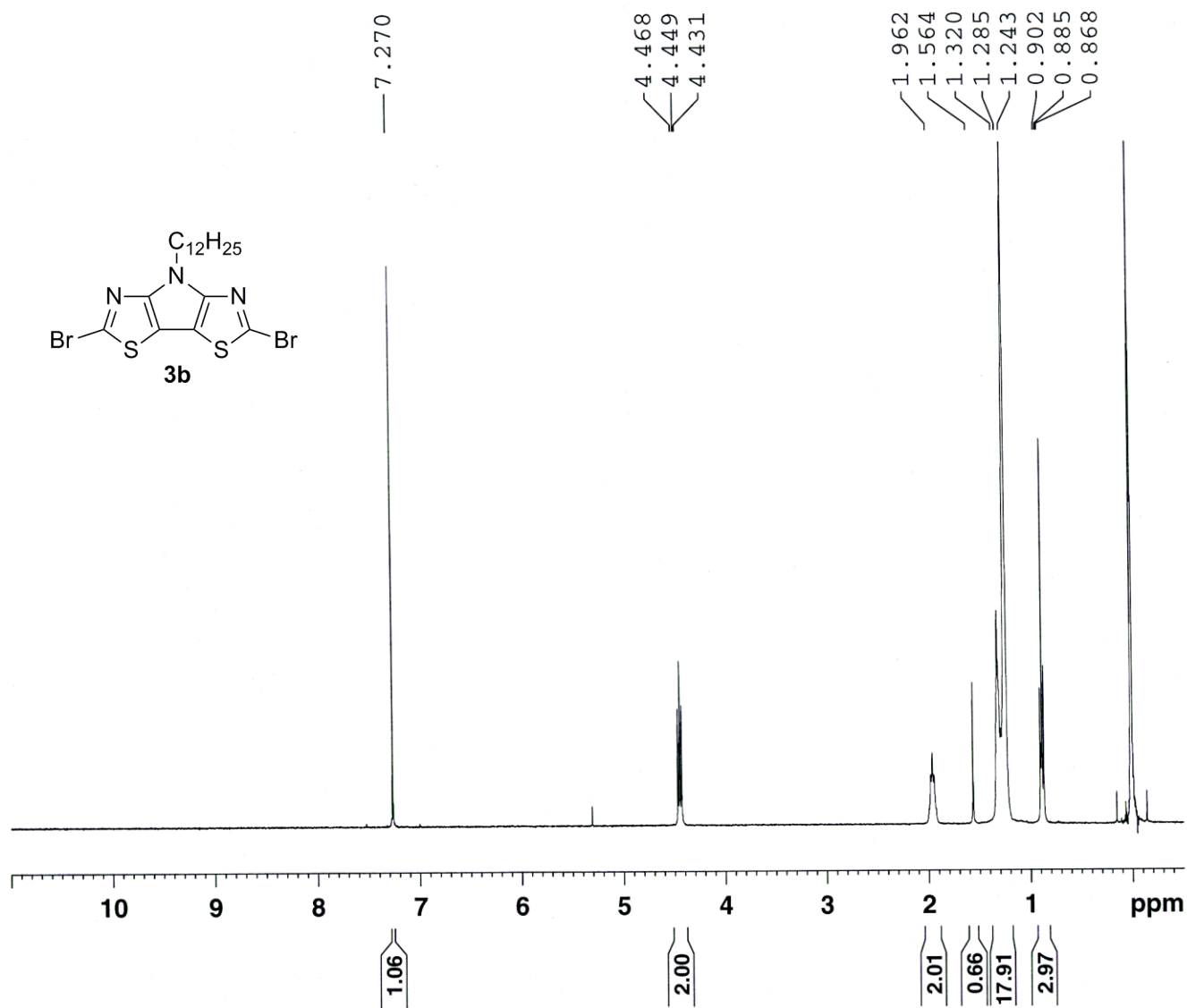


Figure S45. ^1H NMR (400 MHz, CDCl_3) spectrum of 3b.

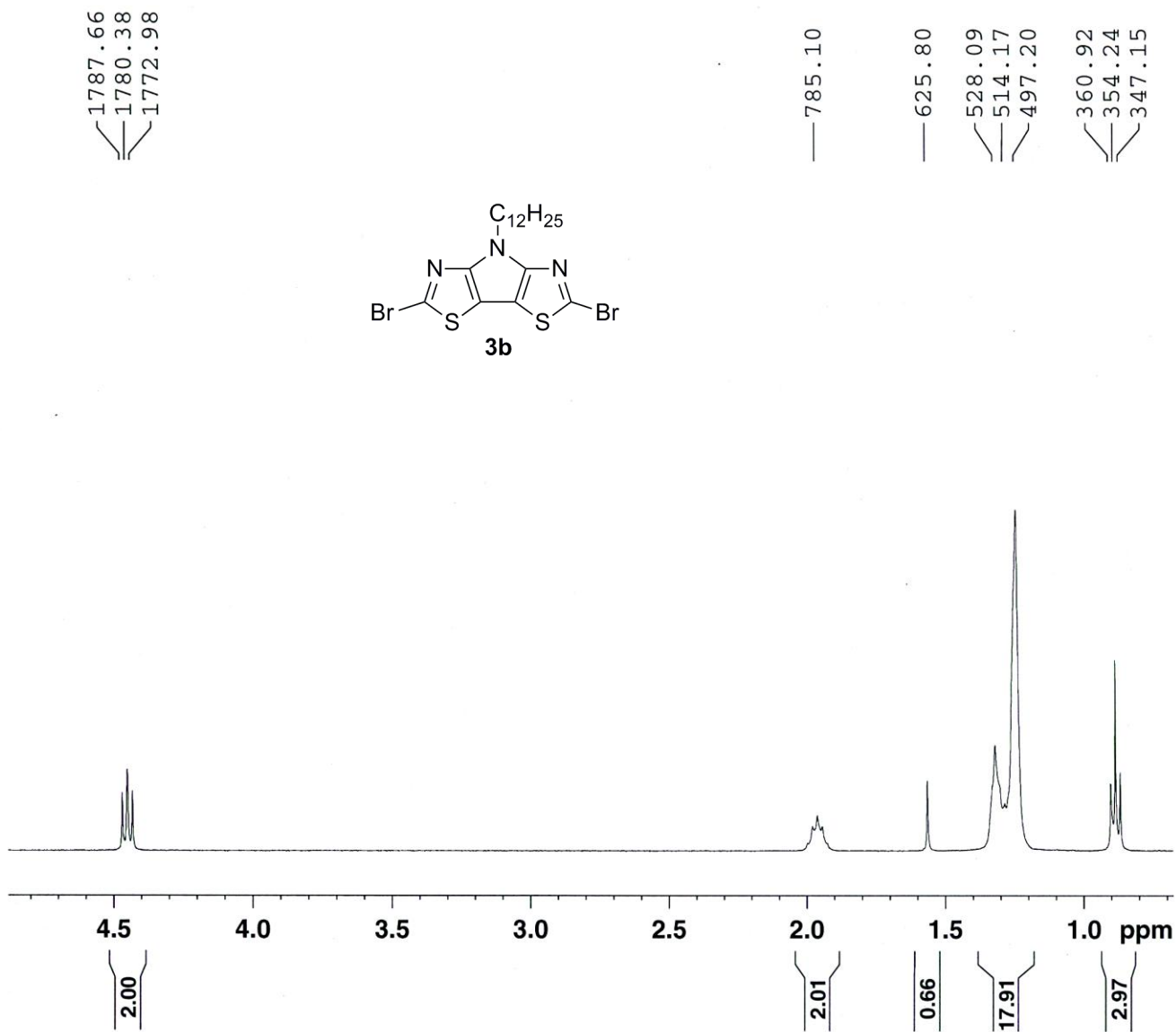


Figure S46. ¹H NMR (400 MHz, CDCl₃) spectrum (aliphatic region) of 3b.

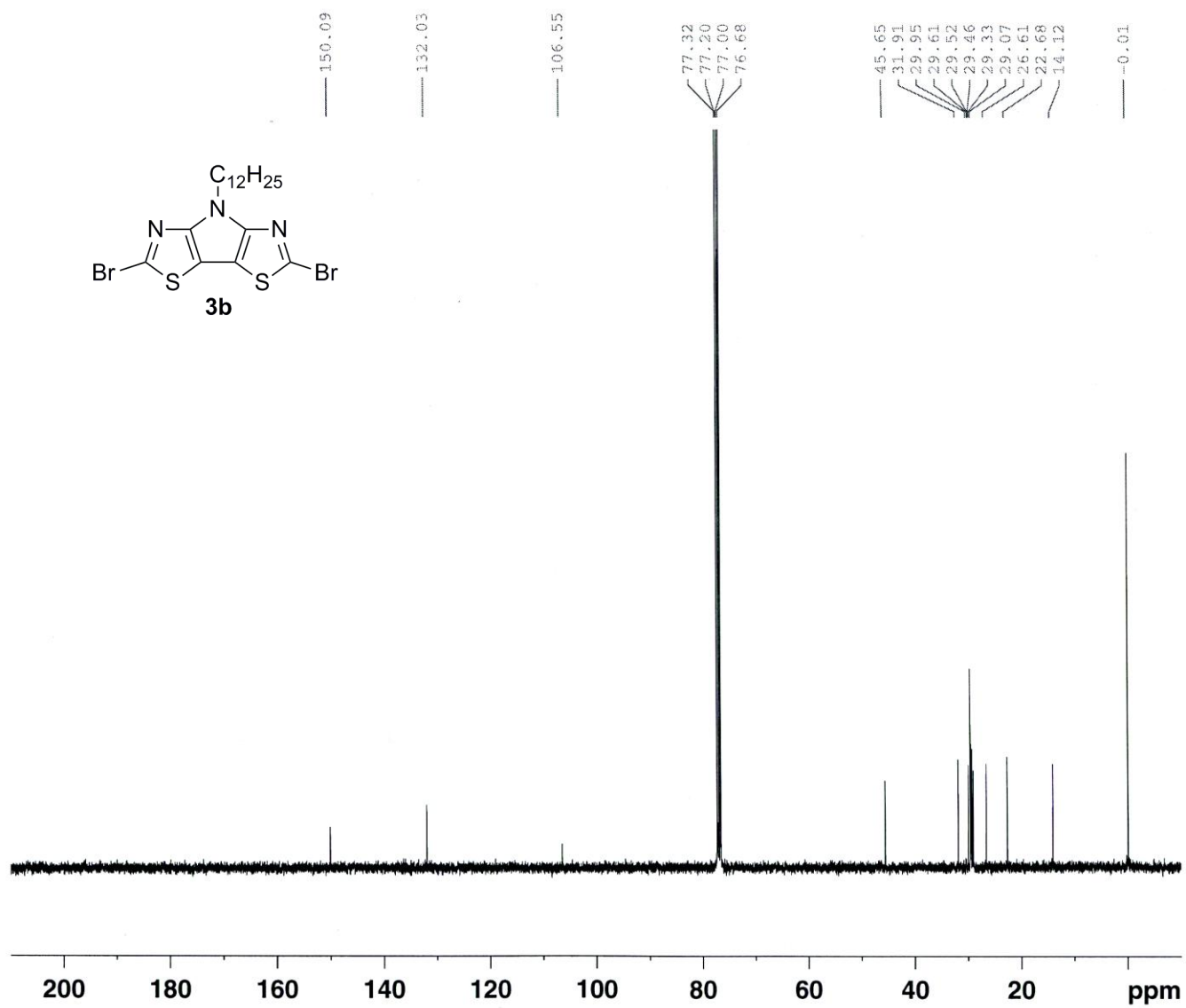


Figure S47. $^{13}\text{C}\{^1\text{H}\}$ NMR (100 MHz, CDCl_3) spectrum of **3b**.

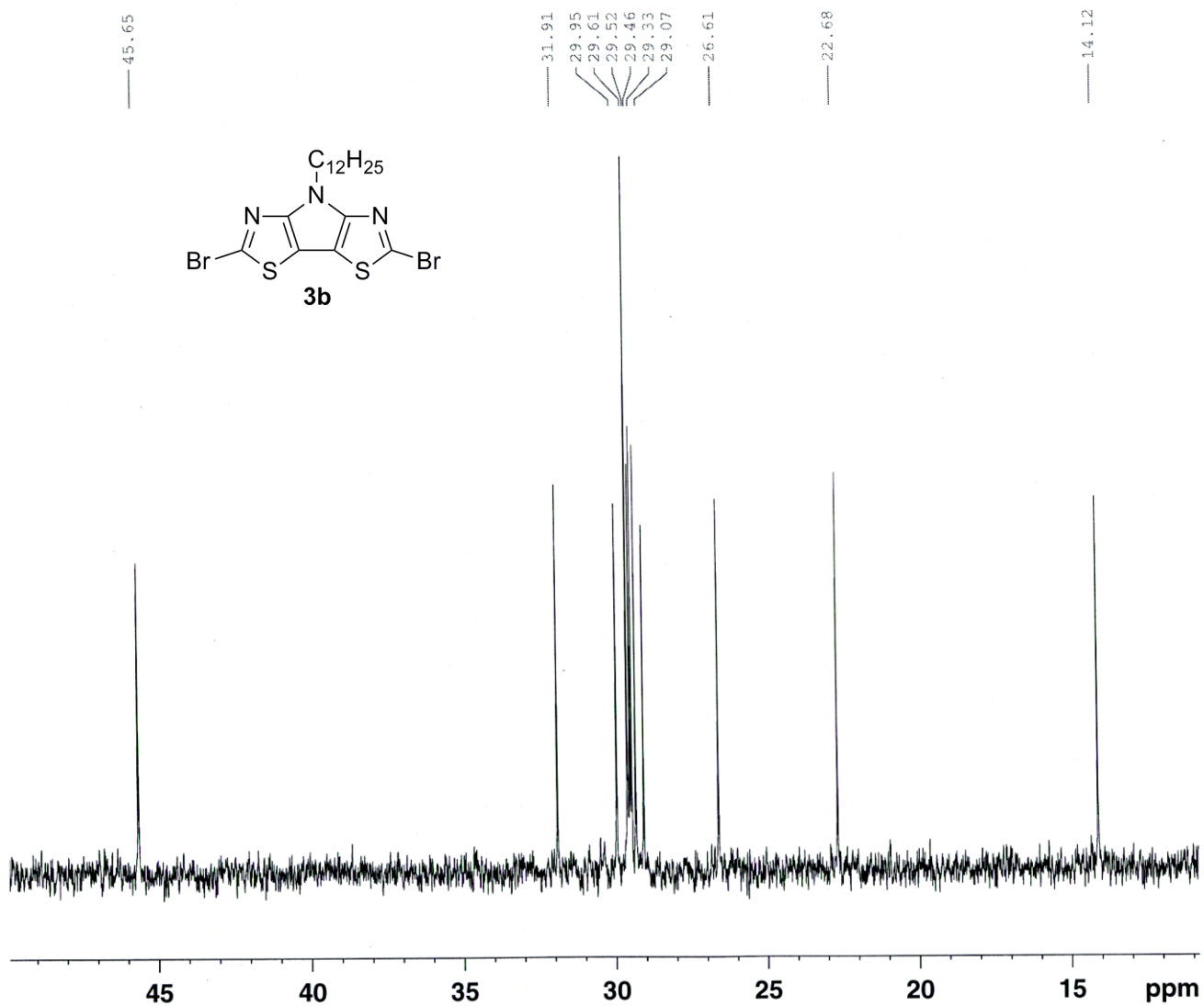


Figure S48. $^{13}\text{C}\{^1\text{H}\}$ NMR (100 MHz, CDCl_3) spectrum (aliphatic region) of **3b**.

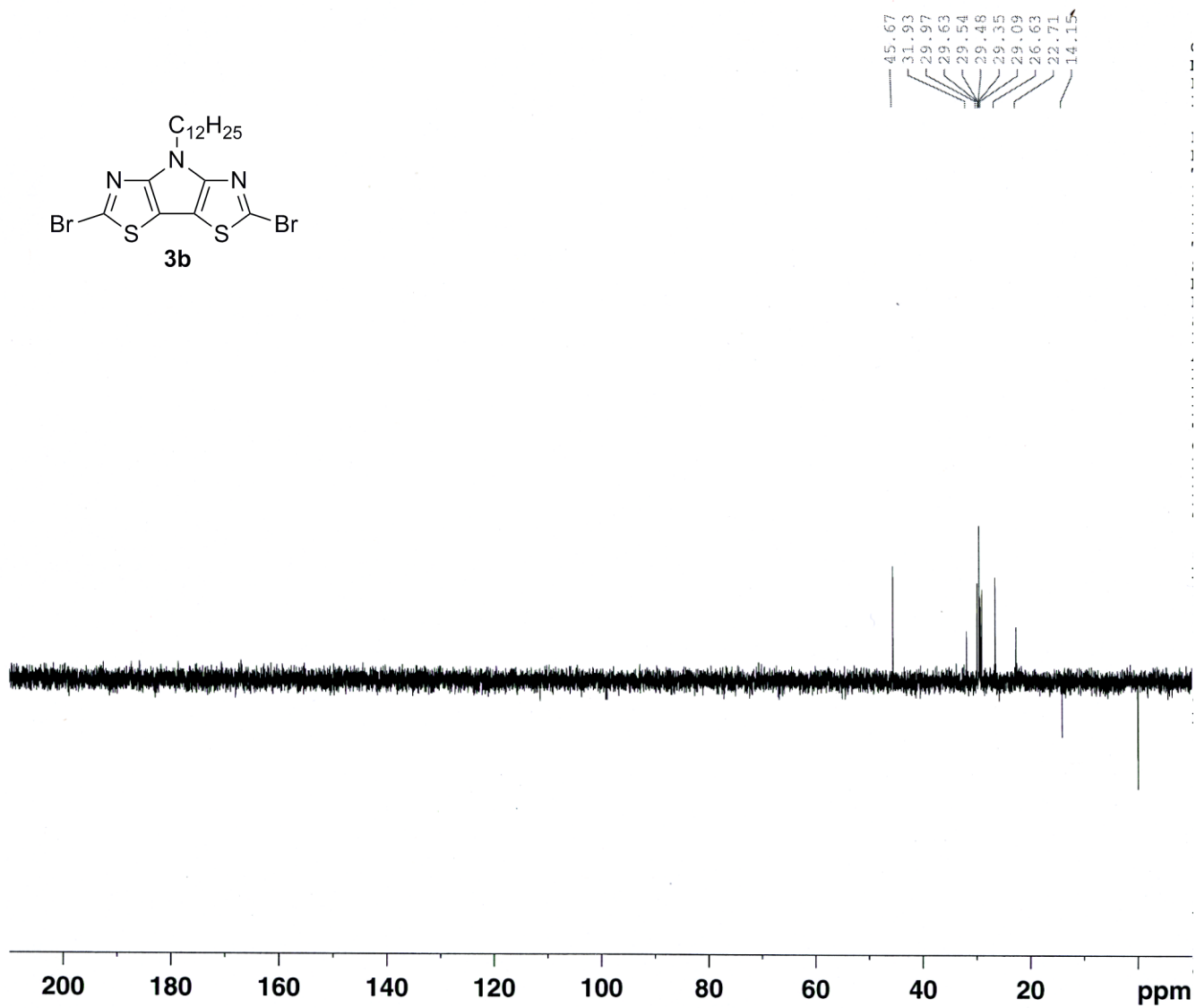


Figure S49. $^{13}\text{C}\{^1\text{H}\}$ NMR (100 MHz, CDCl_3) spectrum (aliphatic region) of **3b**.

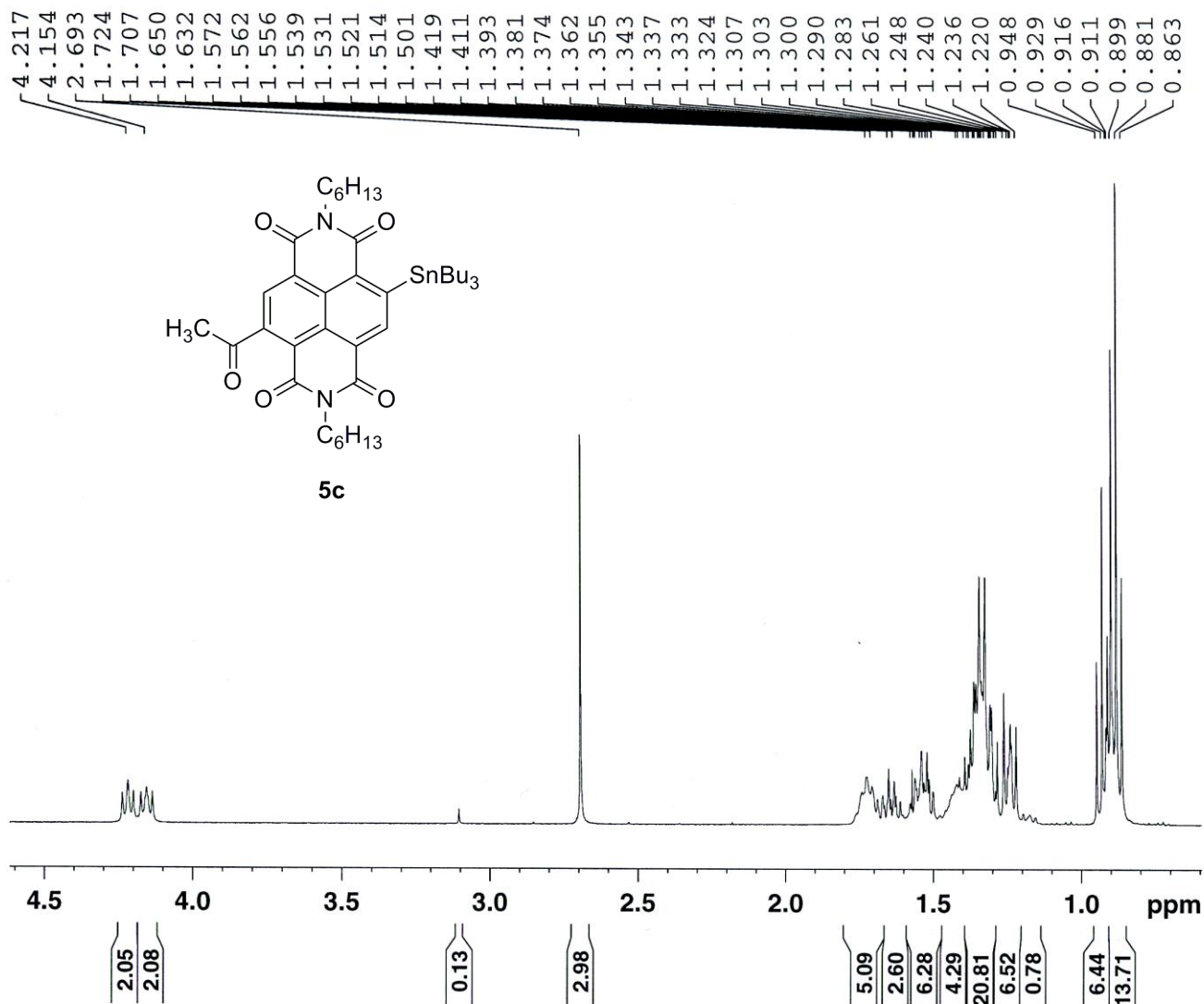


Figure S51. ^1H NMR (400 MHz, CDCl_3) spectrum (aliphatic region) of **5c**.

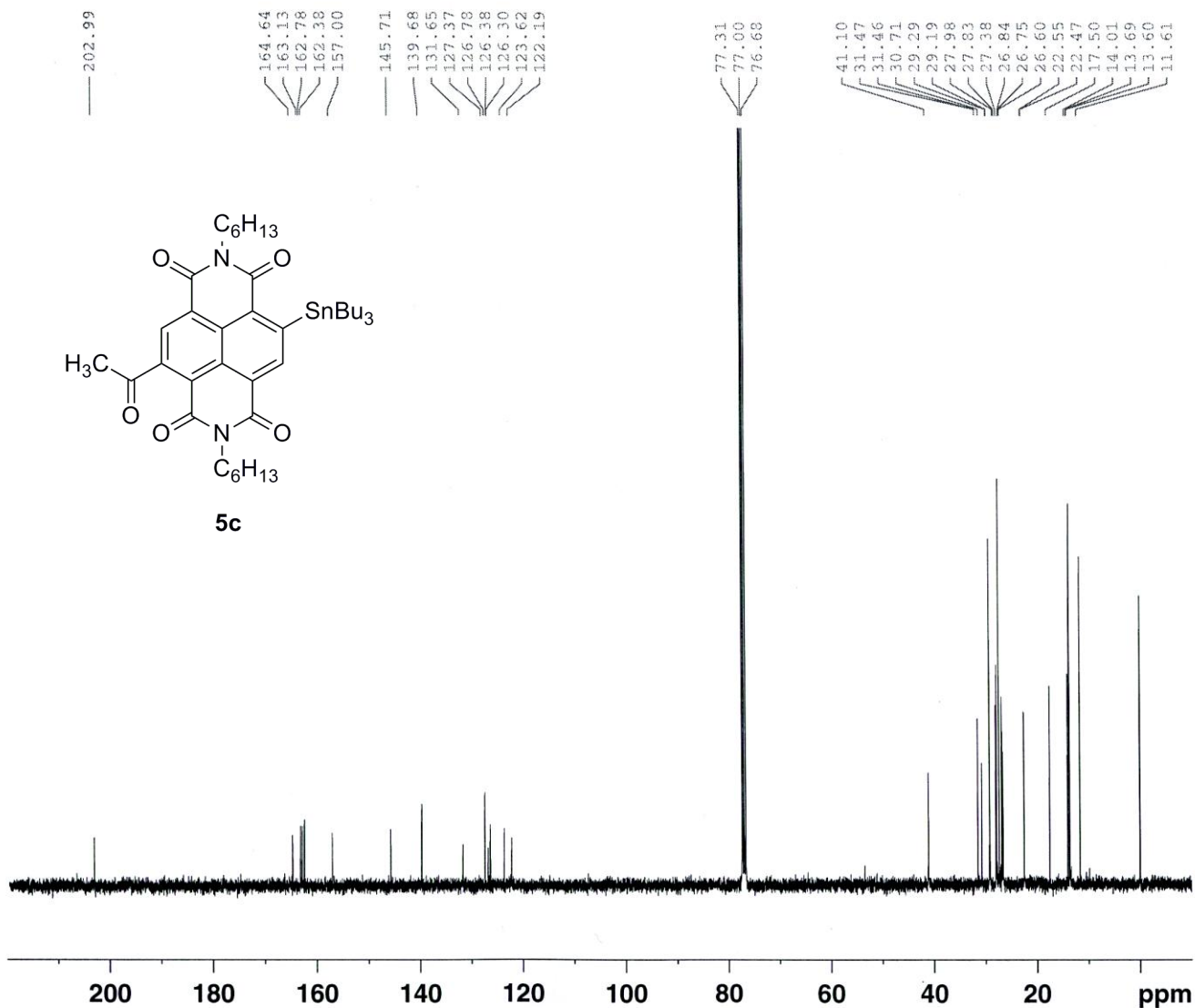


Figure S52. $^{13}\text{C}\{^1\text{H}\}$ NMR (100 MHz, CDCl_3) spectrum of **5c**.

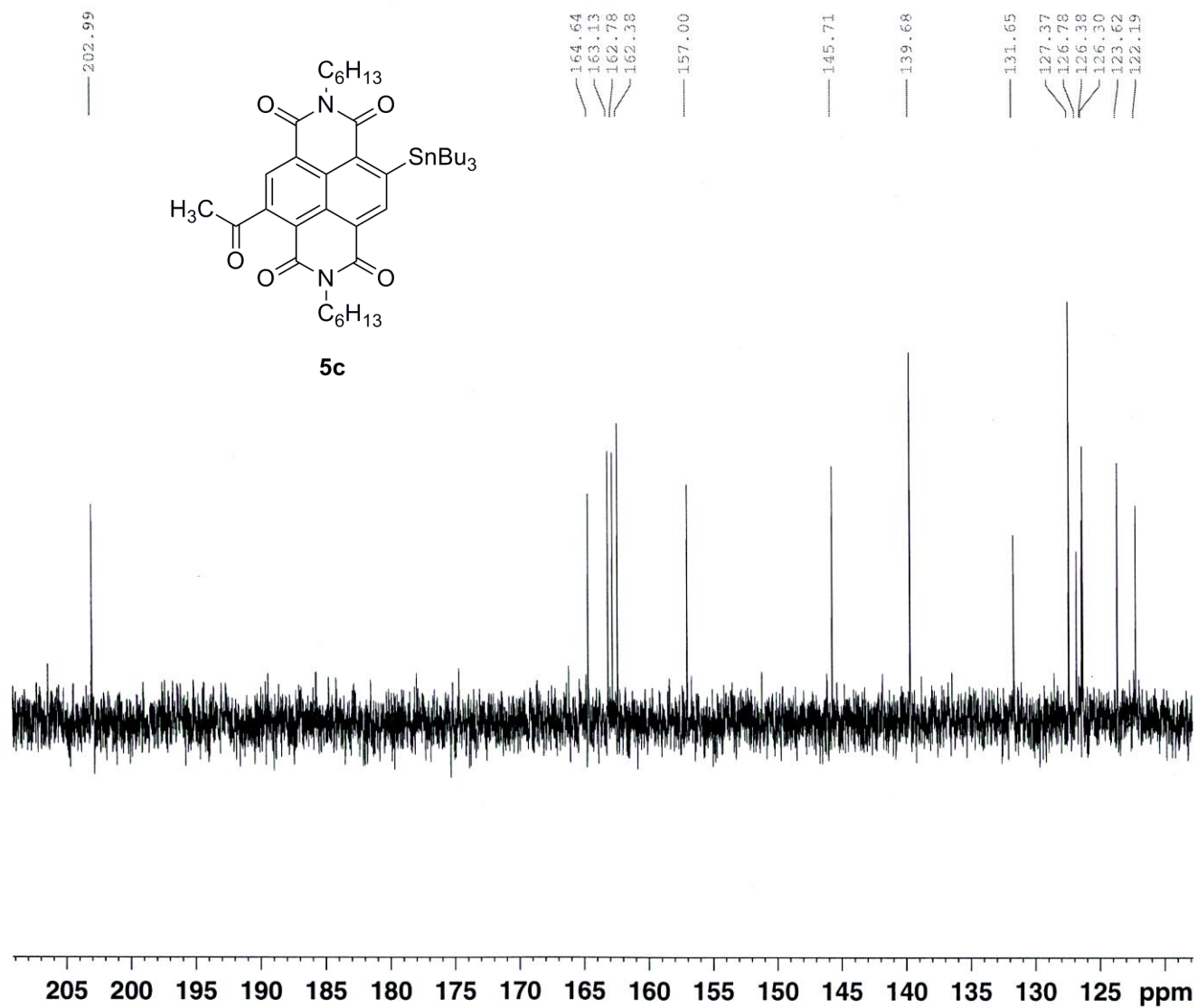


Figure S53. $^{13}\text{C}\{^1\text{H}\}$ NMR (100 MHz, CDCl_3) spectrum (aromatic region) of **5c**.

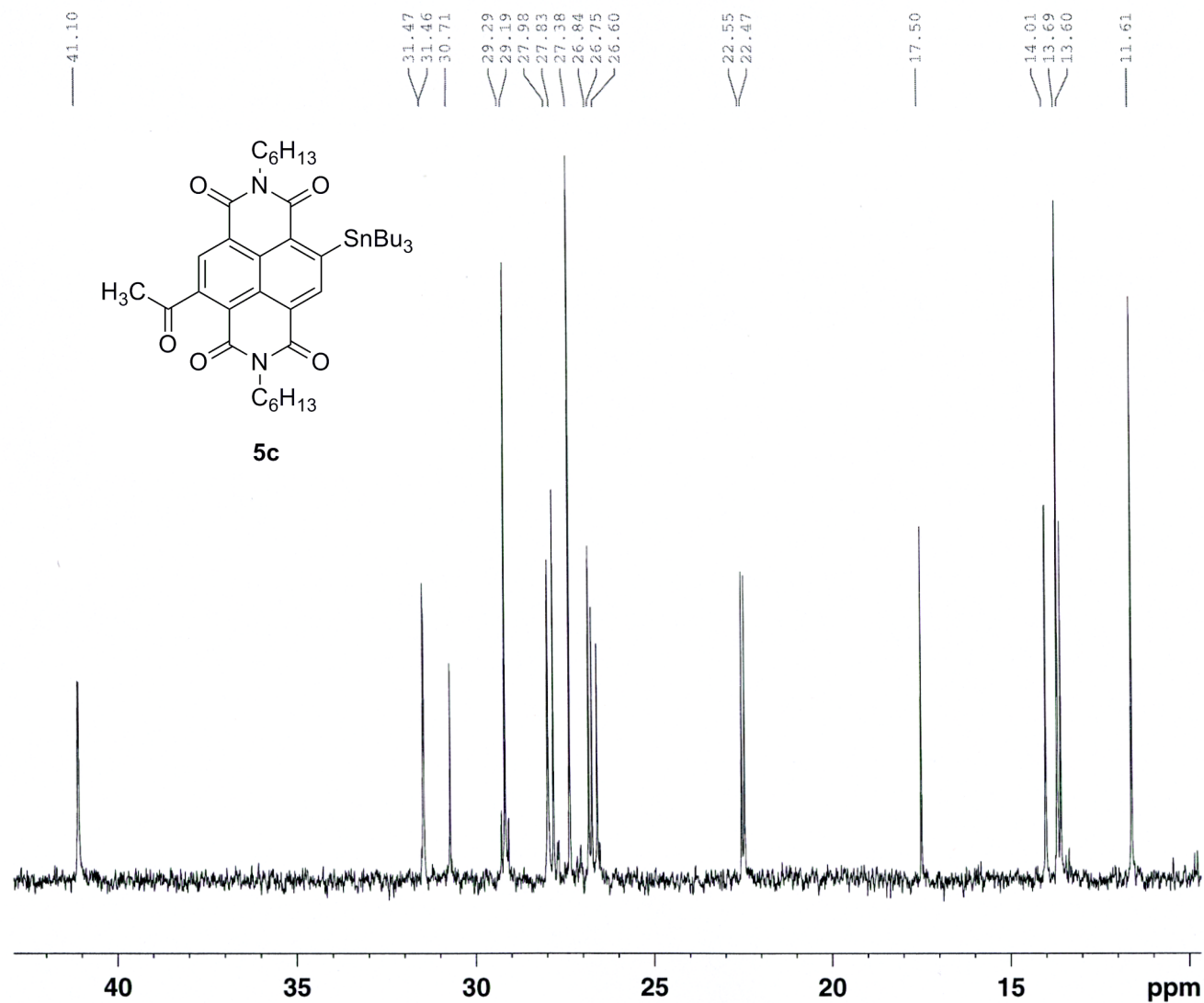


Figure S54. $^{13}C\{^1H\}$ NMR (100 MHz, $CDCl_3$) spectrum (aliphatic region) of **5c**.

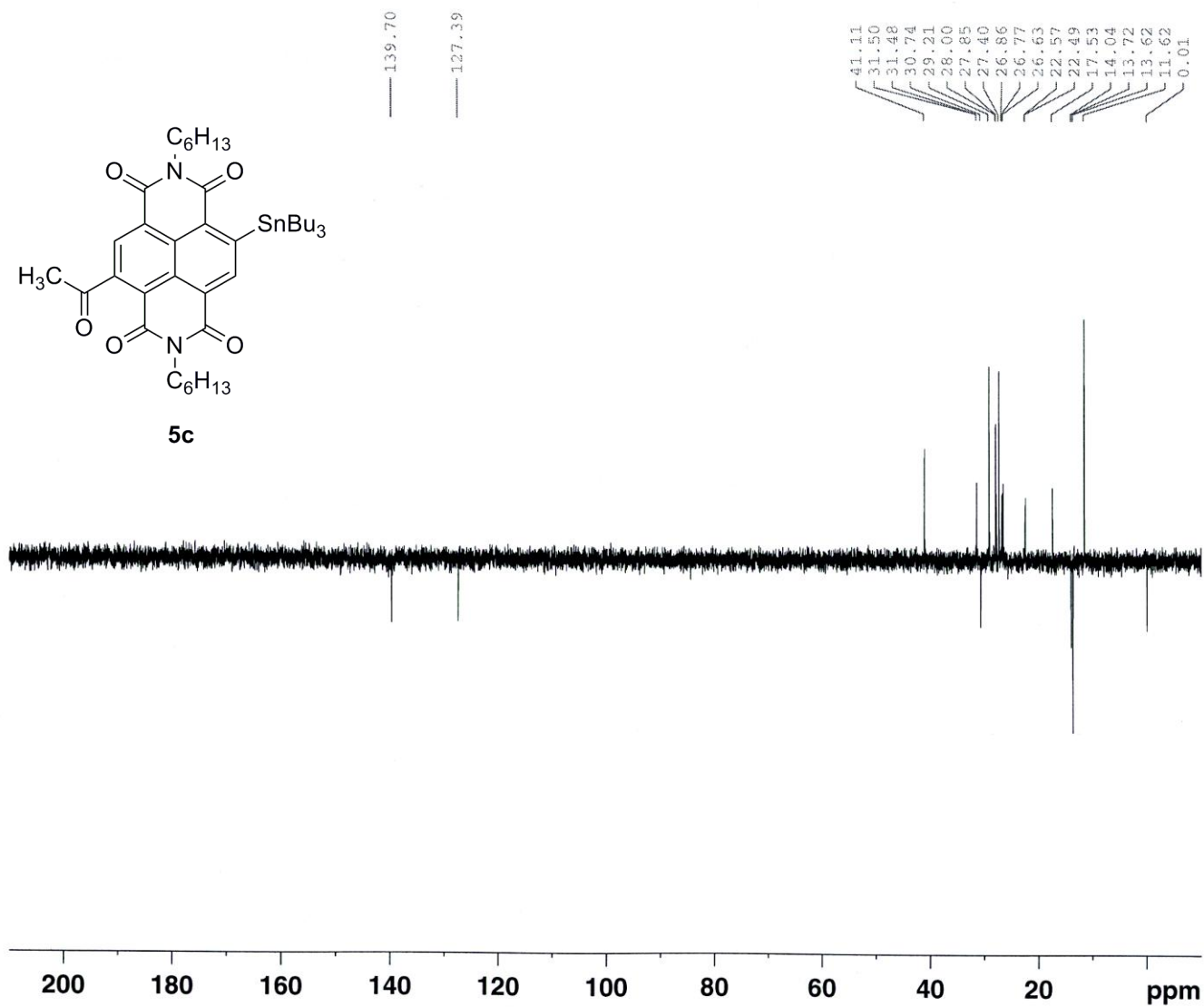


Figure S55. DEPT-135 spectrum of **5c**.

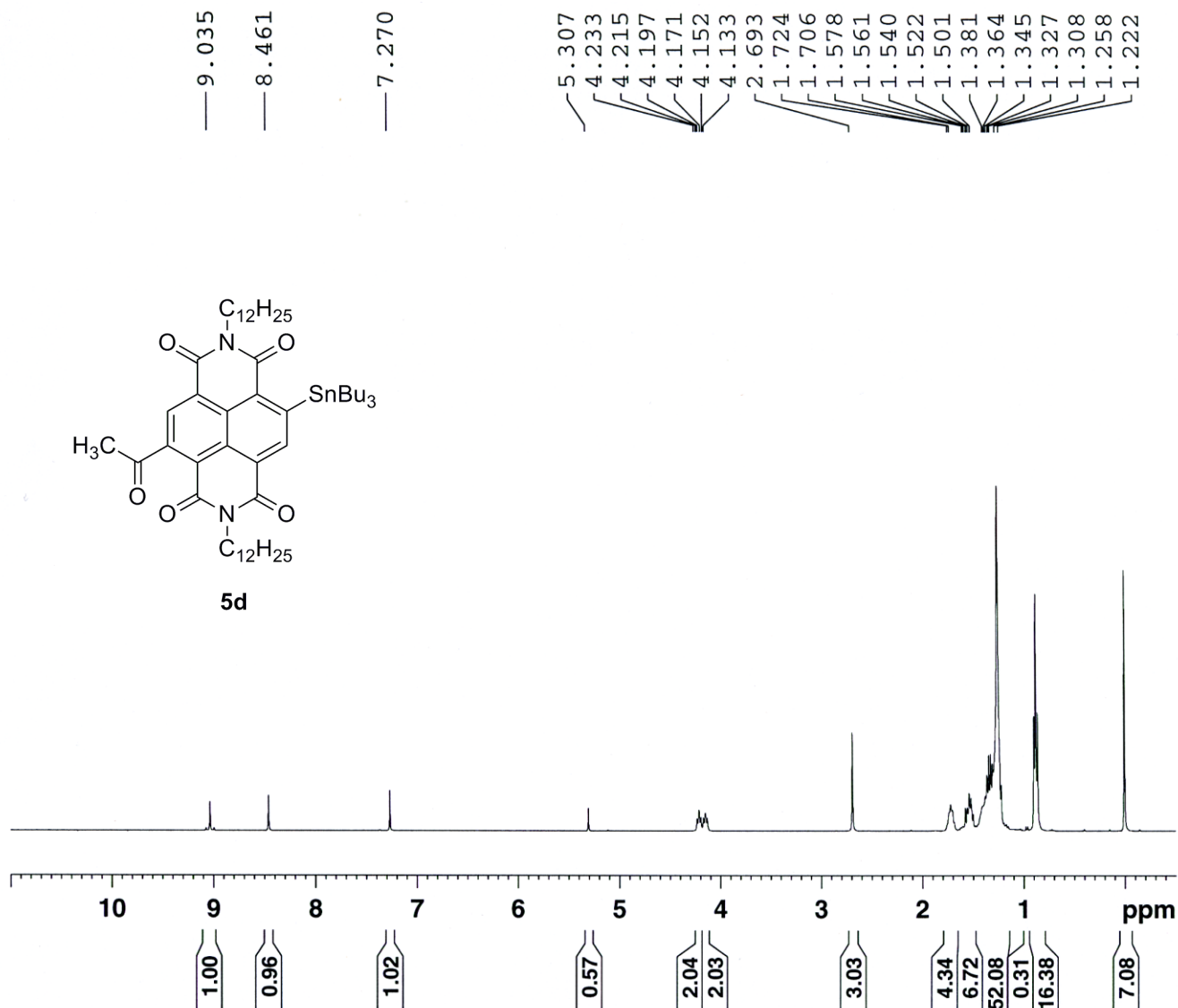


Figure S56. ^1H NMR (400 MHz, CDCl_3) spectrum of **5d** (peak at 5.31 ppm belongs to residual CH_2Cl_2).

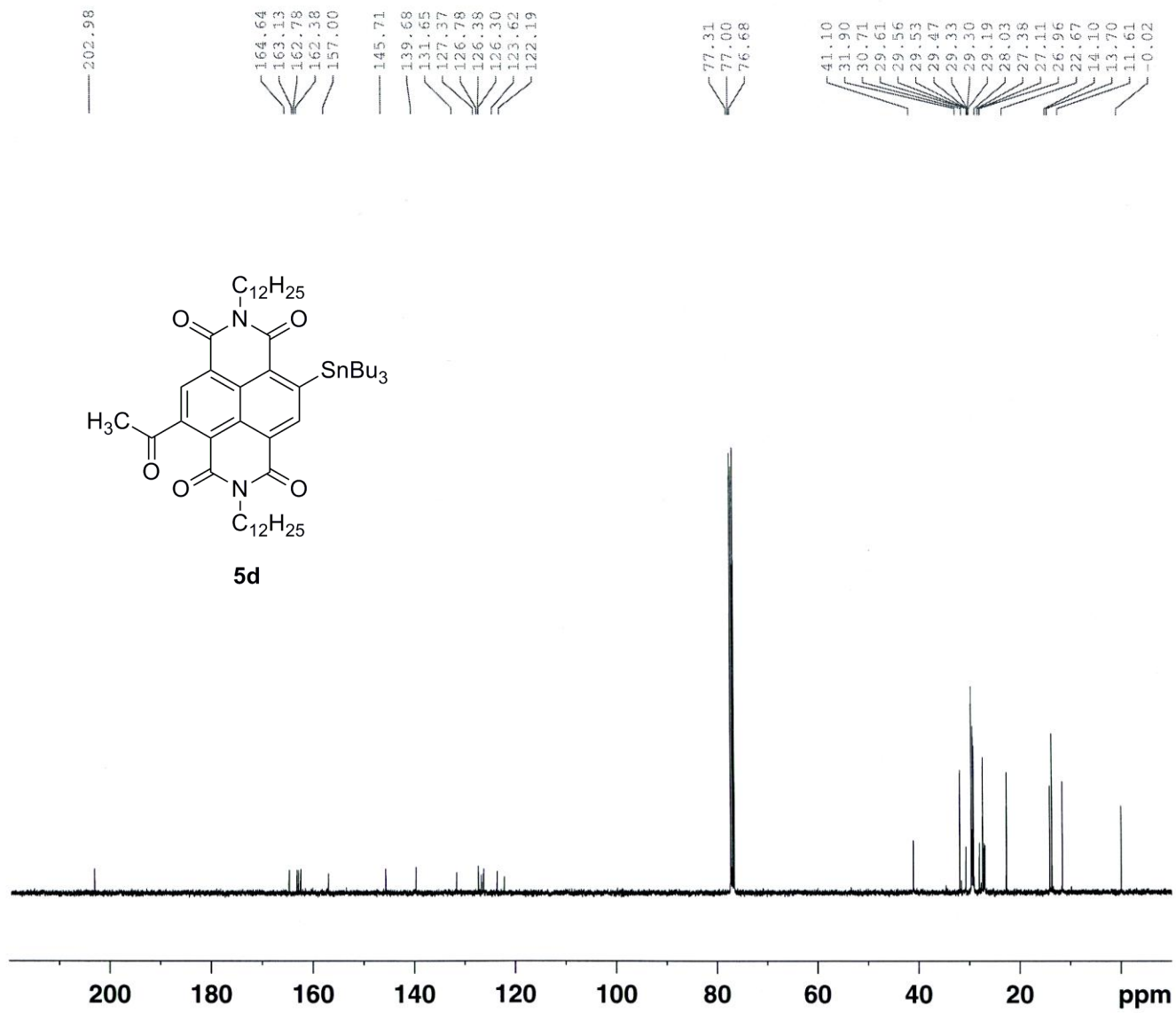


Figure S57. $^{13}\text{C}\{^1\text{H}\}$ NMR (100 MHz, CDCl_3) spectrum of **5d**.

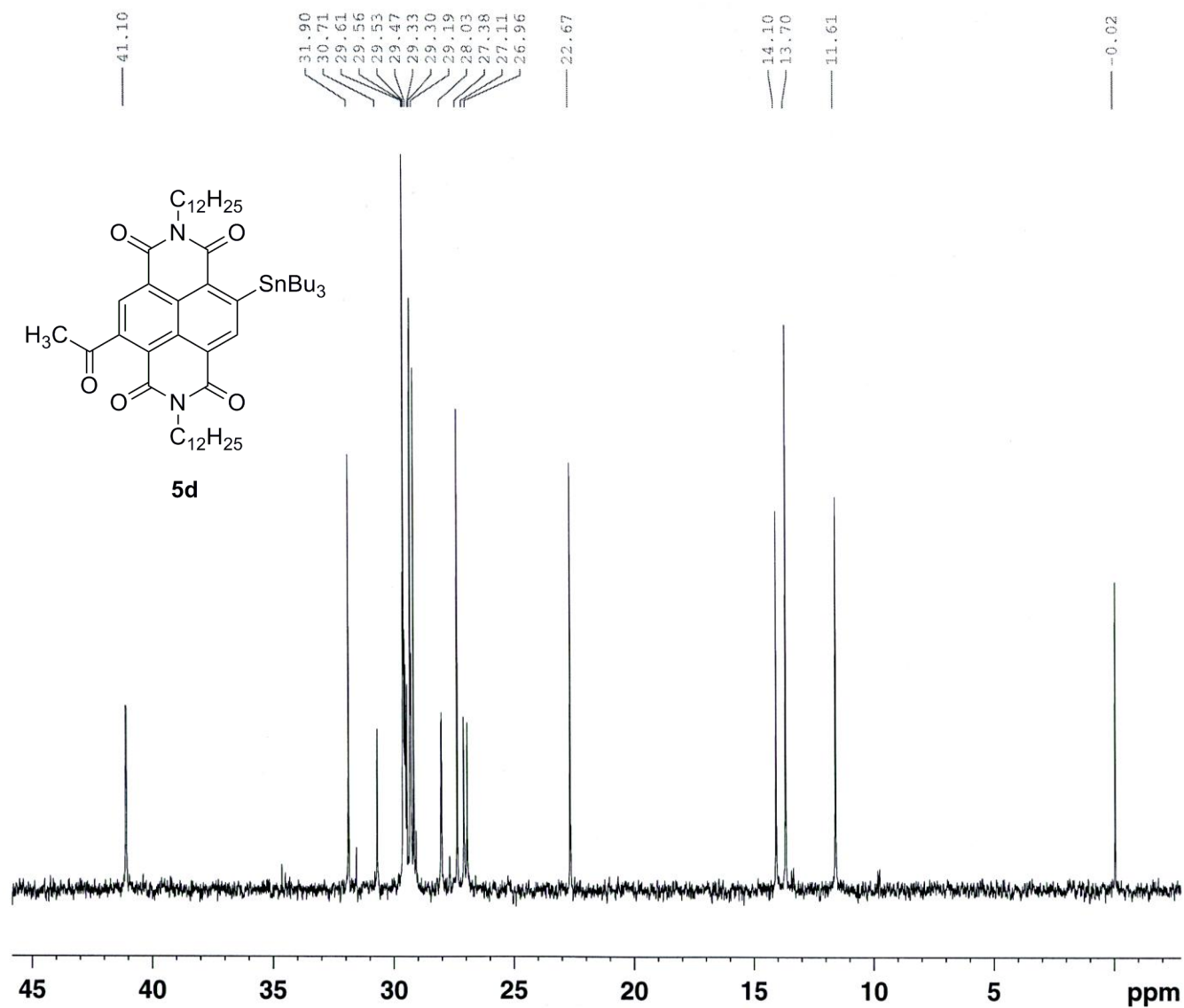


Figure S59. $^{13}\text{C}\{^1\text{H}\}$ NMR (100 MHz, CDCl_3) spectrum (aliphatic region) of **5d**.

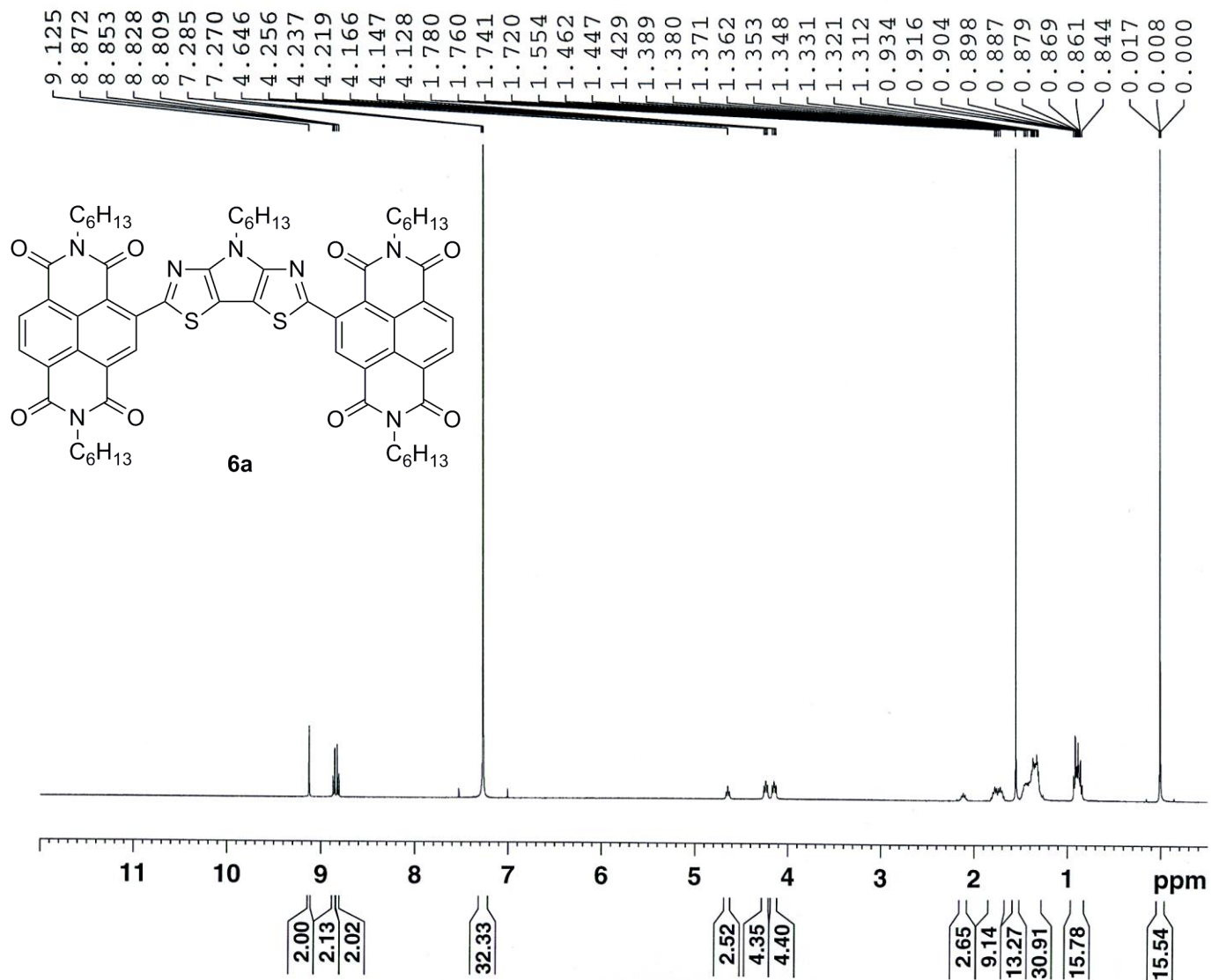


Figure S60. 1H NMR (400 MHz, $CDCl_3$) spectrum of **6a**.

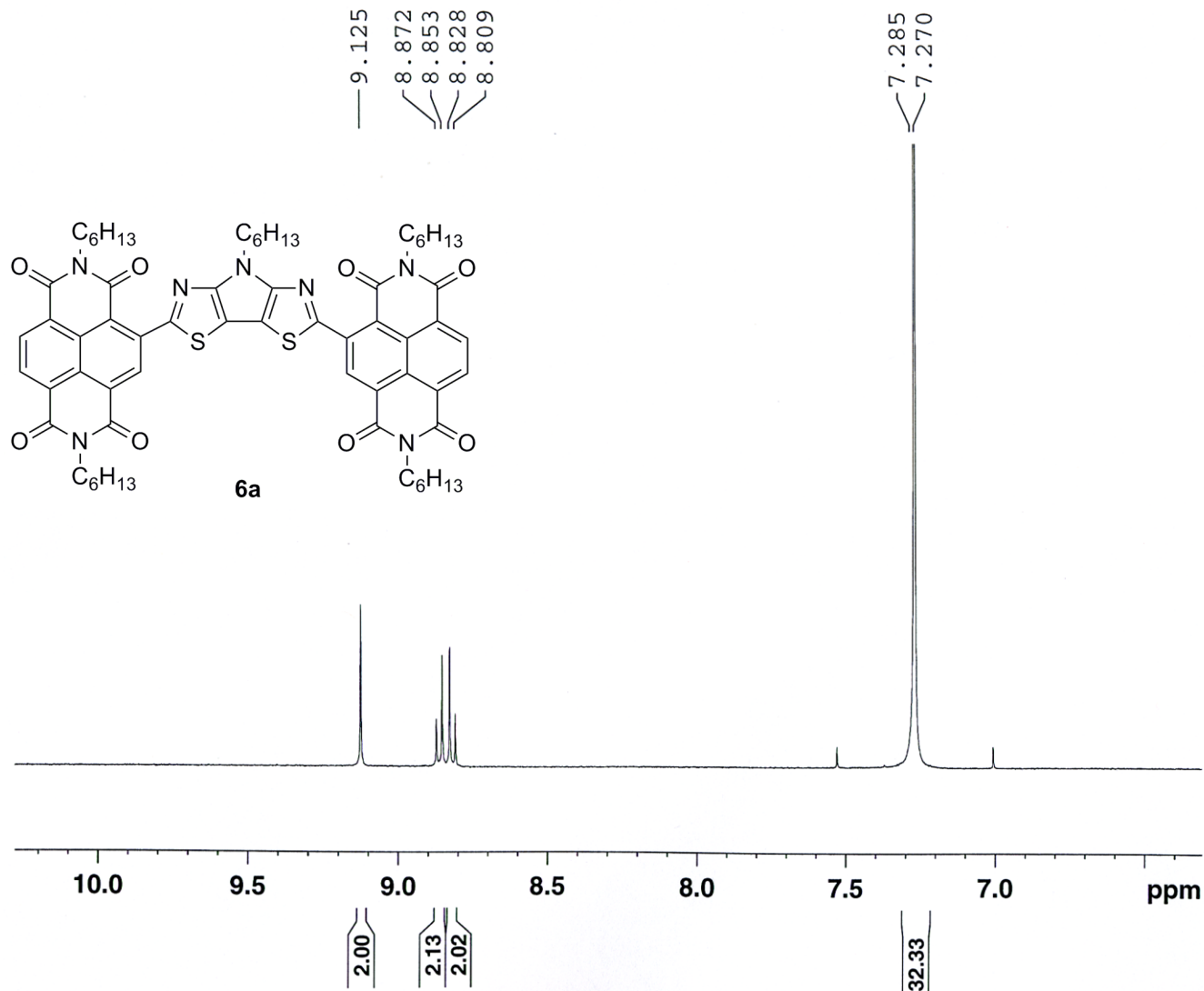


Figure S61. 1H NMR (400 MHz, $CDCl_3$) spectrum (aromatic region) of **6a**.

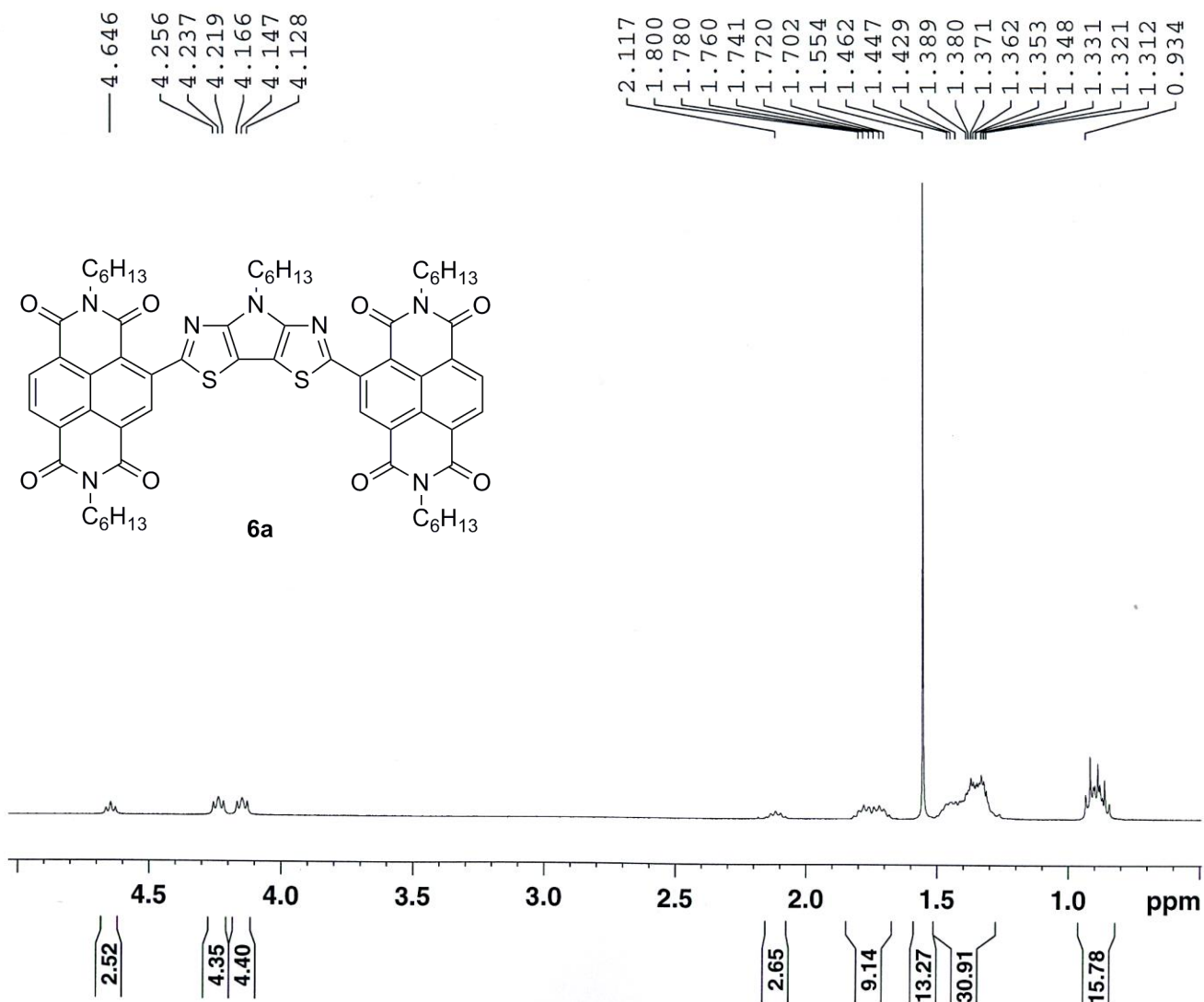


Figure S62. 1H NMR (400 MHz, $CDCl_3$) spectrum (aliphatic region) of **6a**.

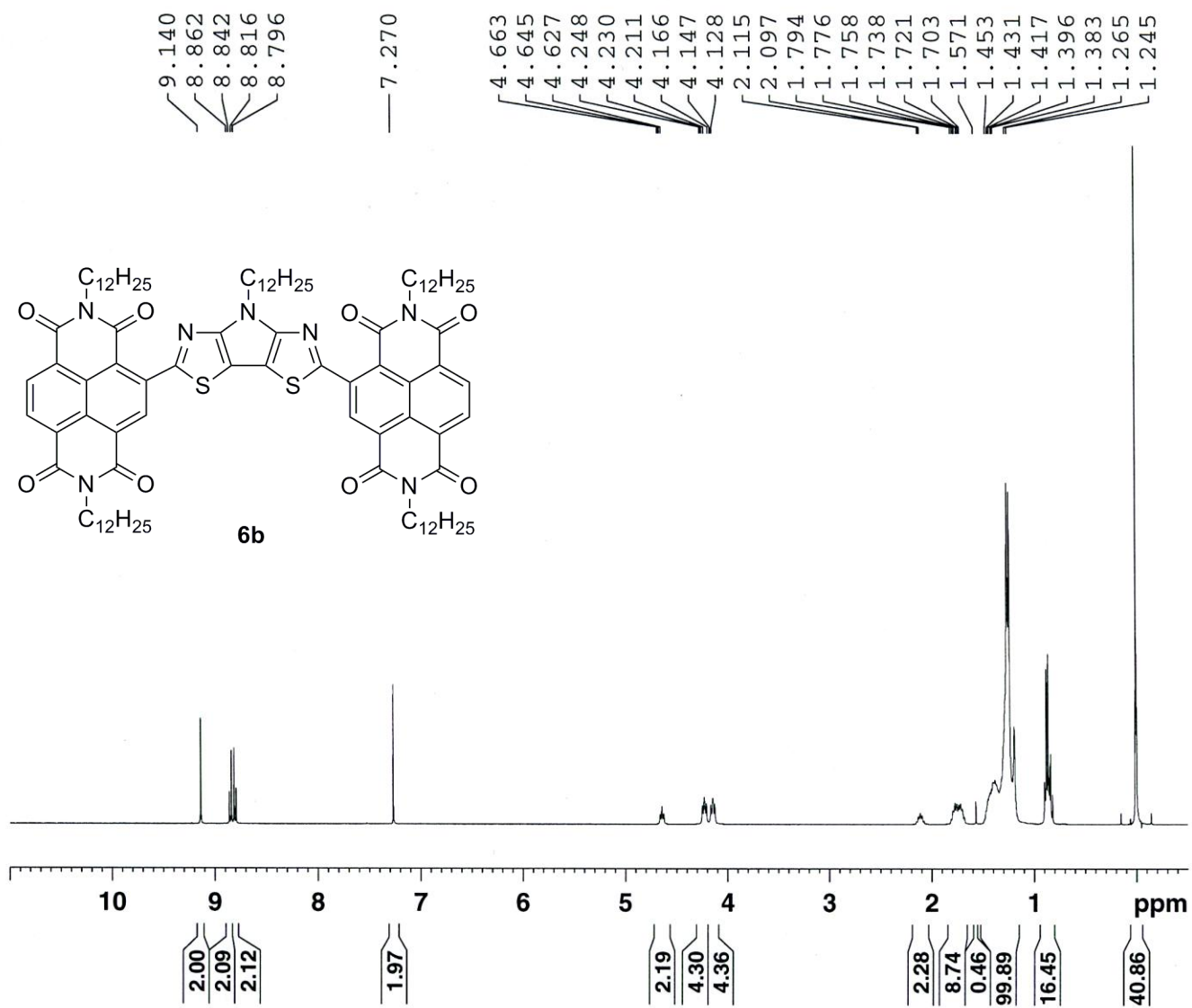


Figure S63. ^1H NMR (400 MHz, CDCl_3) spectrum of 6b.

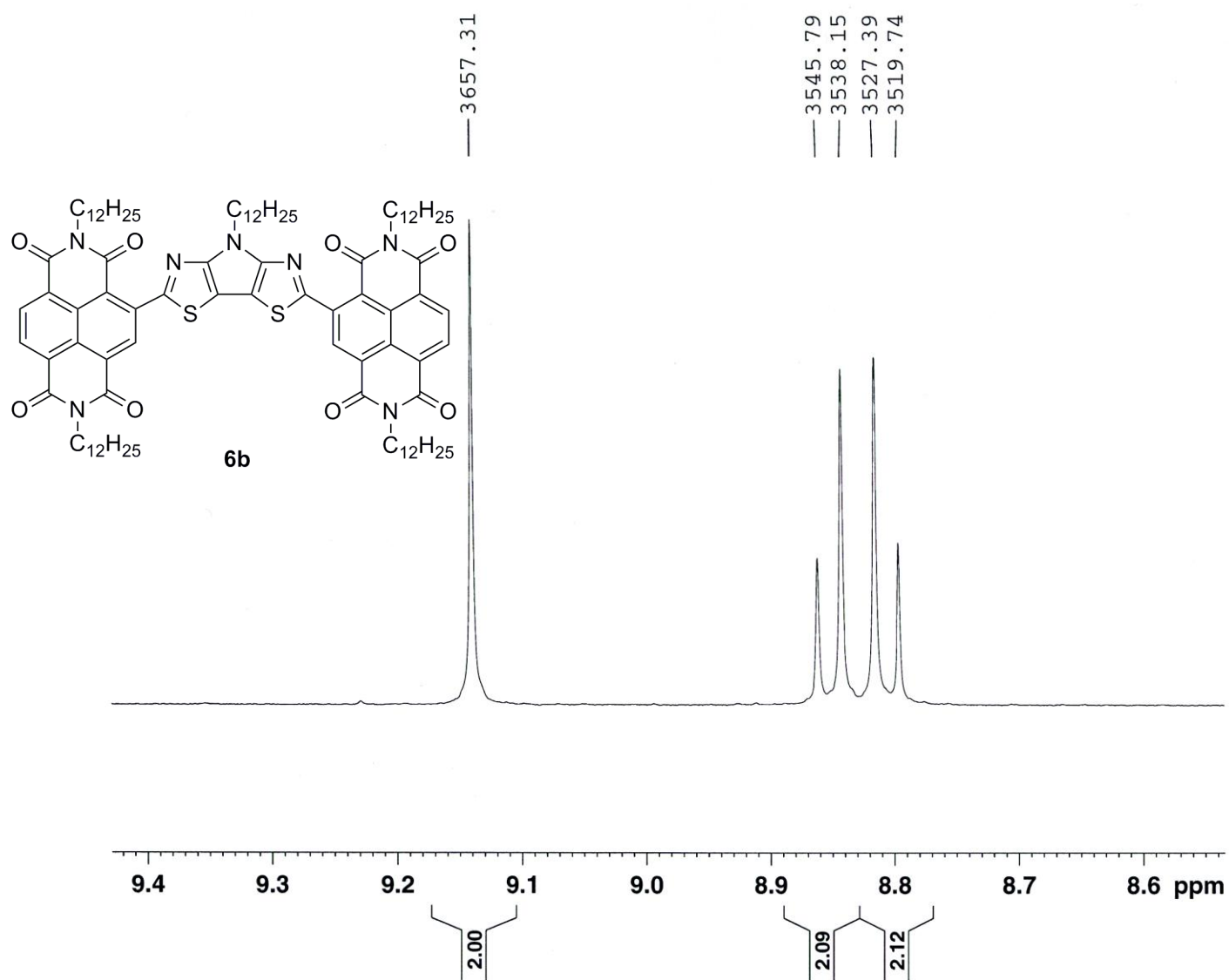


Figure S64. ^1H NMR (400 MHz, CDCl_3) spectrum (aromatic region) of 6b.

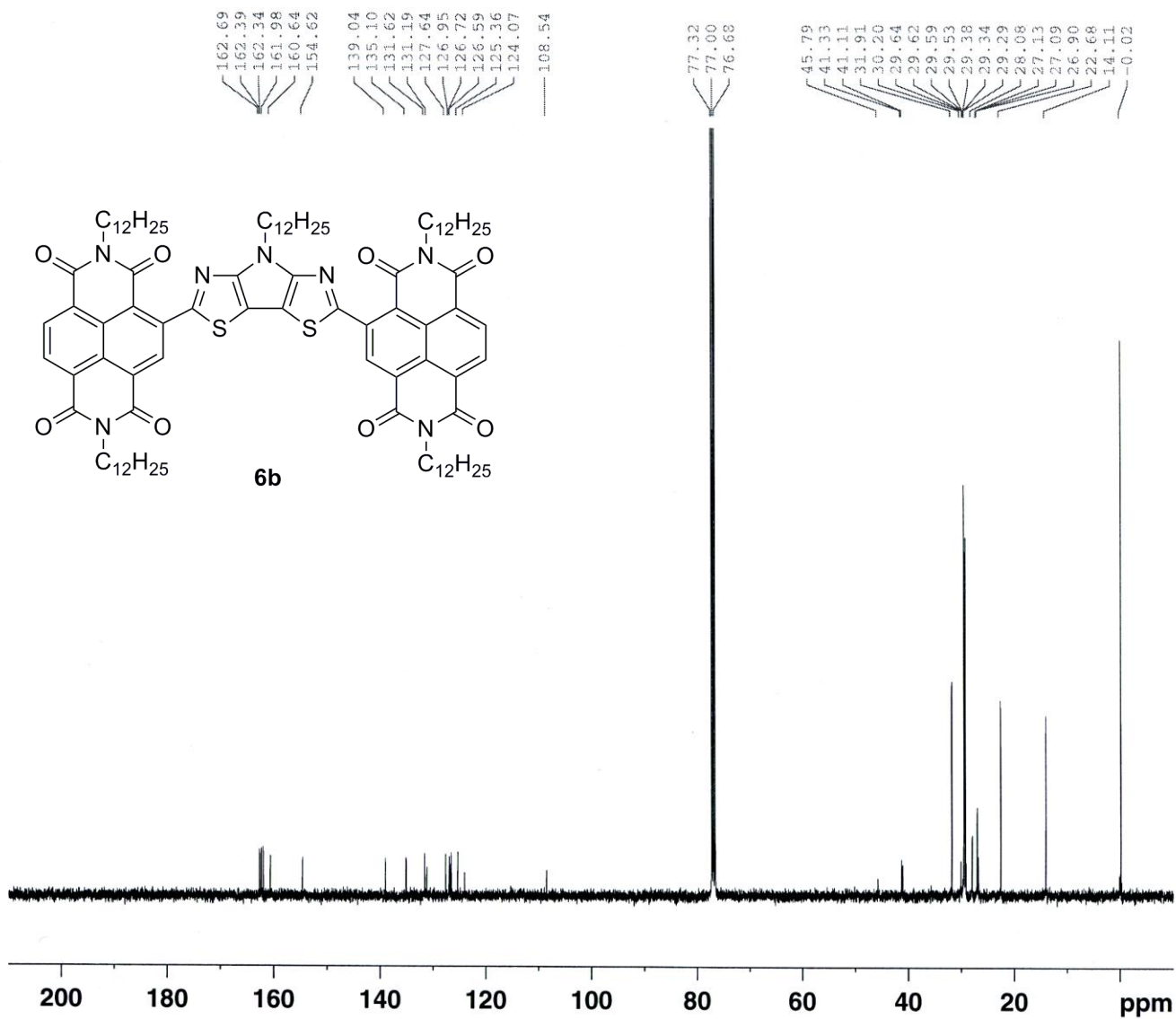


Figure S65. $^{13}C\{^1H\}$ NMR (100 MHz, $CDCl_3$) spectrum of **6b**.

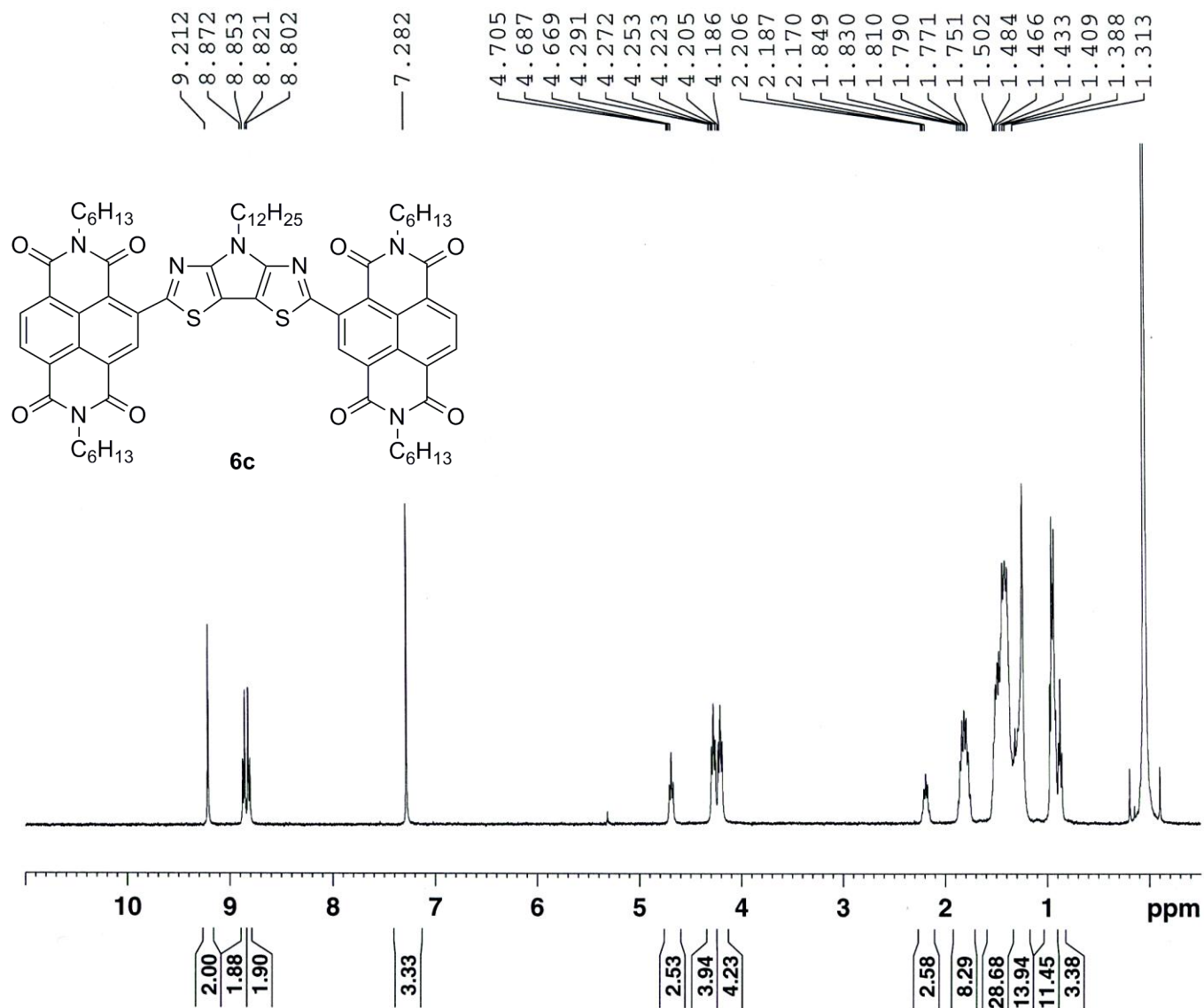


Figure S66. 1H NMR (400 MHz, $CDCl_3$) spectrum (340 K) of **6c**.

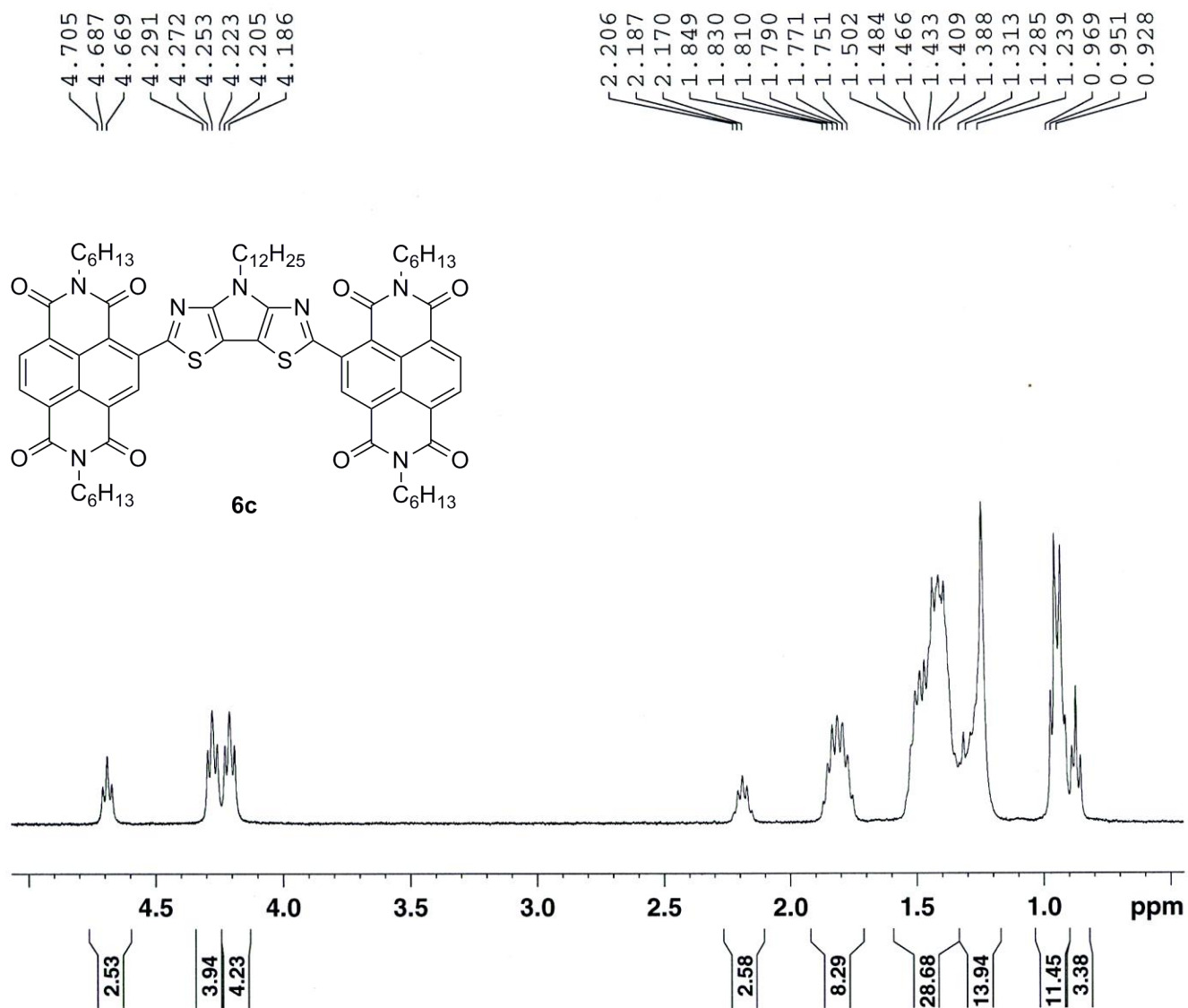


Figure S67. ^1H NMR (400 MHz, CDCl_3) spectrum (340 K; aliphatic region) of **6c**.

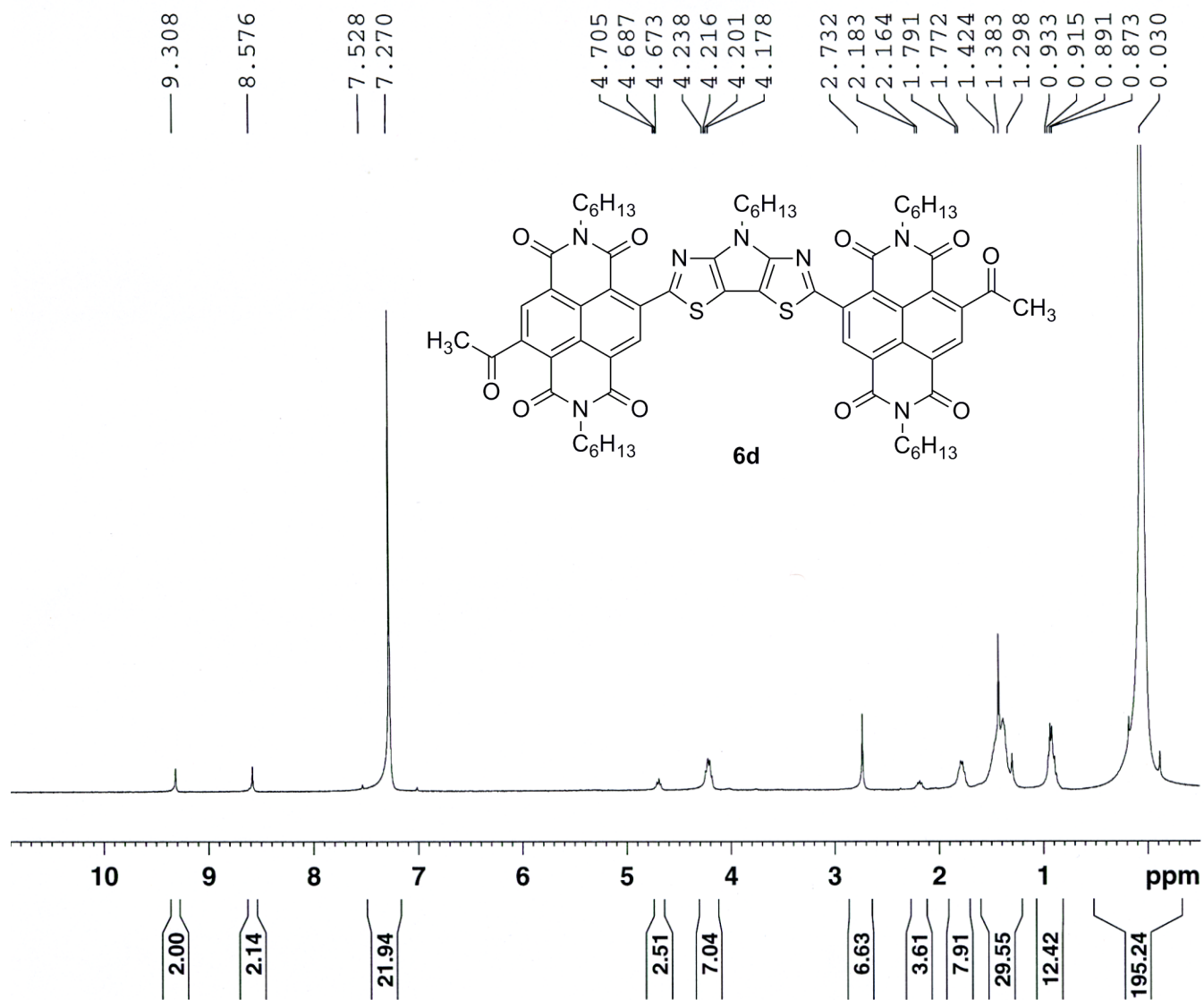


Figure S68. ¹H NMR (400 MHz, CDCl₃, 340 K) spectrum of **6d**.

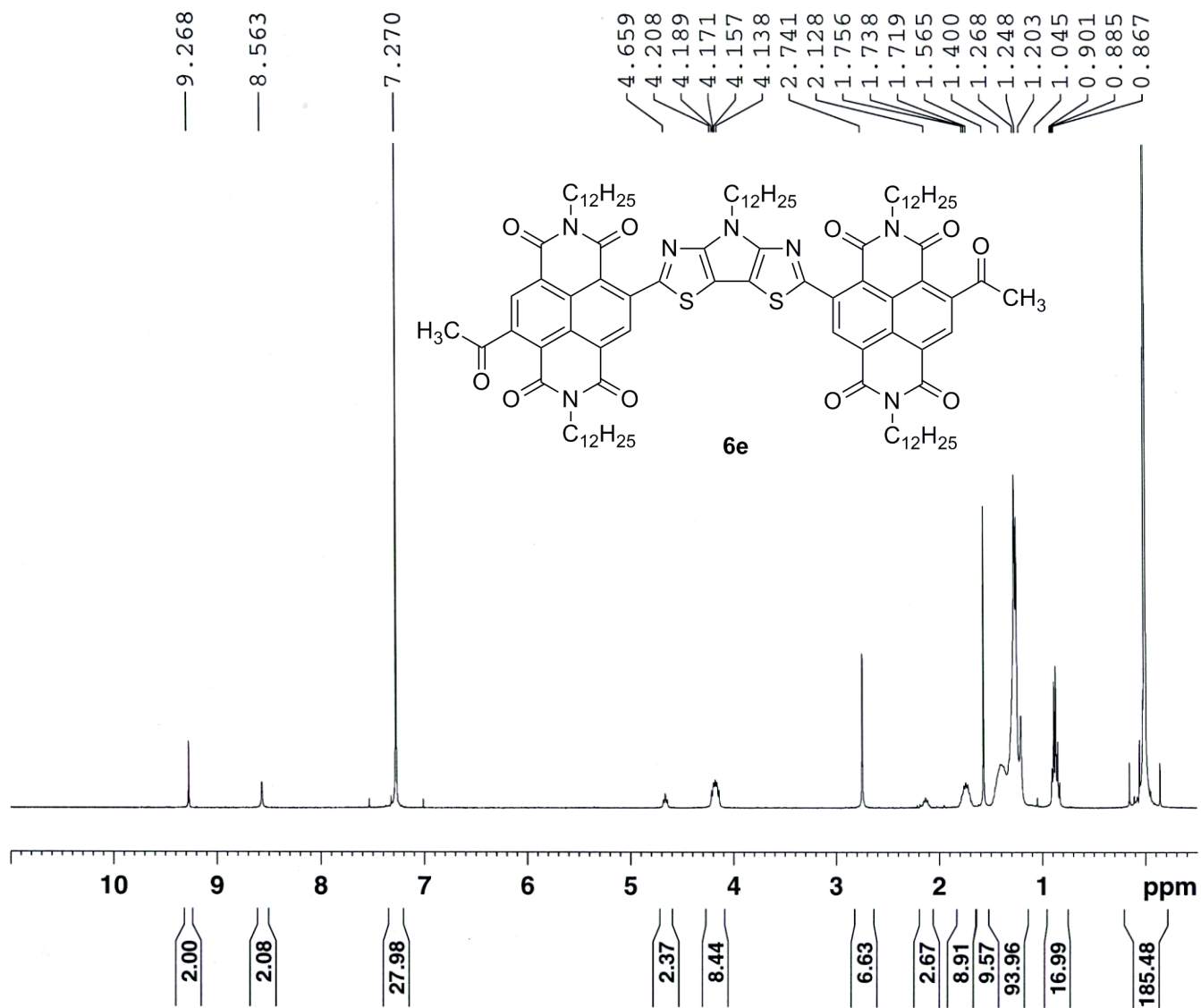


Figure S69. ^1H NMR (400 MHz, CDCl_3 , 340 K) spectrum of **6e** (peak at 1.57 ppm (9.6H) belongs to water present in CDCl_3).

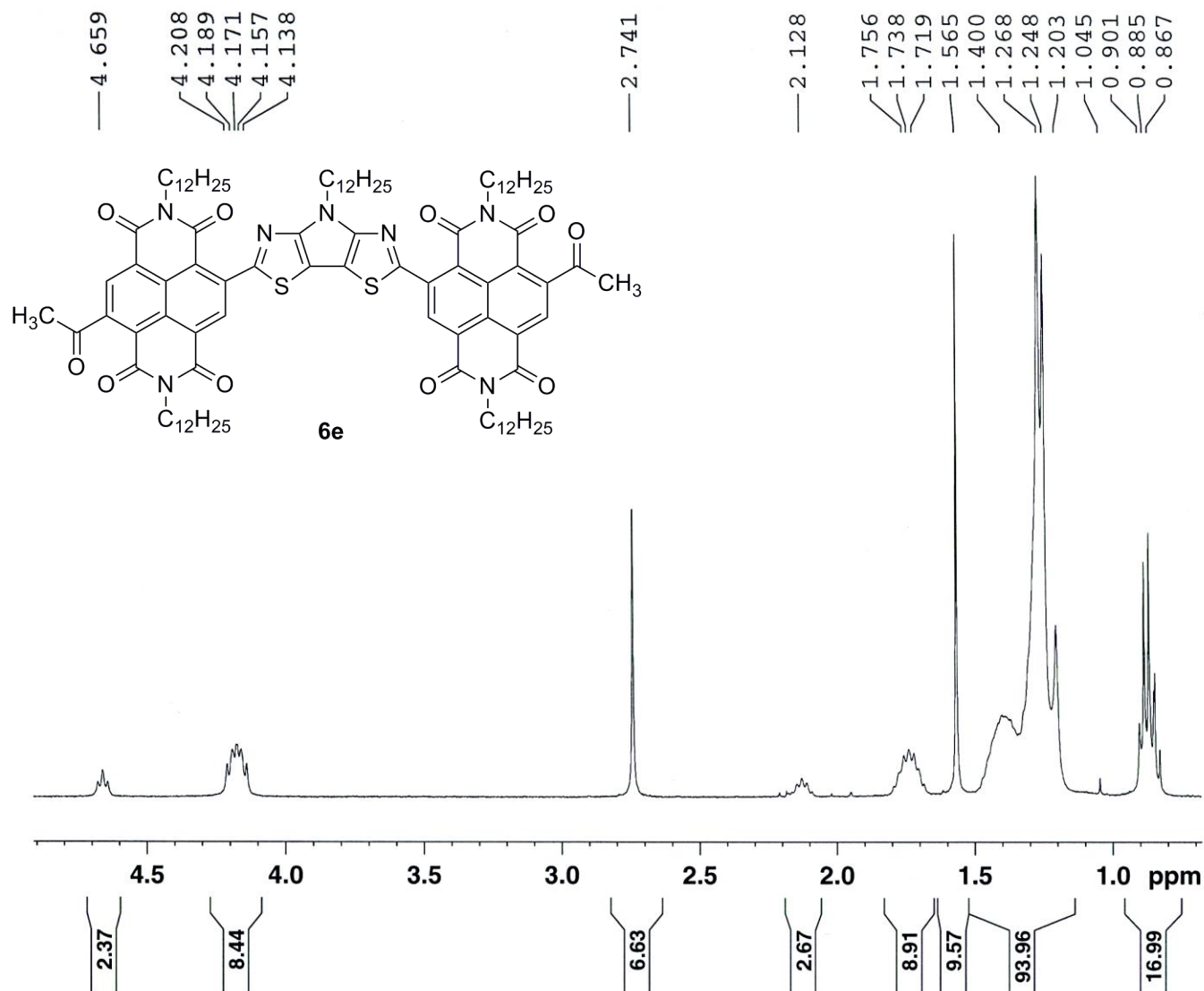


Figure S70. ¹H NMR (400 MHz, CDCl₃, 340 K; aliphatic region) spectrum of **6e**.

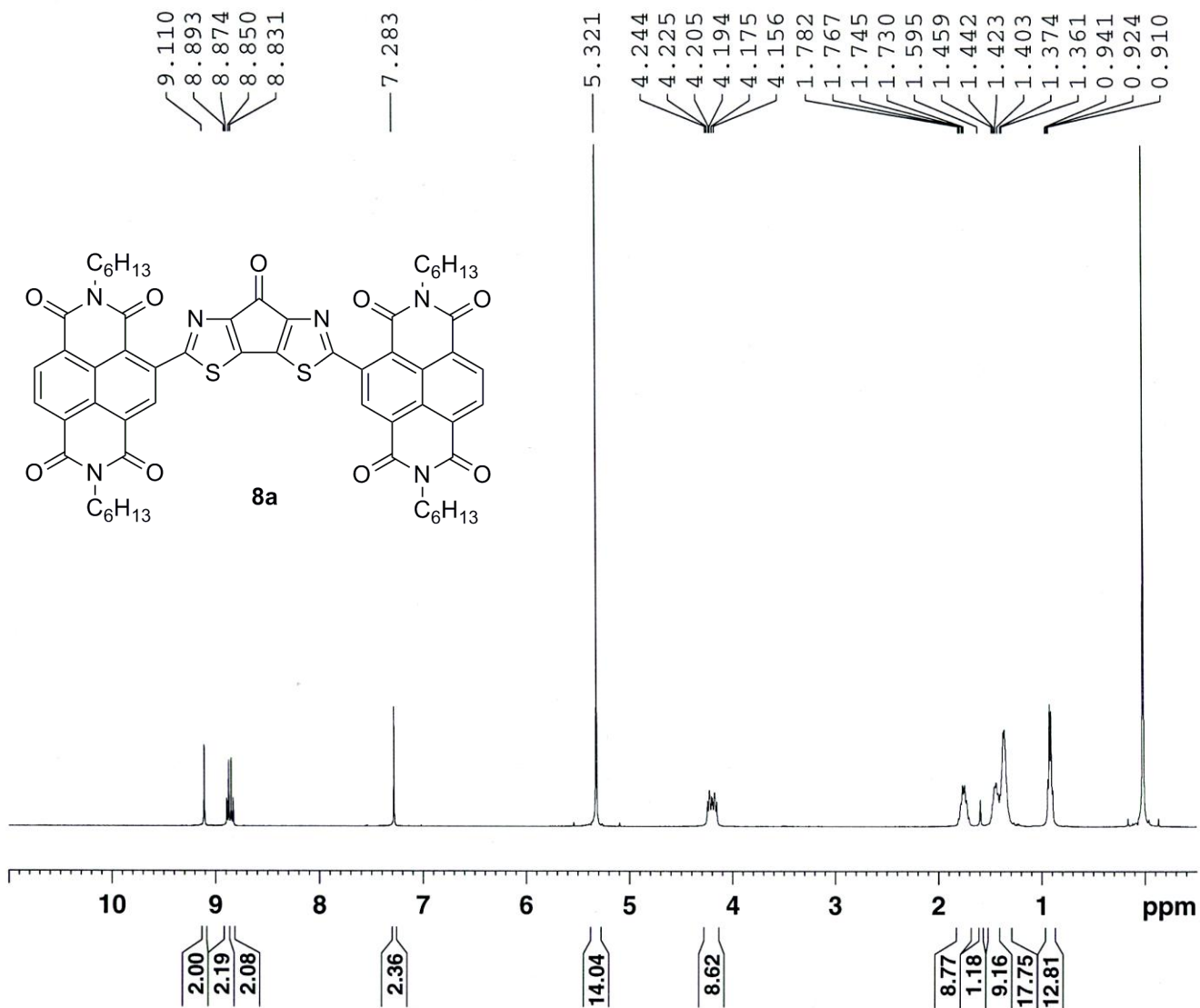


Figure S71. 1H NMR (400 MHz, $CDCl_3$) spectrum of **8a** (peak at 5.32 ppm belongs to dichloromethane which was used to wash NMR tube).

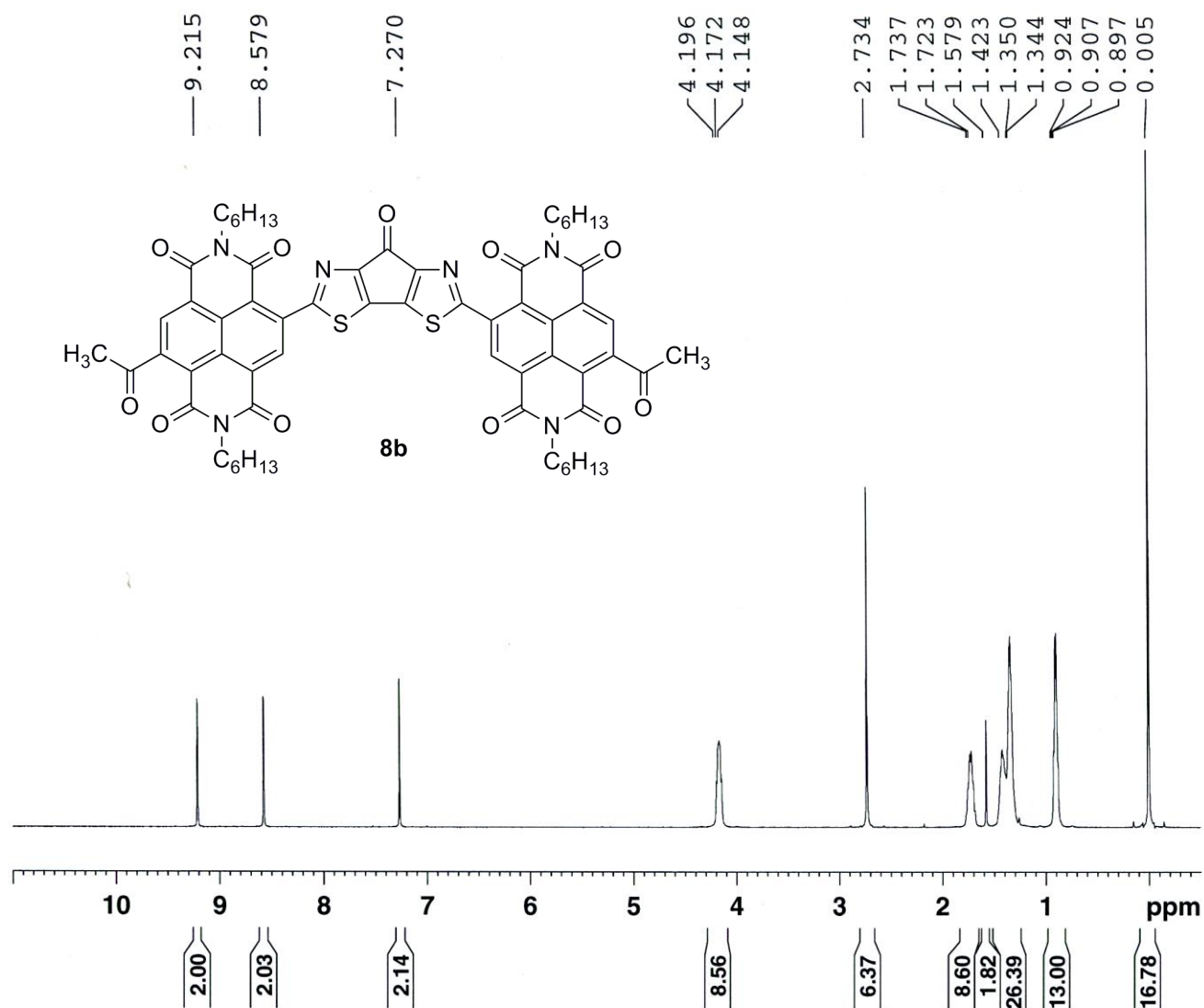


Figure S72. ^1H NMR (400 MHz, CDCl_3) spectrum of **8b**.

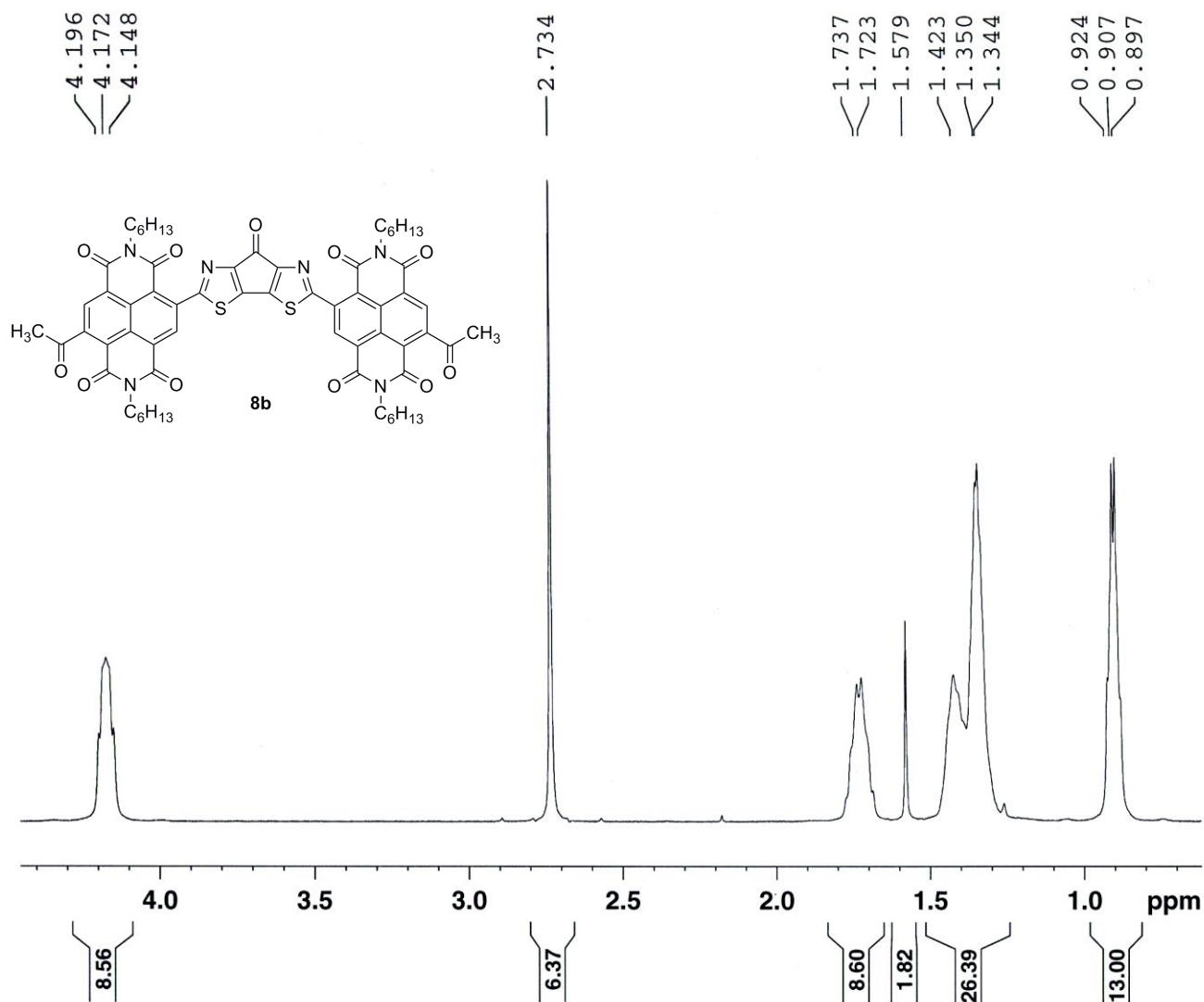


Figure S74. ¹H NMR (400 MHz, CDCl₃) spectrum (aliphatic region) of **8b**.

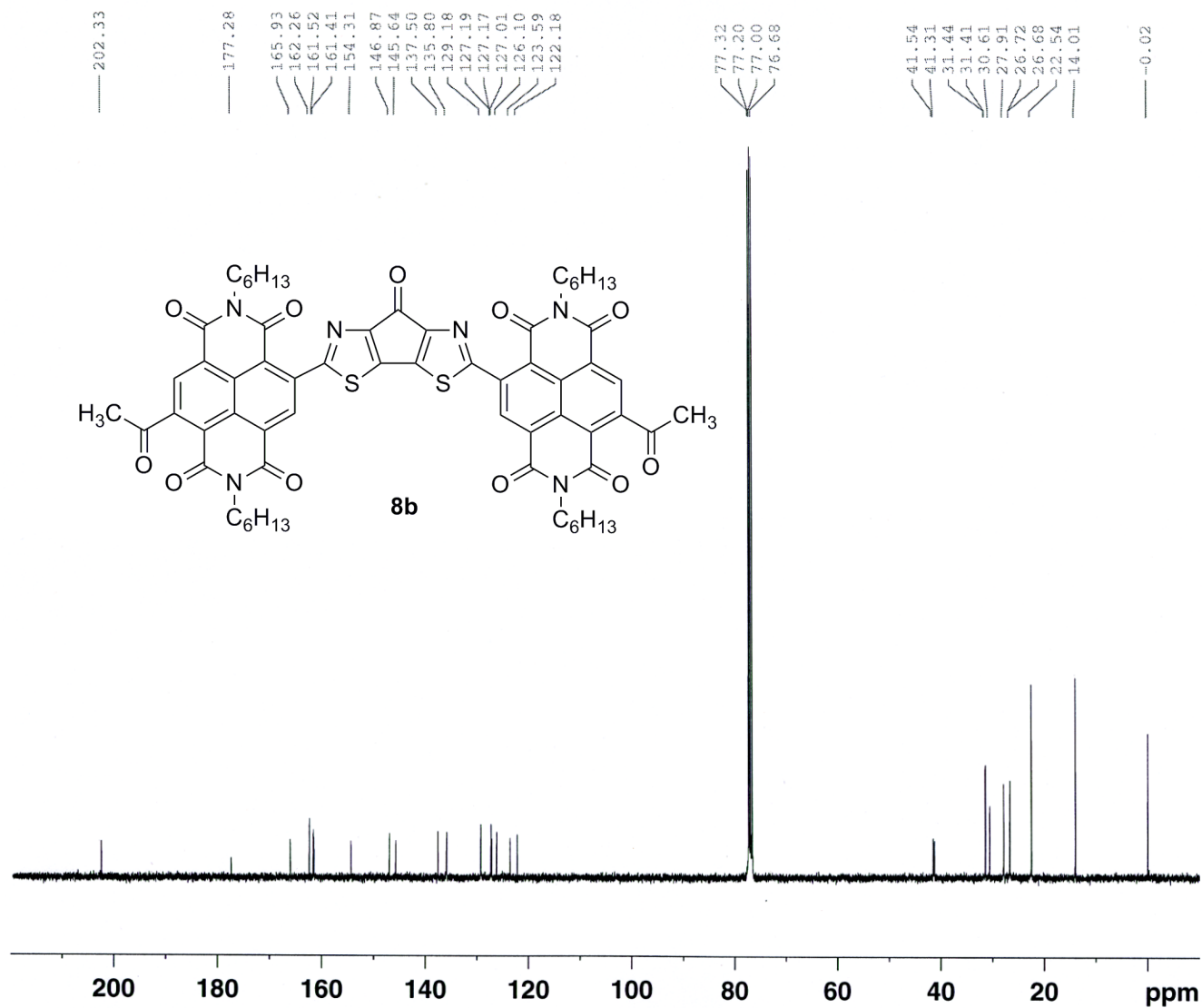


Figure S75. ^{13}C $\{^1\text{H}\}$ NMR (100 MHz, CDCl_3) spectrum of **8b**.